NDR2 AND FILAMIN A AS MODULATORS OF INTEGRIN ACTIVATION DURING DENDRITIC GROWTH

Dissertation
zur Erlangung des akademischen Grades
doctor rerum naturalium (Dr. rer. nat.)
genehmigt durch die Fakultät für Naturwissenschaften
der Otto-von-Guericke-Universität Magdeburg

von
Yunus Emre Demiray, MSc.
geboren am 27.08.1990 in Goztepe/Istanbul

eingereicht am 24.11.2020.

verteidigt am 07.05.2021.

Gutachter: Prof. Dr. Oliver Stork

Gutachter: Prof. Dr. Amparo Acker-Palmer

DDC: 573.848

TABLE OF CONTENTS

LIST OF TABLES

LIST OF FIGURES

LIST OF ABBREVIATIONS

^{0}C	degree of celcius
AAK1	ap2 associated kinase
AAV	adeno associated virus
ABD	actin binding domain
AIS	autoinhibitory segment
AP-2	adapter protein 2
AS	activation segment
BDNF	brain derived neurotrophic factor
CamKII	ca2+/calmodulin dependent protein kinase 2
CMV	cytomegalovirus
CNS	central nervous system
CRISPR	clustered regularly interspaced short palindromic repeats
dCas9	catalytically defective Cas9
DIg24	loss of Ig24
DIV	days in vitro
DMEM	Dulbecco's Modified Eagle Medium
ECM	extracellular matrix
FAK	focal adhesion kinase
FBS	fetal bovine serum
FlnA	filamin A
FN	fibronectin
gRNA	guide RNA
HBSS	Hank's Balanced Salt Solution
HDR	homology-directed-repair
HM	hydrophobic motif
HPC	hippocampal primary culture
HSBP1	heat shock factor binding protein 1
Ig	immunoglobulin like repeat
ILK	integrin linked kinase
KO	knockout
LETS	large external-transformation sensitive proteins
LN111	laminin-111
LSD	least significant difference
Luc	luciferase
MAPK	mitogen activated protein kinase
MIDAS	metal ion dependent adhesion site
miniCMV	minimal CMV promoter
NBM	neurobasal media

Ndr2	nuclear dbf2-related 2
NGF	nerve growth factor
NTR	N-terminal regulatory motif
PAK1	p21 activated kinase
PC12	rat adrenal phaeochromocytoma cell line
PDL	poly-D-lysine
PFA	paraformaldehyde
PH	periventricular heterotopia
PI3K	phosphoinositide 3-kinase
PKA	protein kinase A
PKC	protein kinase C
PSI	plexin-semaphorin-integrin
PTEN	Phosphatase and tensin homolog
PTPRA	receptor-type tyrosine-protein phosphatase alpha
ROCK	Rho associated protein kinase
RSK	ribosomal S6 kinase
S2152	serine 2152
tdTom	tdTomato
Trc	tricornered
VPR	VP64-p65-Rta

ABSTRACT

M.Sc. Demiray, Yunus Emre

Ndr2 and Filamin A as modulators of integrin activation during dendritic growth

During maturation newborn neurons polarize and start extending neurites. In the adult brain, as dendrites and axons are precisely wired, numerous synapses are formed between them. The architecture of the neural circuitry is essential since it lays the foundation of signal transmission in brain. Therefore, dendritic branching patterns are pivotal for regulating the specificity and capacity of the synaptic input in the developing and the adult brain. In this study, two intracellular components, Ndr2 kinase and its recently identified substrate Filamin A, are examined for their critical role in neurite extension and dendritic arborization during neuronal development in vitro. Ndr2 kinase has been previously shown to increase β_1 integrin activity and to be involved in neurite growth mechanisms. In the present study, experiments using primary neurons and neurally differentiated pheochromacytoma (PC12) cells further demonstrated that Ndr2 kinase also determines the substrate specificity of neurite extension via surface expression of $\alpha_1\beta_1$ integrins. Secondly, given that the Ndr2 mediated modulation of β_1 integrins is not direct, its recently identified substrate FlnA was tested in detail regarding its role during dendritic branching. FlnA manipulations in neurons resulted in significant dendritic hypertrophies, which are mediated by β_1 integrin receptor activity and actin cytoskeleton crosslinking. Finally, biochemical analysis of the FlnA silenced neurons revealed a disturbance in Akt signaling that might be the downstream mediator of the observed differential neuronal growth effects in FlnA manipulated neurons. Together, these results suggest that Ndr2 and FlnA are involved in integrin receptor activation and downstream cascades and play critical roles during dendritic arborization.

ZUSAMMENFASSUNG

M.Sc. Demiray, Yunus Emre

Ndr2 and Filamin A as modulators of integrin activation during dendritic growth

Neugeborene Neurone polarisieren sich während der Reifung und verlängern ihre Neuriten. Im adulten Gehrin reifen Neuriten zu Dendriten und Axonen, die über Synapsen präzise miteinander verschaltet sind. Da die Architektur solcher neuronalen Schaltkreise die Grundlage der Signalübertragung im Gehirn bildet, sind dendritische Verzweigungsmuster sowohl im adulten als auch im sich entwickelnden Gehirn entscheidend für die Regulierung der Spezifität und Kapazität des synaptischen Inputs. In dieser Studie werden zwei intrazelluläre Komponenten, die Ndr2 Kinase und ihr kürzlich identifiziertes Substrat Filamin A, auf ihre grundlegende Rolle bei der Neuritenausdehnung und der dendritischen Verästelung während der neuronalen Entwicklung in vitro untersucht. Es wurde bereits früher gezeigt, dass die Ndr2 Kinase die Aktivität von β_1-Integrin erhöht und dadurch am Wachstumsn von Neuriten beteiligt ist. In der vorliegenden Studie wird mittels Experimenten mit primären Neuronen und neural differenzierten Phäochromazytom-Zellen (PC12) außerdem gezeigt, dass auch die Substratspezifität der Neuritenausdehnung durch die Ndr2 Kinase bestimmt wird. Dies erfolgt über die Oberflächenexpression von $\alpha_1\beta_1$ Integrinen. Da die Ndr2-vermittelte Modulation der β_1 Integrine indirekt erfolgt, wurde das kürzlich identifizierte Substrat FlnA hinsichtlich seiner Rolle bei der dendritischen Verzweigung eingehend getestet. FlnA Manipulationen in Neuronen führt zu signifikanten dendritischen Hypertrophien, die durch β_1 Integrinrezeptor-Aktivität und Aktin-Zytoskelett-Vernetzung vermittelt werden. Die biochemische Analyse von FlnA defizienten Neurone ergibt außerdem, dass der Akt Signalweg gestört ist, der als nchgeschaltetere Mediator für die beobachteten differentiellen neuronalen Wachstumseffekte in FlnA manipulierten Neuronen in Frage kommt. Zusammengenommen deuten

diese Ergebnisse darauf hin, dass Ndr2 und FlnA an der Aktivierung der Integrinrezeptoren und den nachgeschalteten Kaskaden beteiligt sind und während der dendritischen Arborisierung eine entscheidende Rolle spielen.

INTRODUCTION

1.1 Integrin Receptors

The transition from unicellular microbes to multicellular organisms required novel cell-cell communication and cell adhesion mechanisms. To adapt into this new cellular environment, one of the most important mechanism that emerged specifically in the animal kingdom is the integrin mediated cell signaling (Whittaker and Hynes, 2002; Nichols *et al.*, 2006; Sebé-Pedrós *et al.*, 2010). However, it took scientists a long time until they successfully purify and study structure and functions of integrin receptors.

The notion that there must be a transmembrane bridge on the cell membrane between extracellular matrix proteins (ECM) and cytoskeleton was emerging in 1970s. Early evidence of such receptors came from the studies linking the large external-transformation sensitive proteins (LETS, which coined the term "fibronectin" later) to the actin cytoskeleton of the cells. Using human, mouse and hamster cells, scientists showed that adhesion and morphology of the cells can be modified via actin cytoskeleton after addition or removal of fibronectins from the extracellular space (Ali *et al.*, 1977; Heggeness, Ash and Singer, 1978). Accumulating evidences and hypotheses resulted to first papers speculating a transmembrane receptor (Hynes and Yamada, 1982) that can specifically bind fibronectin and induce intracellular signaling cascades via candidates such as vinculin or spectrin to modify actin cytoskeleton. With the discovery of more and more antibodies that can block adhesion of cells to specific extracellular proteins (Greve and Gottlieb, 1982; Neff *et al.*, 1982; Knudsen, Horwitz and Buck, 1985), it did not take very long time for the first receptors to be fully identified from cDNA libraries that encodes the receptor protein involved in fibronectin-induced cell adhesion (Tamkun *et al.*, 1986). This cDNA sequence also revealed that the receptor has

transmembrane domains and several phosphorylation residues on its intracellular tail. As an integral membrane complex bridging intra- and extracellular proteins, the name "integrin" was given which gave rise to the integrin receptor family (Tamkun *et al.*, 1986).

1.1.1 Structure of integrin receptors

Like many other adhesion receptors on the membrane, an integrin receptor has an extracellular domain receiving the outside cues, a transmembrane domain and finally an intracellular part that interacts with downstream components (Askari *et al.*, 2009). Furthermore, integrins are heterodimers that consist of two non-covalently bound α and β subunits (Figure 1). Since integrins are relatively large membrane receptors, it took a lot of effort to resolve its 3D structure in high resolution. When the crystal structure of $\alpha_V\beta_3$ integrins was published very first time in 2001, it revealed further structural details: two globular head domains on the extracellular side of each subunit; a seven-bladed β-propeller structure (each is about 60 amino acids) on α and a von Willebrand factor A domain on β subunit respectively (Xiong *et al.*, 2001). Globular head structures of integrins also contain an I-domain, either between beta sheets 2-3 on α subunit or on the β subunit head depending on the integrin subtype. These I-domains are important for the integrin ligand binding (Luo, Carman and Springer, 2007). I-domains are also flanked with metal ion dependent adhesion sites (MIDAS), in which divalent cations can bind to the integrins and modulate its conformation. Studies show that while divalent ions such as Mg^{2+} and Mn^{2+} promotes ligand binding and activation of the integrins, Ca^{2+} has more biphasic effects depending on its concentration (Zhang and Chen, 2012). It has been shown that millimolar concentrations of calcium ion (which is close to the body fluid concentration) inhibits the integrin adhesion. Lower

concentrations of calcium can still increase integrin-ligand binding combined with low Mn^{2+} concentrations (Chen, Salas and Springer, 2003).

Ligand binding head domains of integrin subunits are followed by so-called leg structures which provide the moving parts for the bent and active conformation. α subunit has relatively a simpler leg domain which is divided into thigh domain (upper leg) and calf-1 / calf-2 domains (lower leg). Besides the MIDAS in the head domains, an extra Ca^{2+} binding site is present between thigh and calf-1 domain, which is involved in concentration dependent Ca^{2+} modulation of integrin conformation (Luo, Carman and Springer, 2007). β-subunit's leg domain is a hybrid structure that consist of a plexin/semaphorin/integrin (PSI) domain and four epidermal growth factor-like domains. As shown by electron microscopy, the "joint" that provides the bending movement of the integrins is located between the thigh and calf-domain 1 on a subunit and between the EGF-domains 1 and 2 on β subunit (Nishida *et al.*, 2006). The bent conformation of the receptor masks the hybrid domain on the β subunit; hence it often serves as the target of integrin activity reporter or integrin activating antibodies (Mould *et al.*, 2005).

Extracellular domains of each integrin subunit are followed by single spanning transmembrane helices. Resolving the structure of $\alpha_{2b}\beta_3$ integrins via NMR revealed hydrophobic and electrostatic interactions between the transmembrane helices of α and β subunits, which consequently stabilizes the overall integrin heterodimer structure (Lau *et al.*, 2009). Moreover, introducing stable disulfide bonds between the subunits via amino acid substitutions impairs the outside-in ligand activation of the integrins. Hence disassociation of these transmembrane helices upon ligand binding is also required for integrin activation (Zhu *et al.*, 2007).

Finally, at the intracellular side, integrins have a C-terminal tail domain where the intracellular components can interact with the receptor. Although tails are short (20-80 amino acid long), they interact with a large set of intracellular proteins and these interactions are orchestrated with the activation state of the receptor. Integrin tail domains also display a flexible structure, which can mask/unmask binding domains depending on the interacting partners (Morse, Brahme and Calderwood, 2014).

Sequences of α integrin tails are rather distinct from each other among different subtypes except for a conserved GFFKR motif close to the cell membrane (Morse, Brahme and Calderwood, 2014). The conserved GFFKR motif has been shown to interact with integrin modulators such as SHARPIN, PP2A and Rab21 (Gushiken *et al.*, 2008; Pellinen *et al.*, 2008; Rantala *et al.*, 2011). Unlike α integrins, β subunit tails share higher homology among subtypes (except for integrin β_4, see below). Thus, β integrin tail/intracellular protein interactions are well studied due to their similar mode of action among different integrin β subtypes. The most studied motif on β integrin tails is the NPxY sequence which occurs at two different locations on C terminal and binds to most integrin regulatory proteins (Morse, Brahme and Calderwood, 2014). Talin and Kindlin proteins are the two most important interacting partners that binds the NPxY motifs and are required for integrin activation (Moser *et al.*, 2008; Margadant *et al.*, 2012). Moreover, actin-binding protein Filamin A also binds the β integrin tail using the NPxY which overlaps with Talin/Kindlin binding. Therefore, Filamin A serves as a competitive negative regulator of integrin activity (Kiema *et al.*, 2006; Nieves *et al.*, 2010).

The relatively short C-terminal tail of β integrin subunits have one exception: integrin β_4. It contains a uniquely long C-terminal, around 1072 amino acids (Hogervorst *et al.*, 1990), which

could be explained by its function. Studies have shown that this long tail is required to concentrate intracellular components of the hemidesmosomes, a distinct connection of epithelial cells to ECM via integrin β_4, which maintains integrity of the skin (Spinardi *et al.*, 1995).
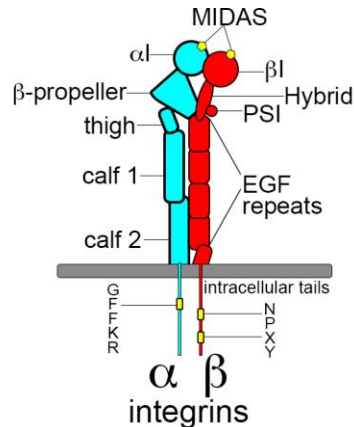
Figure 1: Structure of integrin heterodimers on the membrane.
While the leg of α subunit consists of two calf and a moveable thigh domain, stem of β subunit compromises four EGF repeats. Ligand binding head domains (globular αI and βI structures) are followed by a β propeller and a plexin-semephorin-integrin (PSI) hybrid domain respectively. These globular I domains at the N-terminal also contain the metal ion dependent adhesion sites (MIDAS) that can bind divalent cations which promotes ligand binding. Lastly, membrane spanning transmembrane parts are followed by C-terminal intracellular tail peptides which acts as a docking structure for integrin accessory proteins (Luo et al., 2007; Askari et al., 2009).

1.1.2   Integrin subtypes and their ligand specificity

While integrin receptors can only be found in the Metazoan kingdom, invertebrates and vertebrates utilize different integrin heterodimers for adhesion. Unlike the vertebrate counterparts, invertebrates have much fewer integrin subtypes (i.e.: C. elegans have only two α and one β integrin subunit) yet their structures are remarkably similar to vertebrate integrins (Baum and Garriga, 1997; Burke, 1999). In vertebrates, 18 α and 8 β subunits have been discovered so far and these different subunits can combine up to 24 different integrin heterodimers and provide the necessary ligand specificity of integrin mediated signaling (Shimaoka and Springer, 2003).

Early studies on the cell-ECM communication were particularly focused on the interaction of the cell membrane with a newly discovered extracellular protein of the same era: Fibronectins. First, this extracellular protein appeared as a large band missing in tumor cell protein extracts compared to control cells (hence named as large external transformant sensitive protein, LETS) (Hynes, 1973). Further studies revealed the tripeptide present in the fibronectin sequence, RGD, that is necessary for its binding to the cell membrane. This paved the way to the discovery of the first sub-group of integrin heterodimers that specifically binds to RGD-containing extracellular proteins with different affinities (Ruoslahti and Pierschbacher, 1987).

Among different integrin subtypes, integrin β_1 can make heterodimers with almost all different alpha subtypes (α_1, α_2, α_3, α_4, α_5, α_V, α_6, α_7, α_8, α_9, α_{10} and α_{11}) and hence functions as the central player integrin mediated signaling (Hynes, 2002). While β_1 integrin activity and availability is tightly regulated via intracellular binding partners and kinases (on C terminal NPxY motifs and at Threonine[788/789] respectively (Nilsson *et al.*, 2006; Margadant *et al.*, 2012)); the α subunit partner of the heterodimer mainly determines the ligand specificity of the receptor. Ligands of β_1-integrin containing receptors are composed of ECM members which can be classified into 3 major groups: Laminins which bind the α_3, α_6, and α_7; RGD containing fibronectins which bind to α_5, α_V, and α_8; and finally GFOGER containing collagens that bind to the α_1, α_2, α_{10}, and α_{11} (Hynes, 2002; Barczyk, Carracedo and Gullberg, 2010). Moreover, these ECM groups can further be divided into their corresponding isoforms, such as collagen I, II, III and IV subtypes under GFOGER containing ECMs (Turner, Flier and Carbonetto, 1987) or laminin-1 and laminin-2 subtypes (Hamill *et al.*, 2009). Similarly, different α integrin subtypes mediate isoform specificity: for instance in T cells, which depends on the integrin receptors for adhesion, $\alpha_1\beta_1$ expressing cells are enriched on collagen IV rich areas and $\alpha_2\beta_1$ expressing cells localize more on collagen I rich areas (Richter *et al.*, 2007).

Besides β_1 integrins, 7 more integrin β subunits are present in vertebrates: β_3, β_5, β_6, and β_8 containing heterodimers bind to fibronectins while β_4 integrin can make a heterodimer with α_6 integrin as serve as a receptor for laminins (Hynes, 2002). Lastly, β_2 and β_7 integrins are only expressed in leukocytes and make heterodimers with other leukocyte specific α subunits (such as alpha L,M,X,D and E) and play an important role in leukocyte recruitment (Barczyk, Carracedo and Gullberg, 2010).

To test the role of integrin subunits in vivo, previous studies knocked out different subunits in mice and revealed different phenotypes varying from mild developmental impairments to embryonic lethality (Hynes, 2002). As expected, full knockout (KO) of β_1 integrin results embryonic lethality with embryos failing in gastrulation phase (Fässler and Meyer, 1995; Stephens *et al.*, 1995). Hence, functional studies of β_1 integrin was often done using promoter-driven transgenic mice to restrict the β_1 mutation to a temporal window or a subset of cell population instead of full body KO (such as using CamKII (Ca^{2+}/calmodulin-dependent protein kinase) or Emx1 promoter driven β_1 integrin KO, see 1.1.3 Function of integrin receptors in neurons). While integrin α_1 KO shows no significant developmental impairment, integrin α_4 KO results in embryonic lethality with severe heart defects (Yang, Rayburn and Hynes, 1995; Gardner *et al.*, 1999). As expected, leukocyte specific integrins such as αL or β_2 knock out mice are viable with leukocyte recruitment impairments (Schmits *et al.*, 1996; Scharffetter-Kochanek *et al.*, 1998). These results suggest that, although integrin subunits have overlapping and redundant functions, they serve distinct roles and can cause varying impairments upon knockdown in vivo.

1.1.3   *Function of integrin receptors in neurons*

Once neurons are produced from progenitor cells in subventricular zone, they are guided to their target region via adhesion mediated migration. As they are reaching to their destination, they start to polarize and extend neurites to join the brain circuitry. For all these steps, neurons rely on integrin heterodimers on their membrane because of their ECM ligand specificity and downstream cytoskeleton signaling. Throughout the brain development, integrin subunits have different spatial and temporal expression which is critical for proper brain architecture (Schmid and Anton, 2003). β_1 integrin is the central player in integrin mechanisms in the brain and ablation of β_1 subunit causes severe developmental perturbations of cortical and cerebellar structures (Graus-Porta *et al.*, 2001). While $\beta_3, \beta_5, \beta_6, \beta_7$ and β_8 integrin subunits are also expressed throughout the brain, leukocyte specific β_2 integrin was not detected in neurons (Schmid and Anton, 2003; Nieuwenhuis *et al.*, 2018). While earlier studies reported an exceedingly rare β_4 integrin labelling in neurons, further studies implicated its expression with reactive oxygen species in neurons (Pinkstaff *et al.*, 1999; Su *et al.*, 2007). Among α integrins, all subunits are expressed in the neurons except for leukocyte specific alpha integrins (as αL, M, X, D and E), α_{10} and α_{11}. Lastly, α_9 can be detected in glial cells and not in neurons (Schmid and Anton, 2003; Nieuwenhuis *et al.*, 2018).

During brain development, neural stem cells divide into undifferentiated progenitors which then produces the glia and neurons (Gage, 2000). Several studies have found that integrin β_1 can be used as a marker as it is enriched in neural stem cells and integrin β_1 mediated MAPK (mitogen activated protein kinase) signaling is critical for neural stem cell function (Campos *et al.*, 2004; Hall *et al.*, 2006). Besides, lack of integrin β_1 results to a significant reduction of neural stem cell proliferation and decreases the lifespan of produced neurons (Leone *et al.*, 2005). As in for cerebral

development, proliferation of granule cell precursors in developing cerebellum is also severely impaired in β_1 integrin CNS (central nervous system) KO mice (Blaess *et al.*, 2004).

Neurons that are made from progenitor cells in ventricular/subventricular zones then migrate tangentially and radially to their final destinations (Buchsbaum and Cappello, 2019). Earlier studies showed that injection of antisense RNAs against β_1 integrin resulted in to neural migration deficiencies in chicken optic tecta (Galileo *et al.*, 1992). Interestingly, despite its indispensable role in cortical development, β_1 integrin ablation in excitatory cells (using Emx1 promoter) did not affect the hippocampal morphology while severe cortical lamination defects were reported (Huang *et al.*, 2006). Later on, by using integrin blocking antibodies, it has been shown that different α integrin subunits also have distinct roles during neuronal migration: While α_3 integrins are necessary for glia-neuron recognition during initial steps of neuronal migration; αV integrins are needed to provide necessary adhesion between the glial fiber and the migrating neuron (Anton, Kreidberg and Rakic, 1999). Besides CNS, integrins are also required for migration of PNS neurons derived from neural crest, as neural crest specific integrin β_1 KO mouse models display severe defects in peripheral nervous system development (Pietri *et al.*, 2004). Even in adult brain, which neural progenitor cells that are located in the ventricular/subventricular zone still produce new neurons, β_1 integrins support the migration of new immature neurons towards to injury sites in post-stroke brain to replace the damaged cells (Fujioka *et al.*, 2017).

Neurons are highly polarized cells, and their neurite outgrowth is tightly controlled, mainly via ECM ligands acting on integrin receptors. Several early studies have already revealed that $\alpha_1\beta_1$, $\alpha_3\beta_1$ and $\alpha_6\beta_1$ heterodimers mediate neurite growth of sympathetic neurons by interacting with the neural ECM (Tomaselli *et al.*, 1993; DeFreitas *et al.*, 1995; Weaver *et al.*, 1995). $\alpha_8\beta_1$ integrins on

neurons can also bind to Tenascin-C, another important neural ECM molecule that is associated with neurite outgrowth (Varnum-Finney *et al.*, 1995). A number of other studies also demonstrated that activation of β_1 integrins promotes the neurite outgrowth of neurons using β_1 ligands such as laminins and semaphorins (Pasterkamp *et al.*, 2003; Moresco *et al.*, 2005; Tucker, Rahimtula and Mearow, 2005). Interestingly, loss of responsiveness to ECM ligands and in late embryonic neurons can be rescued by increasing integrin receptor activity (for instance via divalent cations) and this rescue is sensitive to β_1 integrin blocking (Ivins, Yurchenco and Lander, 2000). These findings suggest a developmental decrease in activity of integrin receptors in CNS, which could explain the decreased regeneration of CNS neurons over time. Even on chondroitin sulphate proteoglycan ligand, which accumulates at nerve injury sites and inhibits regeneration, forced activation of integrins via divalent cations or activating antibodies can overcome the inhibitory effect and can improve the axon regeneration (Tan *et al.*, 2011). β_1 integrin heterodimers are also implicated in dendritic stability, as inactivation of β_1 integrins causes rapid dendritic retractions and loss of distal filopodia dynamics (Marrs *et al.*, 2006).

Besides neurite extension and stability, integrin receptor activity can promote spine maturation and stability (Shi and Ethell, 2006; Bourgin *et al.*, 2007; Ning *et al.*, 2013). Because of their involvement in spine dynamics, blocking the integrin β_1 activity results in impaired synaptic responses and decay of LTP both in mouse and rat models (Chun *et al.*, 2001; Huang *et al.*, 2006). As expected from its role in dendritic morphogenesis and spine maturation, neuron specific ablation of integrin β_1 reduces synaptic density and impairs novel object recognition and working memory tasks in mouse models (Chan *et al.*, 2006; Warren *et al.*, 2012).

Overall, the past twenty years have seen numerous studies suggesting that integrin receptors play an important role during brain development due to its role in neurite extension and are critical in mature brain for signal transmission. However, while previous studies mostly consider outside-in signaling mechanisms at integrin binding sites for adhesion, recent evidence support the dynamic regulation of integrin signaling also through intracellular regulatory proteins. These molecules regulating the integrin inside-out signaling range from protein phosphatases such as PP2A (Liu *et al.*, 2016) to scaffold proteins such as Talin and ADAP (Tan *et al.*, 2015; Thiere *et al.*, 2016). Previous work from our group has further identified Ndr2 kinase, a novel member of Hippo pathway signaling (Hergovich, 2016), as an intracellular modulator of β_1 integrin activity and surface expression (Rehberg *et al.*, 2014).

1.2 Ndr2 Kinase

Protein kinases are the key regulators of cellular processes and act as modulatory switches on their target proteins. Kinases can affect localization, stability and activity of their substrates by adding phosphate groups on either Serine, Threonine or Tyrosine residues. Until now, over 500 different kinases have been discovered in humans and human kinome can be clustered 8 main groups: AGC (Protein kinase A,G,C families), CAMK (Calcium regulated kinases), CK1 (Cell kinases), CMGC (CDK-MAPK-GSK3 and CLK families), STE (STE homologs family), TK (Tyrosine kinases), TKL (Tyrosine kinase-like) and RGC (Receptor guanylate cyclase) (Manning *et al.*, 2002). Kinases are clustered in these subgroups mainly due to their sequence homology and evolutionary conversation, whereas their functions are also considered. Lastly, kinases without any structural similarity to any main families are grouped into Atypical kinases family.

1.2.1 Ndr2 kinase: Structure and Homologs

The AGC kinase family contains around 60 members that are implicated in diverse cellular functions. Their malfunction can result to many diseases such as cancer and diabetes (Pearce, Komander and Alessi, 2010). Some members of the AGC kinase family are the protein kinase A, protein kinase G, protein kinase C, Akt, RSK and nuclear Dbf2 related kinases (Pearce, Komander and Alessi, 2010).

Ndr2 (nuclear Dbf2 related-2) kinase (also known as serine/threonine kinase 38-like protein, STK38l) belongs to the nuclear Dbf2 related (NDR) kinases along with Ndr1 and Lats1/2. While Ndr1 and Ndr2 are very close homologs, both Lats and Ndr kinases are under control of Hippo pathway, which mainly controls cell proliferation (Gógl *et al.*, 2015). Conserved homologs of mammalian Ndr2 is also present in other species: As its name refers (nuclear Dbf2 related), Dbf2p is the Ndr2 homolog present in yeast (Frenz *et al.*, 2000). Ndr2 homologs Tricornered (Trc) and Sax-1 are also widely studied in Drosophila and C. elegans species respectively (Zallen *et al.*, 2000; Emoto *et al.*, 2006). Although they are close isoforms, previous studies have shown that Ndr2 is the primary Ndr kinase in mouse brain and Ndr1 protein was not detected in neither cortex nor hippocampus tissue from mice (as opposed to rats) (Cornils *et al.*, 2010; Rehberg *et al.*, 2014).

Catalytic core of Ndr2 consists of 12 kinase domains that is also conserved among other AGC kinases (Hanks and Hunter, 1995) (Figure 2). Different than other of AGC kinases, an N-terminal regulatory motif (NTR) is also present in Ndr2. This motif contains a Threonine residue (T^{75}) which is absent in lower organisms such as S. cerevisiae's Dbf2p (Stegert *et al.*, 2004). Moreover, the NTR domain contains a stretch of hydrophobic amino acids where S100B and Mob proteins can interact with Ndr2 kinase (Millward *et al.*, 1998; Bichsel *et al.*, 2004).

Another conserved phosphorylation domain is present at Serine^{282} which is between catalytic domains VII and VIII. This subdomain is also referred as activation segment (AS) of Ndr2 (Hergovich *et al.*, 2006). N-terminal of the AS is known as autoinhibitory segment (AIS), a 30-60 amino acid stretch enriched with basic amino acids (lysine and arginine) that reduces the catalytic activity of the Ndr2 kinase (Bichsel *et al.*, 2004). Recently, it has been shown that deletion of AIS from Ndr1 increases Ndr association with its activators thus stimulates its kinase activity (Xiong *et al.*, 2018). AIS also acts as a nuclear localization signal in Ndr1 kinase, a close homolog of Ndr2 that mainly localized in nucleus (Millward, Cron and Hemmings, 1995).

Lastly, at the C-terminal of Ndr1/2 kinase, a hydrophobic motif (HM) can be found that is conserved among AGC kinases. The HM domain contains a Threonine^{442} phosphorylation site that is important for the Ndr2 catalytic activity (Stegert *et al.*, 2005).
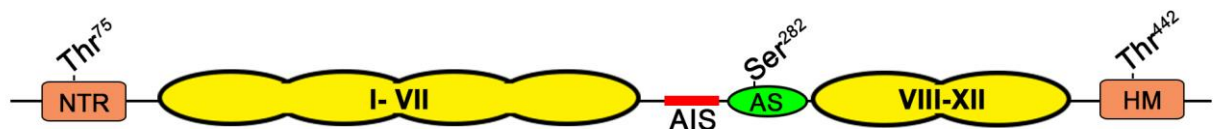
Figure 2: Structure of Ndr2 kinase.
Catalytic core of Ndr2 consists of 12 subdomains surrounded by a N-terminal regulatory domain (NTR) and C-terminal hydrophobic domain (HM) (Rehberg et al., 2014). NTR contains the Thr^{75} residue that is important for Ndr2 activity. Moreover, Ndr2 regulators S100B and Mob can also interact with NTR domain. Thr^{442} residue, another important switch for Ndr2 activity, can be found on HM. Lastly, activation segment (AS) containing Ndr2 autophosphorylation target residue (Ser^{282}) is located between subdomains VII and VIII. Upstream of AS compromises autoinhibitory segment (AIS), which the release of the catalytic inhibition depends on association of Ndr2 activators.

1.2.2 Regulation of Ndr2 kinase activity

The N-terminal regulatory domain (NTR), which is unique to Ndr kinases in the AGC kinase family, is important for the activation state of Ndr2. S100B, a Ca^{2+} binding EF-hand protein, can directly bind to NTR of Ndr2. This interaction increases the phosphorylation of Serine^{282} on

activation segment and Threonine[442] on C-terminal hydrophobic motif. Importantly, S100B mediated Ndr2 activation is calcium dependent, thus connecting Ndr2 catalytic activity to intracellular calcium concentration (Tamaskovic *et al.*, 2003). Besides S100B, Mob1 also binds to NTR of Ndr2 and acts as a co-activator by releasing the autoinhibition from the AIS subdomain (Bichsel *et al.*, 2004). Mst1 and Mst2 phosphorylation of Mob1 co-activator can also affect the affinity of Mob1 for the NTR domain (Ni *et al.*, 2015; Kim *et al.*, 2016). Due to its binding to S100b and Mob1 co-activator proteins, NTR domain of Ndr kinases is also known as S100B/hMob1 association domain (Hergovich *et al.*, 2006).

Serine[282] on activation segment (AS) and Threonine[442] on hydrophobic motif (HM) are the main regulatory sites of Ndr2 kinase. Interestingly, Serine[282] site is not the main target of upstream kinases but rather it is auto phosphorylated by Ndr2 after activation. Threonine site on the N-terminal regulatory domain (Threonine[75]) is also important as its T75A mutations significantly decreases Ndr2 catalytic activity (Stegert *et al.*, 2004).

Threonine[442] on HM is the main target of the upstream kinases on Ndr2, which increases its catalytic activity upon phosphorylation. Previous studies showed that Ste20-like kinases can act upstream of Ndr2 homologs in other organisms: for example, in Saccharomyces cerevisiae, Ste20-like kinase Cdc15p can phosphorylate Dbf2p on Serine[374] and Threonine[544] (Mah, Jang and Deshaies, 2001). In the same line, mammalian Ste20-like kinase Mst3 can selectively phosphorylate Threonine[442] on Ndr2 kinase and increase its kinase activity up to 10-fold (Stegert *et al.*, 2005). Another follow-up study also reported that Mst1 kinase phosphorylates Threonine[442] and activate Ndr2 upon TNFα stimulation (Vichalkovski *et al.*, 2008).

Overall, previous studies suggest that binding of co-activators such as Mob1 to N-terminal of Ndr2 kinase induces its activity by releasing the auto-inhibitory mechanisms. The Threonine[442] at the C-terminal is the main switch for the Ndr2 activity and can be phosphorylated by upstream Mst kinases whereas auto-phosphorylation of Serine[282] on the activation segment is also critical for full Ndr2 activity. Involvement of Mst kinases and Mob proteins for the Ndr2 activation also indicates the importance of Ndr2 kinase in Hippo pathway, a highly conserved tumor suppressor pathway that regulates proliferation and tissue growth (Hergovich, 2016).

1.2.3   Functions of Ndr2 kinase in neurons

Neuronal tiling is an important process during circuit formation as it allows neurons to extend neurites to innervate a subfield with minimal overlap, via extension and retraction dynamics (Cameron and Rao, 2010). Ndr homologs Sax-1 and Sax-2 are important in tiling of mechanosensory neurons during C. elegans nerve development. While Sax mutants fail to slow down neurite growth and inhibit tiling, Sax overexpression leads to early neurite termination and impair neurite growth (Gallegos and Bargmann, 2004). Another study also reported that Sax-1 mutant neurons have enlarged somas and excess neurites suggesting a crucial role for Ndr2 in neuronal shape (Zallen et al., 2000). Similarly, Ndr homolog Trc in Drosophila contributes to the dendritic arborization during neuronal tiling of class IV neurons (Emoto et al., 2006). Same study also demonstrated that Trc mediated neurite tiling in Drosophila is controlled by Hippo signaling pathway.

Analysis of gene expression changes in mouse amygdala has led to identification of Ndr2 kinase during an mRNA screen after fear conditioning. Ndr2 expression was significantly increased in amygdala 6 hours after Pavlovian conditioning and returned to baseline levels within 24 hours

(Stork *et al.*, 2004). Furthermore, Ndr2 mRNA was also detected in several brain regions and associated with actin cytoskeleton in soma, neurites and spines in subcellular level (Stork *et al.*, 2004). In the same study, neurite outgrowth of rat pheochromocytoma (PC12) cells were significantly increased by Ndr2 overexpression, which indicates a similar role of Ndr2 in mammalian neurons as in lower organisms. In addition, another group reported that mammalian Ndr kinases are required for the polarity of hippocampal neurons and Ndr loss of function results to mutant neurons with ectopic axons (Yang *et al.*, 2014). Accordingly, it was demonstrated that Ndr2 is required for hippocampal dendritic development and loss of Ndr2 results to arbor specific impairments and premature branching in the hippocampus of Ndr2 deficient transgenic mice and rats (Ultanir *et al.*, 2012; Rehberg *et al.*, 2014). By addressing the cellular mechanisms of Ndr2 mediated dendritic growth, it was shown that Ndr2 is involved in inside-out signaling of β_1 integrins by modulating its trafficking to the surface and activity state (Rehberg *et al.*, 2014).

Both the transient increase of Ndr2 mRNA expression in amygdala after fear conditioning (Stork *et al.*, 2004) and control of β_1 integrin activity by Ndr2 kinase (Rehberg *et al.*, 2014; Demiray *et al.*, 2018) suggested an important role for Ndr2 in memory consolidation. Therefore, how Ndr2 kinase might affect synaptic processes, signal transmission and memory formation in mouse hippocampus has been under investigation. On-going studies have demonstrated a significant reduction of PSD95 labelling in Ndr2-deficient hippocampal neurons which can be rescued by re-expression of Ndr2. Moreover, Golgi-Cox staining of the Ndr2 KO mice revealed decreased spine density on both apical and basal CA1 dendrites of hippocampus compared to the wild type mice (Atsuhiro Tsutiya & Oliver Stork, unpublished data). Accordingly, electrophysiological characterization of the Ndr2 KO mice demonstrated a deficit in long term potentiation in CA1 area (Hussam Hayani & Alexander Dityatev, personal communication). Finally, behavioral analysis of

these mutants revealed impairments in water cross maze task, a spatial learning paradigm dependent on CA1 area of hippocampus (Kul Madencioglu, 2019- Doctoral Thesis). Collectively, these on-going studies indicate that Ndr2 kinase is critical for spine formation and signal transmission in the hippocampus and identify a novel role of Ndr2 in learning and memory.

1.2.4 Role of Ndr2 in neurite extension of PC12 cells

PC12 cells are originated from rat pheochromocytoma cell line and can be maintained in a routine cell culture either in an immortalized proliferative state or in a differentiated state (into sympathetic neuron-like morphology with extended neurites) after addition of NGF. Despite originating from rat adrenal medulla, these cells are extensively used in neurite-growth assays due to their ease of cell culturing, genetic manipulation and pharmacological/extracellular matrix assays (reviewed in Wiatrak *et al.*, 2020).

Previous research has shown that Ndr2 kinase controls integrin dependent dendritic and axonal growth in mouse hippocampal neurons (Rehberg *et al.*, 2014). However, how extracellular substrates and Ndr2 mediated morphology may interact via integrin heterodimers had not been examined. To investigate the role of Ndr2 kinase in neurite growth on different substrates, a previously established EGFP-Ndr2 stable-transfected PC12 cell line (Ndr2 PC12) was used along with EGFP transfected PC12 cells as controls (EGFP PC12) (Stork *et al.*, 2004). These cells were seeded on different substrates (such as collagen IV, laminin, fibronectin etc.) and treated with NGF (nerve growth factor) to analyze their neurite growth (in cooperation with Dr. Kati Rehberg, Demiray *et al.*, 2018). Both cell lines showed efficient neurite formation in which >98% of cells showed discernible neurites on both PDL (poly-D-lysine) and collagen IV. Laminin was also efficient at inducing neurite formation both cell lines, whereas fibronectin, gelatin and collagen I

was less favorable where only less than 50% of control PC12 cells displayed neurites (Figure 3A). Moreover, on those less efficient substrates, Ndr2 PC12 cells displayed significantly higher proportion of cells with neurites compared to EGFP PC12 (Figure 3A, two way ANOVA genotype x substrate interaction $F_{(5,24)}= 4.575$, $p= 0.0045$). To test any differences in neurite extension by Ndr2, cells were further analyzed for neurites extending beyond 100 μm. For neurite extension, PDL, laminin and collagen IV substrates were selected since they resulted to almost complete neuronal differentiation in both cell lines. As in measure of cells with neurites, Laminin did not cause a significant difference in proportion of cells bearing >100μm neurites between EGFP and Ndr2 PC12 cells (Figure 3B; on Laminin: $X^2_{(1)}= 0.1364$, $p= 0.71$). On PDL, Ndr2 PC12 line showed significantly higher proportion of cells bearing long neurites (**Error! Reference source not found.**Figure 3B; on PDL: $X^2_{(1)}= 4.276$, $p< 0.05$). On the other hand, on collagen IV substrate, Ndr2 PC12 cells displayed significantly reduced neurite extension compared to control cells (Figure 3B; on Col IV: $X^2_{(1)}= 81.45$, $p< 0.001$). Therefore, PDL and collagen IV substrates were tested in further experiments to examine how Ndr2 kinase affects this substrate specific control of neurite extension.
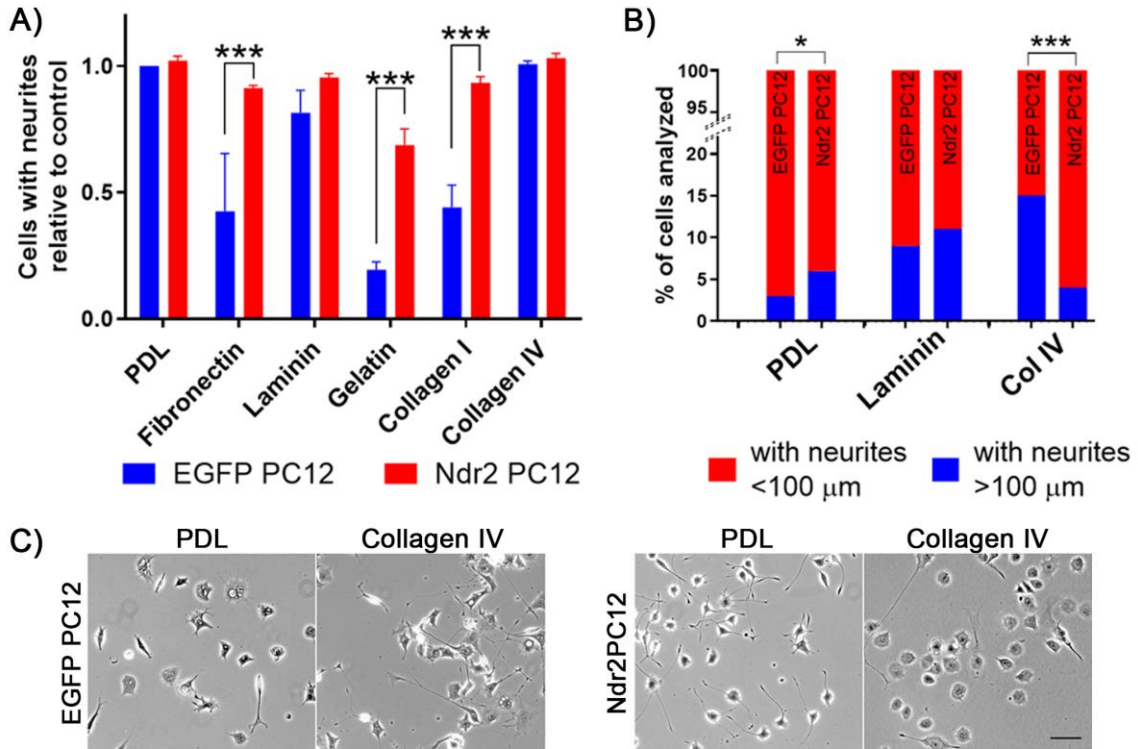
Figure 3: Substrate specific control of neurite outgrowth of PC12 cells via Ndr2 kinase.
(A) While number of cells with neurites did not change between control and Ndr2 PC12 cells on PDL, Laminin and Collagen IV substrates; Ndr2 PC12 cells showed significantly higher proportion of cells with neurites on Fibronectin, Gelatin and Collagen I substrates (two way ANOVA genotype x substrate interaction $F_{(5,24)}= 4.575$, $p= 0.0045$). **(B)** Furthermore, when cells bearing neurites at least 100 μm long are analyzed, Ndr2 PC12 cells show higher proportion of cells having long neurites on PDL ($X^2_{(1)}= 4.276$, $p< 0.05$). However, Collagen IV substrate fails to stimulate neurite extension in Ndr2 PC12 cells while this enhancement is evident in control EGFP PC12 cells ($X^2_{(1)}= 81.45$, $p< 0.001$). (**C**) Representative microscopy images of EGFP and Ndr2 PC12 cells after NGF treatment on PDL and Collagen IV substrates, displaying morphological differences. Values are mean± SEM; N= 3; *$p< 0.05$; ***$p< 0.001$. Scale bars: 100 μm (in cooperation with Dr. Kati Rehberg, Demiray *et al.* 2018).

$\alpha_1\beta_1$ integrin heterodimers are one of the main receptors on the surface that recognizes and responds to collagens, especially collagen type IV substrate (Carmeliet, Himpens and Cassiman, 1994). To identify the processes underlying the growth deficiency on Collagen IV by Ndr2 kinase; control and Ndr2 PC12 cells were tested either with general integrin receptor stimulation (Mg^{2+}) or with a KTS ligand (obtustatin) specific to $\alpha_1\beta_1$ integrin heterodimer on both substrates (in cooperation with Dr. Kati Rehberg). When cells were analyzed for extended neurites, a significant

interaction between Ndr2 expression, integrin stimulation and coating substrate (three way ANOVA genotype x substrate x treatment interaction $F_{(2,24)}= 19.16$, $p< 0.0001$) were observed. Moreover, neurite extension between Ndr2 genotypes on different substrates revealed a significant difference between treatments (genotype on substrates x treatment interaction $F_{(6,24)}= 41.05$, $p< 0.0001$) (Figure 4). Under NGF-only treatment, a significant enhancement of neurite growth by collagen IV substrate was observed in EGFP PC12 cells as previously. However, Ndr2 PC12 cells again failed to enhance growth on collagen IV coating. Next, Mg^{2+} ions were used as a divalent cation to increase general affinity of integrin receptors via MDIAS (Luo, Carman and Springer, 2007; Nunes *et al.*, 2018). Under NGF+ 0.3mM Mg^{2+} treatment, EGFP PC12 cells again showed an increased neurite growth on Collagen IV substrate. While Ndr2 PC12 cells under Mg^{2+} treatment also increased neurite growth regardless of the substrate; they remained significantly lower than EGFP PC12 cells on collagen IV, re-iterating the deficiency of collagen IV mediated neurite extension in Ndr2 PC12 cells. In order to specifically address the role of $\alpha_1\beta_1$ integrin receptor in PC12 neurite extension, a synthetic KTS ligand peptide (CW**KTS**LTSHYC) was applied on control and Ndr2 PC12 cells (Marcinkiewicz *et al.*, 2003; Moreno-Murciano *et al.*, 2003). This specific stimulation of $\alpha_1\beta_1$ integrin receptor via KTS peptide resulted the maximal growth of EGFP PC12 cells on both substrates. In Ndr2 PC12 cells, however, $\alpha_1\beta_1$ integrin agonist KTS ligand entirely failed to induce neurite growth on any substrate; in spite of the previously shown increase in β_1 integrin phosphorylation and surface expression (Rehberg *et al.*, 2014), (Figure 4). Overall, this data indicated a substrate specific growth deficiency in Ndr2 PC12 cells which is likely to involve α_1 integrin regulation during differentiation.
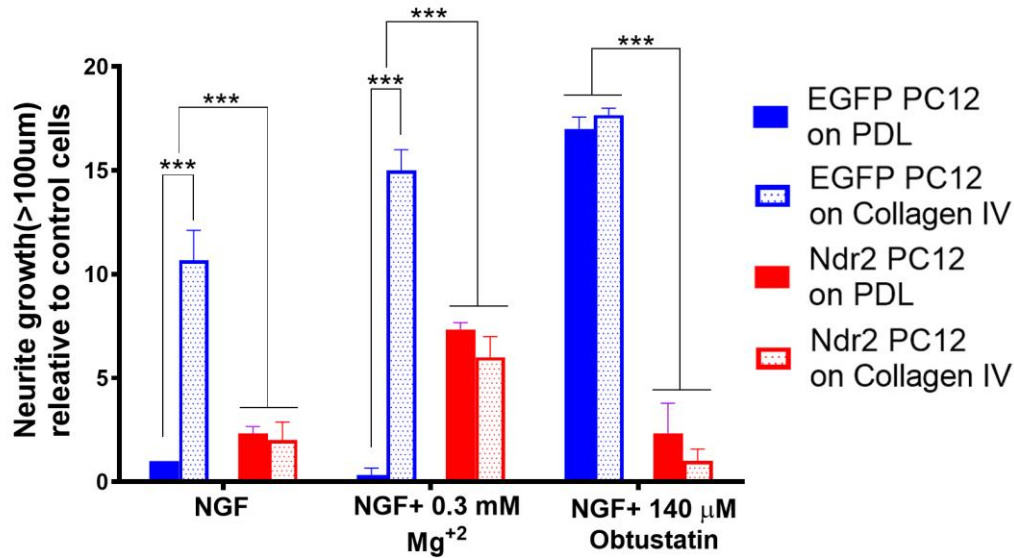
Figure 4: Lack of $\alpha_1\beta_1$ integrin receptor activation in Ndr2 overexpressing PC12 cells.
Under NGF only, Collagen IV substrate stimulated a significant enhancement in neurite extension only in control and not in Ndr2 PC12 cells. General enhancement of integrin mediated adhesion by 0.3 mM Mg^{2+} somewhat increases the neurite growth in Ndr2 PC12 cells, however, still significantly below the proportion of neurite extended EGFP PC12 cells on Collagen IV. The synthetic KTS peptide obtustatin induces neurite growth in control cells on PDL to the same high levels as in Collagen IV. On the other hand, $\alpha_1\beta_1$ integrin ligand did not stimulate neurite growth of Ndr2 PC12 cells on neither substrate. To summarize, $\alpha_1\beta_1$ integrin stimulation by either with Collagen IV or KTS ligand obtustatin only stimulates growth in EGFP PC12 and not in Ndr2 PC12 cells (two way ANOVA: genotype on substrates x treatment interaction $F_{(6,24)}= 41.05$, $p< 0.0001$). Values are mean± SEM; N= 3; ***$p< 0.001$. (in cooperation with Dr. Kati Rehberg, Demiray e*t al.* 2018).

Despite the fact that previous studies have shown that Ndr2 induces β_1 integrin Thr^{788}/Thr^{789} phosphorylation, in vitro kinase assays demonstrated no evidence of direct phosphorylation of β_1 integrins by Ndr2 (Rehberg *et al.*, 2014). We have recently identified Filamin A as a downstream substrate of Ndr2 kinase (Figure 13, Figure 14, Appendix Figure 43), which can modulate β_1 integrin activity therefore might be involved in Ndr2 mediated inside-out integrin signaling in neurons.

1.3 Filamin A

Most eukaryotic cells have a highly polarized shape and finely tuned movements as a consequence of their cytoskeleton dynamics. Cytoskeleton provides this mechanical support through three major classes of fibers: Microtubules are the largest filament with 25 nm diameter, intermediate filaments are around 10 nm and microfilaments are the smallest sized filaments with 6 nm diameter (O'Connor, Adams and Fairman, 2010). Microfilaments consist of highly conserved actin monomer subunits, which in fact makes it the most abundant protein in eukaryotic cells. Microfilaments are very dynamic structures that undergo constant polymerization/depolymerization, which is the main, but not the only way to maintain its flexibility (Dominguez and Holmes, 2011). Besides actin treadmilling, interaction of actin-binding-proteins with microfilaments can further modify the actin cytoskeleton. For instance, actin filaments can be bundled together by Fimbrin to form tightly packed filaments (Glenney, Kaulfus and Weber, 1981), form multiple branches via Arp2/3 nucleation (Goley and Welch, 2006) or assemble into networks through Filamin mediated cross-linking (Popowicz *et al.*, 2006).

In early 1970s, two independent group successfully purified a cytoskeletal accessory protein from both muscle and non-muscle cells. It was simultaneously named as actin-binding-protein 280 due to its large size and Filamin since it was found to associated with actin filaments (Hartwig and Stossel, 1975; Wang, Ash and Singer, 1975; Baldassarre and Calderwood, 2018). In the past four decades of research, Filamin A has been extensively studied regarding with respect to its actin-binding features, involved signaling pathways and surface receptor interactions.

1.3.1 Structure of Filamin A

Filamin has three isoforms in humans that are encoded by three different genes, referred as Filamin A (FlnA), Filamin B and Filamin C. All three isoforms share around 70% homology between their

sequences except their loop domains which is more divergent (around 55%). Among different isoforms, Filamin C is mostly restricted in striated muscle cells. While FlnA and Filamin B are ubiquitously expressed in variety of tissues such as bone, kidney and skin cells; FlnA is the more dominant isoform in brain tissue (van der Flier and Sonnenberg, 2001; Hu *et al.*, 2017).

FlnA protein, also referred as actin binding protein 280 or Filamin-1 in earlier studies, is encoded by the gene on X chromosome (Xq28, NCBI GeneID: 2316) (Gariboldi *et al.*, 1994). It is a homodimer consists of two 280 kDA subunit which forms a V-shaped structure (Figure 5). Each subunit is around 2691 amino acid long and contains 24 immunoglobulin-like tandem repeats (Ig). Each repeat-domain is ≈96 amino acid long and divided with two hinge domains (≈34 amino acids) that are located between Ig 15-16 and Ig 23-24. These hinge domains provide further flexibility to the overall FlnA structure (Yue, Huhn and Shen, 2013). N-terminal of FlnA protein contains an actin-binding-domain (ABD) that is ≈275 amino acid long and resembles the ABD of other cytoskeleton accessory proteins such as alpha-actinin (van der Flier and Sonnenberg, 2001). On the C-terminal, last ≈60 amino acids function as the dimerization domain (Ig 24) for the FlnA subunits, which confers the V-shape of the overall protein and plays a crucial role in FlnA-induced actin gelation (Nakamura *et al.*, 2007).
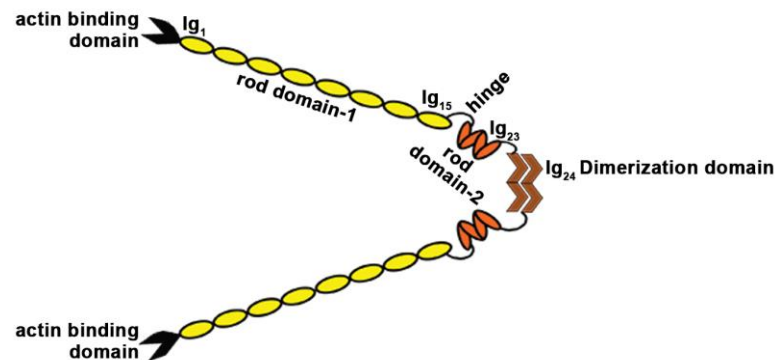
Figure 5: Structure of FlnA
Two identical subunits consisting of 24 immunoglobulin-like repeats (Ig) are dimerized at Ig_{24} and result to mature FlnA protein. These 24 tandem repeats are divided by two hinge domains after Ig_{15} and Ig_{23}. N-terminal of the protein contains the actin binding domain. Rod-domain-2 closer to the tip of V-shape structure is also the main substructure that can interact with other proteins such as integrin receptors (Yue *et al.*, 2013).

1.3.2   Regulation of Filamin A expression and activity

During brain development, FlnA serves critical roles due to its interaction with cytoskeleton and membrane receptors (see section 1.3.3), therefore it is highly expressed throughout all cortical layers (Sheen *et al.*, 2002). While its expression subsequently downregulated postnatally in mature brains (Fox *et al.*, 1998), FlnA can still be detected in adult brains and serve important functions to regulate membrane receptor dynamics (Petrecca, Miller and Shrier, 2000; Wang, Frankfurt and Burns, 2008). Moreover, in-depth characterization of FlnA in adult rat brain revealed an intense labelling of FlnA in pyramidal neurons in neocortex, hippocampus and basolateral amygdala along with other basal forebrain nuclei (Noam *et al.*, 2012). Subcellular analysis of FlnA immunoreactivity exhibits FlnA puncta in soma and dendrites while labelling in dendritic spines could not detected in early studies (Nestor *et al.*, 2011; Noam *et al.*, 2012). However, using a high-resolution structured illumination microscopy and YFP-filled neurons for better spine visualization, a recent study reported a prominent FlnA labelling on dendritic spines of hippocampal neurons (Segura *et al.*, 2016).

Due to its function as a bridge between actin cytoskeleton and ECM receptors, FlnA expression levels can also be controlled by external mechanical force applied on cells. Mechanical force induces p38 mitogen activated kinase redistribution, which in turn phosphorylates Sp1, a zinc finger transcription factor. This results to transcriptional activation FlnA gene due to the Sp1-binding sites on its promoter (D'Addario *et al.*, 2002). Next to its expression levels, external mechanical stimuli also affect FlnA activity by modulating its overall flexible structure. FlnA

interacts with its association partners mostly via domains located between hinge 1 and hinge 2 (Figure 5). β-sheet repeats that are responsible for this interaction can be masked and auto-inhibited due to overall conformation of FlnA domains. Applied mechanical forces can alter FlnA conformation and expose these hidden binding sites on FlnA (especially between Ig 16-24) (Pentikäinen and Ylänne, 2009). This force-activatable characteristics of FlnA can rapidly change upon stimuli and plays an important role controlling the FlnA-β_1 integrin binding dynamics (Ehrlicher *et al.*, 2011; Rognoni *et al.*, 2012).

Phosphorylation is a crucial posttranslational mechanism that can regulate the function of downstream targets by changing their overall conformation, kinetic activity or cellular localization/stability. FlnA is a substrate of several protein kinases and the Serine residue at 2152 (S2152) in Ig-repeat-domain 20 is the main target of the kinases (see below). Phosphorylation status of S2152 is an important modulator of FlnA function by affecting its stability, interaction-partners and cellular localization.

Protein kinase A (PKA), a cAMP dependent protein kinase, phosphorylates FlnA on S2152 in the presence of cAMP-elevating agents such as forskolin and isobutyl methylxanthine (Jay, García and de la Luz Ibarra, 2004). Moreover, this PKA-mediated phosphorylation can protect FlnA from proteolysis, especially from calpain cleavage (Chen and Strachers, 1989). Calpains are calcium-dependent proteases which can bind and cleave the FlnA from both hinge domains. This cleavage produces a 190 kDA fragment (repeats 1-15) and 90 kDA fragment (repeats 16-23) (Dyson *et al.*, 2003). Interestingly it has been also shown that the smaller cleaved fragment can still be transported into nucleus and can interact with transcription factors, such as transactivated androgen receptors (Loy, Sim and Yong, 2003). S2152 of FlnA is also subjected to dephosphorylation by calcineurin,

a calmodulin dependent serine/threonine phosphatase, which can mediate calpain-induced proteolysis of FlnA (García, Stracher and Jay, 2006).

Besides PKA, protein kinase C (PKC), a family of phospholipid dependent kinases, can also phosphorylate FlnA on S2152 and regulate FlnA-actin interactions in membrane invaginations (Muriel *et al.*, 2011). The PKC mediated FlnA phosphorylation has shown to be isoform specific: only FlnA and FlnC can be phosphorylated by PKC while FlnB is not a substrate (Tigges *et al.*, 2003). Ribosomal S6 kinase (RSK) is an important member of Ras-mitogen activated kinase pathway and can be activated by MAPK/Erk activity. It has been shown that RSK phosphorylates FlnA on S2152 in response to growth factors such as EGF (Woo *et al.*, 2004). It has also been reported that a well-known carcinogen, trivalent Arsenic (As^{3+}), activates Akt kinase which in turn phosphorylates FlnA on S2152 (Li *et al.*, 2015). Recently, studies in T-cells showed that Ndr2 kinase phosphorylates S2152 on FlnA upon T-cell receptor stimulation and induce the disassociation of FlnA from integrin LFA-1 receptors (Waldt *et al.*, 2018). The phosphorylation status of S2152 also determines the subcellular localization of FlnA protein. By expressing either phosphodeficient (S2152A) or phosphomimetic (S2152D) FlnA in neuroblastoma cells, it was demonstrated that S2152A FlnA prominently localized around the cell membrane and overlapped with actin fibers where S2152D FlnA was more uniformly diffused throughout the cytoplasm (Zhang *et al.*, 2012).

Overall, all these upstream kinases that act on S2152 affects the stability of the full protein (Chen and Strachers, 1989; García, Stracher and Jay, 2006), can change the steric hindrance on the C-terminal of FlnA which in turn affects its affinity for interaction partners such as integrin receptors in a cell type specific manner (Chen, Kolahi and Mofrad, 2009; Waldt *et al.*, 2018) or controls the

localization of the protein in the cells with respect to actin cytoskeleton (Muriel *et al.*, 2011; Zhang *et al.*, 2012).

1.3.3   Functions of Filamin A

1.3.3.1   Filamin A and integrin receptors

As mentioned in section 1.1.3, various studies have demonstrated the role of integrins in dendrite and axon growth (Pasterkamp *et al.*, 2003; Moresco *et al.*, 2005; Marrs *et al.*, 2006). These growth processes are under tight control by integrins, which regulate the dendritic/axonal growth in response to both intrinsic (inside-out) and extrinsic signals (outside-in signaling) (Hynes, 2002). In fact, researchers have found that FlnA can interact with β integrin subunits such as β_1, β_2, β_3 and β_7 (Sharma, Ezzell and Arnaout, 1995; Loo, Kanner and Aruffo, 1998; Travis *et al.*, 2004, Donada *et al.*, 2019). Blocking the β_1 integrin activity in HEK cells reduced the localization of FlnA in cell extensions and silencing of endogenous FlnA impaired the spreading of cells on collagen coated surfaces, suggesting a crosstalk between FlnA and integrin functions (Kim *et al.*, 2008). FlnA-integrin interaction is also implicated in mechanotransduction of cells. External forces are sensed by integrin receptors and translated into local actin accumulations through PKC-mediated FlnA phosphorylation (Glogauer *et al.*, 1998).

Moreover, association of Talin to the integrin tails is one of the main activity markers of integrin receptors (Margadant *et al.*, 2012). FlnA competes for the binding to the same NPxY domains, therefore acts as a negative regulator of integrin activity (Kiema *et al.*, 2006; Nieves *et al.*, 2010). Increased FlnA binding to β integrin subunits also impair cell migration, due to impairments in integrin-dependent membrane protrusions (Calderwood, 2004). One mechanism that can displace FlnA from β_1 integrins is the Migfilin, a cytoskeletal adaptor protein that is enriched in integrin

adhesion sites. Researchers have shown that Migfilin can bind to FlnA and leads to its disassociation from integrin cytoplasmic tail therefore promotes integrin activation (Ithychanda *et al.*, 2009). Furthermore, FlnA can be disassociated from integrin receptors when phosphorylated by Ndr2 kinase on S2152. This dissociation is an important step in inside-out signaling of integrin receptors as it results to subsequent binding of activators such as Talin and kindlin to integrin cytoplasmic tail (Waldt *et al.*, 2018).

1.3.3.2   Filamin A and actin cytoskeleton

Filamin is a very efficient actin cross linker and can stabilize orthogonally branching filaments (Hartwig, Tyler and Stössel, 1980). Besides its high affinity ABD at N-terminal, secondary F-actin binding domains is also present along the rod-1, which provides a high avidity for F-actin binding (Nakamura, Stossel and Hartwig, 2011). A large and growing body of literature has investigated the importance of actin cytoskeleton dynamics in regulating shape and motility of the cells (summarized in Pollard and Cooper, 2009). Therefore, FlnA, as an important actin-binding protein, is also subjected in-depth analysis for its effects on cell spreading and motility. An early study that analyzed human malignant melanoma cell lines reported that in three (named as M1-3) out of seven independent malignant melonama lines showed impaired motility and did not grew any actin bundles (Cunningham *et al.*, 1992). Further protein analysis revealed that while there were not any significant alterations in the levels of actin-binding proteins such as gelsolin, α-actinin or profilin; FlnA protein was undetectable in lines M1 to M3 in which significant impairments of cell motility had been observed. This study was an important cornerstone in the FlnA research as the M2 cell line was later employed by numerous studies as FlnA-null model to study the role of FlnA in actin dynamics (often with cell line A7 as control, where FlnA cDNA is stably transfected into M2 line). For example, FlnA-null M2 cell line was used to demonstrate how lack of FlnA impairs active cell

stiffening and prevents actin remodeling in response to changes in extracellular matrix stiffness (Byfield *et al.*, 2009; Kasza *et al.*, 2009).

The deficiencies in actin mediated cell motility caused by FlnA loss is particularly focused in cancer research, as an approach to inhibit tumor migration and invasion, namely metastasis (Ji *et al.*, 2018). Re-expression of full length FlnA could rescue the migration impairments in Filamin deficient cells, however, re-expression of mutant FlnA lacking the Ig 19-21 was unable to recover neither cell spreading nor cell motility (Baldassarre *et al.*, 2009). It is worth noting that Ig 19-21 of FlnA are the C-terminal structures involved in integrin receptor association (Loo, Kanner and Aruffo, 1998; Travis *et al.*, 2004). These results suggest that, besides ABD at FlnA N-terminals, interaction of integrin and FlnA is also important for FlnA mediated actin dynamics. Actin cytoskeleton controls membrane shape and structure such as fast transitioning membrane ruffles or relatively stable membrane caveolae (invaginations). It has been shown that p21-activated kinase 1 (Pak1), an important serine/threonine kinase upstream of actin cytoskeleton, can phosphorylate FlnA on S2152 and mediates such membrane ruffling events that are important in cell shape and migration (Vadlamudi *et al.*, 2002). Similarly, PKC-dependent FlnA-S2152 phosphorylation and FlnA-actin interaction are required to maintain membrane caveolae dynamics (Muriel *et al.*, 2011). Lastly, it is also important the note that intracellular calcium levels can also affect the affinity of FlnA for the actin. Upon Ca^{2+} increase, calcium-bound calmodulin binds to FlnA ABD and disassociates FlnA from actin cytoskeleton (Nakamura *et al.*, 2005). Considering the prominent role of integrins on actin remodeling, FlnA thereby provides an important link downstream of integrin outside-in signaling to actin cytoskeleton.

1.3.3.3   Role of Filamin A in neurons

As explained above, FlnA is an important adapter between actin cytoskeleton and integrin receptors on the membrane, therefore of major interest for the development and function of the nervous system. In fact, mutations in the FlnA gene in humans result in Periventricular Heterotopia (PH), a neurological disorder that causes brain malformations caused by impaired neuronal proliferation and migration (Fox *et al.*, 1998; Lian and Sheen, 2015). Actin cytoskeleton plays an important role during neural progenitor proliferation, due to actin's role in mitosis. FlnA can also be phosphorylated by cyclin dependent kinase 1 in the beginning of the mitosis and phosphodeficient FlnA mutants impair cytokinesis after mitosis (Cukier, Li and Lee, 2007; Szeto *et al.*, 2015). In the same line, FlnA KO mice show prolonged cell cycle in neural progenitor cells which leads to reduced brain size (Lian *et al.*, 2012). As brain development progresses, neural progenitor cells start to divide asymmetrically to generate the post-mitotic neurons in subventricular zone. These neurons need to migrate along radial glial structures to reach their final destinations using actin cytoskeletal mechanisms (Lian and Sheen, 2015). At this embryonic stage, it has been shown that lack of FlnA disrupts cell adhesion and neuronal migration in a FlnA KO mouse model (Zhang *et al.*, 2013). As a side note, these transgenic mice are only viable for embryonic development studies since full body FlnA KO mice display high embryonic and early postnatal lethality, especially due to cardiac problems (Feng *et al.*, 2006). Interestingly, besides loss of FlnA, increased expression of FlnA or its S2152 phosphorylation also impair neuronal migration (Zhang *et al.*, 2012); suggesting a precise balance of FlnA expression for accurate FlnA function.

As they migrate from ventricular zone through cortical plates, post-mitotic neurons adopt a bipolar shape by extending leading neurite processes. A recent paper showed that FlnA and more importantly its ABD is required for this morphological transformation of newborn neurons (Kurabayashi *et al.*, 2018). Neuronal morphology is under tight control by extracellular factors that

30

are transmitted through integrin receptors and intracellular actin cytoskeleton dynamics. Therefore, it can reasonably be assumed that FlnA, a cytoskeletal bridge that can coordinate these intra and extracellular factors, plays an important role in neuronal morphology. Along this line, it was recently shown that both FlnA and its S2152 phosphorylation are increased in the neurons of TSC1 null mouse, a mouse model for tuberous sclerosis syndrome which is associated with abnormal dendritic complexity. Reducing the increased levels of FlnA in the TSC1 brains lowered the abnormal dendritic complexity and improved the neurophysiological abnormalities (Zhang *et al.*, 2014). Interestingly, same study also demonstrated that both overexpression and silencing of FlnA resulted to abnormal and more complex dendritic trees in olfactory bulb of mice in vivo. In line with its role in dendritic branching, it has also been shown that FlnA contributes axonal dynamics in neurons. Axons of motor neurons travel long distances from CNS to their target neuromuscular junctions and FlnA loss-of-function mutations impair this routing (Zheng *et al.*, 2011). Guidance of axons through this long distance is synchronized with extracellular guidance cues and receptors on growth cones. One important neuronal growth cue is Semaphorin 3a and FlnA S2152 phosphorylation is critical for Semaphorin-3a mediated actin dynamics in growth cones (Nakamura *et al.*, 2014). Moreover, it has been shown that nerve injury increases the FlnA expression in axons and interfering with FlnA function impairs injury-induced microtubule dynamics thus reduces axonal regeneration (Cho, Park and Cavalli, 2015). Besides neurite growth, FlnA contributes to the maturation of actin-rich dendritic spines as both silencing and overexpression of FlnA decreases the dendritic protrusion density and increases the protrusion length, resulting to a, immature spine phenotype (Segura *et al.*, 2016). These results indicate, yet again, how precise regulation of FlnA expression is needed both in neuronal migration, differentiation and maturation mechanisms.

However, the contribution of integrin receptors in these FlnA mediated neural differentiation mechanisms remained largely unexplored.

1.4 Aims of the study

Integrins are an array of heterodimeric surface receptors that can control the neurite growth based on extracellular ligands. Their surface expression and ligand affinity are under tight control and integrin receptors signal bidirectionally: binding to ECM proteins induces signaling cascades within the cell (outside-in signaling) while cytosolic accessory proteins that can bind the intracellular tail of integrins regulate its conformation and ECM ligand binding (inside-out signaling) (Bridgewater, Norman and Caswell, 2012). Previous evidence has suggested that Ndr2 kinase can modulate β_1 integrin inside-out signaling that affects β_1 integrin activity and consequentially neurite outgrowth of hippocampal neurons. However, whether Ndr2 kinase modulates the neurite outgrowth in an ECM ligand-specific manner or whether there are other intermediary proteins between Ndr2 and integrin activation remained unexplored. Therefore, following aims were set to elucidate the Ndr2 dependent integrin inside-out signaling and contribution of FlnA, its recently identified substrate, in this mechanism during dendritic arborization.

Aim 1 - Testing the relevance of Ndr2 mediated integrin regulation of neurite growth: Based on the previous data, which demonstrated an ECM- specific disturbance of neurite extension in Ndr2 overexpressing cells, my first aim was to identify underlying receptor mechanism that causes this selectivity. Based on the integrin-ECM substrate interactions and importance of Ndr2 in integrin surface expression, I tested whether α_1 integrin is differentially regulated by Ndr2 overexpression

in a PC12 cell model. Additionally, I aimed to investigate how this Ndr2-induced differential modulation would manifest in dendritic development of mouse hippocampal neurons.

Aim 2 –Studying the role of FlnA, a newly identified substrate of Ndr2, in integrin mediated dendritic growth: In parallel, in silico and in vitro experiments were conducted which identified FlnA as a downstream substrate of Ndr2 and a potential mediator of Ndr2 developmental effects in neurons. Based on the previously published research about FlnA-integrin interaction and FlnA mediated actin crosslinking, I hypothesized that FlnA is partly responsible for dendritic arborization and acts as a bridge between the integrin receptors and downstream signaling cascades. To elucidate the role of FlnA, different aspects of the dendritic arborization mechanisms, such as ECM, β_1 integrin activity, FAK signaling, and actin crosslinking, were rigorously tested using genetic and pharmacological interventions in mouse neuronal culture.

Aim 3 – Developing tools for future in vivo physiological analysis of FlnA functions: In order to transfer these findings and test the role of FlnA in hippocampal circuitry in vivo, my final aim was to establish a state-of-the-art CRISPR/Cas9 system that enables to genetically disturb or transcriptionally activate the mouse FlnA gene, which can also be delivered efficiently and in a region-specific manner in the mouse brain.

MATERIALS AND METHODS

1.1 DNA constructs

List of all shRNA constructs (Table 2), expression vectors (

Table 3) and CRISPR (clustered regularly interspaced short palindromic repeats) plasmids (

Table 4) are listed in the appendix section. pLL3.7 backbone is used to express shRNAs under U6 promoter using the Hpa1 and Xho1 sites (Figure 6A). shRNAs as sense and antisense configuration with a loop sequence are ordered as an oligonucleotide block (Thermo Fisher) flanked with a 5'blunt end (Hpa1) and 3' Xho1 sticky ends (in cooperation with Dr. Bettina Müller). Addition of poly-T sequence at the 3' end causes RNA pol. III to terminate transcription which results to the shRNA hairpin structure ready for posttranscriptional processing and target-mRNA silencing (Figure 6B). Alignments of the shRNAs against mouse transcriptome can be seen in Appendix Figure 42.
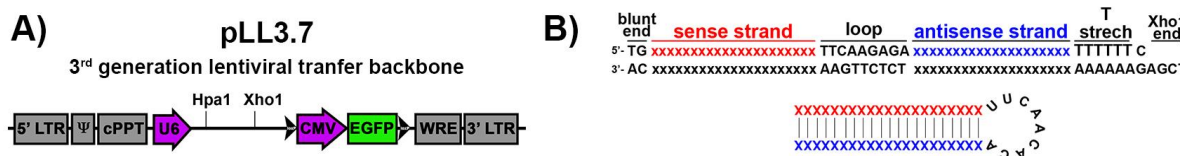
Figure 6: Lentiviral transfer plasmid containing an U6-hairpin and a reporter GFP cassette.
(**A**) Schematic of the pLL3.7, 3rd generation lentiviral backbone showing the flanking long terminal repeats (LTR), RNA target site for Nucleocapsid packaging (Ψ), central polypurine tract (cPPT) and Woodchuck hepatitis virus post transcriptional regulatory element (WRE). (**B**) shRNAs are ordered as oligo nucleotides with sense and antisense strand against the target region flanking a loop sequence. Blunt end on 5' and Xho1 sticky end on 3' is designed intentionally for directional cloning into

pLL3.7. *(below)* Simple representation of an U6 driven shRNA hairpin from pLL3.7 before any processing.

Guide RNAs (gRNA) targeting the mouse FlnA gene (FlnA KO1-4) and mouse FlnA promoter (FlnA1-4) are designed using the online sgRNA designer tools from MIT (crispr.mit.edu) and Broad Institute (https://portals.broadinstitute.org/gpp/public/analysis-tools/sgrna-design), ordered as oligonucleotide blocks and cloned into the gRNA backbone plasmids using type IIs restriction enzymes (Bbs1 for pLenti-sgRNA(SpCas9)-mCherry (Savell *et al.*, 2019), BsmB1 for pLenti-SAMv2 (Joung *et al.*, 2017) and Bsa1 for both pAAV-dCas9VPR-sgRNA (Vora *et al.*, 2018) and pAAV-CMV-SaCas9(HA)-U6-gRNA (Ran *et al.*, 2015) backbones) (Figure 7). Briefly, 10µM of top and bottom oligos were phosphorylated with T4 PNK (NEB) for 30 min at 37^0C (degrees of Celsius) and underwent to subsequent hybridization (95^0C down to 25^0C, 5^0C per minute). 1 µl from 1:10 dilution of the hybridized oligos and 25ng of appropriate backbone gRNA vector were used in a Golden Gate Cloning reaction (1 µl T4 ligase and 1 µl of appropriate Golden Gate restriction enzyme mixed with 0.1µg/µl BSA, 1mM ATP in 1X CutSmart buffer (25 µl final volume, all from NEB)). This mixture is incubated in 15 cycles of 37^0C / 20^0C (5 minutes each) for complete backbone digestion and oligo insertion. Ligation mixtures are then heat-shock transformed (42^0C for 45 seconds) into Stbl3 bacteria (Thermo) and antibiotic selected positive colonies were picked for plasmid extraction. All plasmids are purified in large scale using the GeneJet Midiprep kit (Thermo Scientific) before transfection into the mammalian cells. The integrity and sequence of each plasmid is confirmed with restriction digestions and Sanger sequencing of the cloned insert using appropriate sequencing primers (Seqlab).
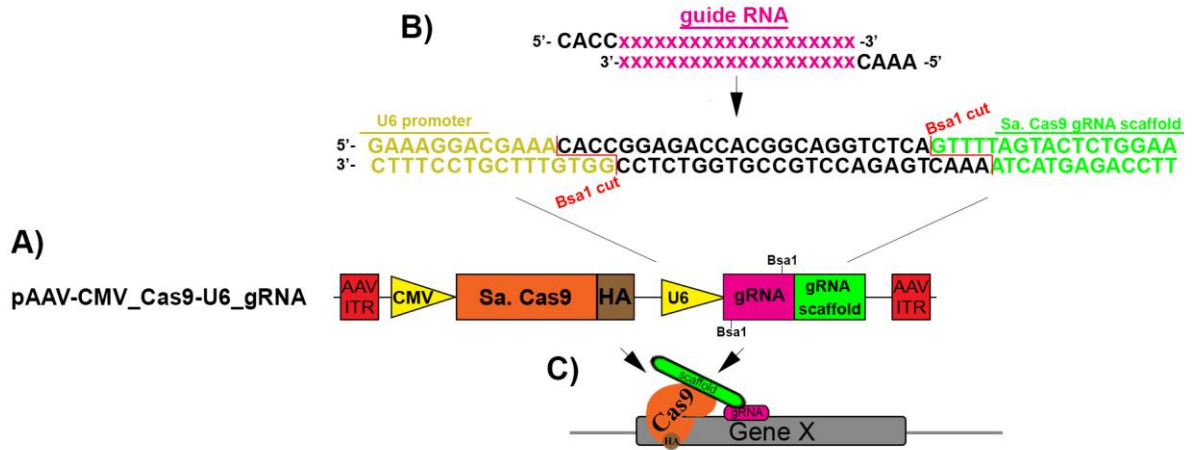
Figure 7: Single AAV transfer plasmid containing the Cas9 and gRNA.
(**A**) Schematic of the pAAV-CMV_Cas9-U6_gRNA AAV backbone showing the flanking AAV inverted terminal repeats (ITR), CMV driven Staphylococcus aureus (Sa. Cas9) with an HA tag and U6 driven gRNA cloning cassette followed by gRNA scaffold sequence. (**B**) *(above)* Guide RNA sequences are ordered as short oligos with 5' and 3' overhangs that would directionally ligate to *(below)* Bsa1 cut sites on pAAV backbone. (**C**) Simple representation of targeted double stranded break created by gRNA guided Cas9.

1.2 NIH3T3 and HEK293T cell culture and transfections

NIH3T3 (mouse fibroblasts) and HEK293T (human embryonic kidney cells) cell lines were kept in DMEM (Dulbecco's Modified Eagle Medium) media (Gibco) with 10% FBS (fetal bovine serum, Gibco) at 37 ^{0}C with 5% CO_2. Cells were grown in T75 flasks (Corning) and passaged at least two times a week to avoid full confluence in the back-up flasks. To split the cells between passages, cells were scraped from the T75 flask using a cell scraper and 1:20 dilution were made with a fresh DMEM+10%FBS media. Cells were routinely tested against mycoplasma contamination using MycoAlert detection kit (Lonza) and constantly kept in antibiotic-free media to detect any contamination quickly before experiments. The day before transfection, adherent cells were disassociated with TrypLE Express (Gibco) and seeded on multiple well plates (Corning) to have full confluency on the day of transfection ($\approx$30000 NIH3T3 cells/cm^2 and $\approx$60000 HEK293T cells/cm^2). Transfection of the cells were done using Lipofectamine 2000 (Thermo Fisher)

according to the manufacturer's instructions. Briefly, for a 6-well plate, 3 µg DNA and 12 µl Lipofectamine 2000 reagent were diluted in 150 µl Opti-MEM media in separate tubes. DNA and lipofectamine tubes were mixed and incubated for 5 min at room temperature (during which media of the cells is replaced with fresh prewarmed media) and added onto cells dropwise for liposome-mediated transfection. Lipofectamine 3000 reagent (Thermo Fisher) was used to transfect cells for Cas9 and gRNA containing plasmid transfections for improved efficiency according to the manufacturer instructions. Briefly, for a 6-well plate, 2.5 µg DNA and 7.5 µl Lipofectamine3000 reagent were diluted in 125 µl Opti-MEM media in separate tubes. 5 µl P3000 enhancer was further added into DNA tube and mixture was vortexed. DNA and lipofectamine tubes were mixed and incubated for 15 min at room temperature (during which media of the cells is replaced with fresh prewarmed media) and added onto cells dropwise for liposome-mediated transfection. Cells were further incubated for 2 days before lysis, protein extraction and subsequent western blotting analysis. Cells were checked under fluorescence microscope the day after with appropriate filter cubes (GFP or tdTom (tdTomato)) to confirm the transfection protocol.

1.3 PC12 cell culturing and differentiation

EGFP expressing control PC12 cells (EGFP PC12) and EGFP-Ndr2 expressing PC12 cells (Ndr2 PC12) were previously established with stable-transfections of the constructs (Stork *et al.*, 2004). Once thawed from liquid nitrogen glycerol stocks, EGFP and EGFP Ndr2 expressing rat pheochromocytoma (PC12) cells were cultured in RPMI medium (Gibco) supplemented with 10% horse serum, 5% fetal bovine serum,100 U/ml Penicillin-Streptomycin (PS) (Gibco) and 200 µg/ml Geneticin (ThermoFisher). PC12 cells were routinely passaged via cell scraper before reaching full confluence for maintenance. For differentiation, PC12 cells were seeded on glass coverslips or

multiwell plates that were coated with 50 μg/ml poly-d-lysine (PDL, SigmaAldrich) in 0.15 M Borate buffer (pH 8.4) overnight at 4 ^{0}C and when indicated with 100 μg/ml Collagen IV (Col IV, SigmaAldrich) in 30% ethanol for few hours in 37^{0}C incubator. Cells were either seeded on glass coverslips with 5000 cells/cm2 density for immunocytochemistry or in 6-well plates with 15000 cells/cm2 for immunoblotting in low RPMI medium (RPMI+ 0.2% horse serum, 1x PS and 200 μg/ml Geneticin). Once the PC12 cells were settled, they were supplemented with 50 ng/ml neurite growth factor (NGF, Gibco) to induce neurite extension until indicated times (3 and 6 days for immunoblotting, 6 days for immunocytochemistry).

1.4 Establishing neuronal and glial cell cultures

Astrocyte cultures: Since the hippocampal neurons were plated on glass coverslips without any glial co-culture, glial factors were supplemented via addition of astrocyte conditioned media (media that was incubated on confluent astrocyte cultures for 72 hours). Astrocytes were isolated from postnatal day 1 (P1) pups using Milteny Biotec Neural Tissue disassociation kit, following the manufacturer's instructions. Cortices from two pups were pooled in one T75 culture flask in DMEM+10%FBS media supplemented with 100U/ml Penicillin-Streptomycin (PS) and 2 mM GlutaMax (both from Gibco). Cells were cultured in T75 flasks with media replacements every 3 days. Once the astrocytes were fully confluent (around after 2 weeks), glial culture media was replaced with neuronal growth media (NBM (neurobasal media) with 1x B27+ 0.5 mM GlutaMax) and kept on the astrocytes for conditioning. 72 hours later, conditioned media was replaced with fresh neural growth media for another round of conditioning. Finally, both conditioned media batches were mixed, filtered with 0.20 μm filter and stored in -20 ^{0}C. Conditioned media aliquots were mixed with 1:1 with fresh neuronal media and used on hippocampal neurons when needed.

Neuronal Culturing: Hippocampi were dissected from embryonic day 18 (E18) to E19 mice were dissected using fine forceps under stereo microscope in ice-cold HBSS (Hank's Balanced Salt Solution) buffer. Dissected hippocampi were then disassociated into neurons using MACS Neural Tissue Disassociation Kit (Milteny). Disassociated cells were plated either on poly-D-lysine (10 µg/cm2, in 0.15 M Borate buffer pH 8.4, Sigma-Aldrich) or with poly- D-lysine+ Laminin111 (0.45 µg/cm^2, in PBS, Biolamina) or poly- D-lysine+ Fibronectin (50 µg/ml, in PBS, Roche) coated coverslips (25,000-30,000 cells/cm^2) when indicated. While poly-D-lysine coating was done overnight at 4^{0}C, fibronectin and laminin-111 was applied at 37^{0}C at least 2 hours. As a side note, coverslips were not let dry at any time after coating. Neurons were plated in plating media (DMEM+10% FBS + 2 mM GlutaMax + 100U/ml Penicillin/Streptomycin) until they adhere to the bottom of the well (≈few hours). Once they settled, media was changed to neurobasal media supplemented with B27 (2%) and GlutaMax (0.5 mM). (for hippocampal cultures, this media had been 1:1 mixed with glial conditioned media, see astrocyte culturing for details). At indicated experiments, neurons were treated with either 25 µg/ml anti-CD29 antibody (clone Ha2/5, 555002, BD Biosciences) and 1 µM FAK (focal adhesion kinase) inhibitor 14 (Y15, Sigma Aldrich) from DIV (days in vitro) 4 to DIV6 to inhibit β_1 integrin and FAK activity, respectively.

1.5 Transfection of neurons with Calcium/Phosphate method

Cultured hippocampal neurons were transfected with calcium phosphate method due to its low but sparse efficiency that allows easier identification/tracing of dendritic morphology. Hippocampal neurons were transfected at DIV3. 1 hour before transfection, neuronal medium was changed with prewarmed and CO_2-conditioned NBM only media. For transfection of shRNAs or expression vectors; 4 µg total transfer plasmid and 0.25 µg pCMV_tdTomato plasmid were dissolved in 60 µl

of 250 mM $CaCl_2$ solution (CalPhos, Takara). Transfer plasmids were used to manipulate gene expression levels while tdTom protein filled the neurons for better tracing of the transfected neurons. After a brief vortex of this mixture, 60 µl of 2x HBS buffer (CalPhos, Takara) was added slowly into to DNA tubes dropwise to acquire a fine and homogeneous DNA/calcium precipitate. This mixture was then added onto neurons dropwise and cells were returned to the incubator immediately for DNA precipitates to settle. Plates were checked every 10 minutes to detect the optimal precipitates formation on neurons (small, homogeneous formation that can be easily endocytosed by neurons with relatively low toxicity). Around 20-30 minutes, the transfection media was aspirated from neurons and dishes were washed with two times with HBSS -/- for 5 minutes to remove remaining precipitates. Finally, prewarmed and CO_2-conditioned neurobasal media supplemented with B27 (2%) and GlutaMax (0.5 mM) was added onto the cells. Neurons were briefly checked 2 days later under fluorescence microscope to confirm the fluorescent signal.

1.6 Production of viral particles and transduction of cells

To achieve the highest efficiency of genetic manipulation for biochemical analysis of proteins, unconcentrated lentivirus and adeno-associated-virus (AAV) viral supernatants were produced using HEK293T cells. For viral production, HEK293T cells were seeded, transfected, and kept in viral packaging medium (Opti-MEM supplemented with 2mM GlutaMax, 1mM Sodium Pyruvate and 5% FBS (all from Gibco)) instead of standard DMEM+10% FBS growth media. All the viral work described below was handled in S2 level certified rooms. Solid materials in contact and liquids containing viral particles were collected separately from any other waste. Replication-incompetent 3rd generation lentiviral production, storage and waste disposal were performed following institutional guidelines.

1.6.1 Lentivirus production

For lentiviral supernatant production, 1.5 million HEK239T cells were seeded in 2 ml viral packaging media per well into 6-well plates. Transfection of 3rd generation lentiviral helper plasmids and transfer plasmids was done using Lipofectamine 3000 reagent according to manufacturer's instructions. DNA mixture consisted of 1.5 μg pLenti transfer plasmid, 750 ng pMDLg/pRRE, 450 ng pMD2.G and 375 ng pRSV-REV packaging plasmids in 250 ul OptiMem media. 6 μl of P3000 reagent was added to the DNA solution prior to the mixing with Lipofectamine 3000 dilution. Once the Lipofectamine 3000 mixture (7 μl of Lipofectamine3000 in 250 μl OptiMem media) was added onto DNA mixture; DNA-lipid complexes were incubated in room temperature for 15 minutes. During this incubation tube, half of the packaging media was removed from the 6-well plates and DNA-lipid complexes were then added dropwise onto the cells. 6 hours post transfection; whole media was replaced with 2ml fresh viral packaging media. Next day, ≈24 hours post-transfection, entire media was harvested and replaced with 2ml fresh packaging media. Harvested supernatant was stored in +4 ^{0}C until the next day. After the second harvest at ≈52 hours post-transfection, all collected 4 ml of supernatant was centrifuged 2000 rpm for 10 minutes to remove any cellular debris and finally filtered using a 45 μm filter. Cleared supernatants were then aliquoted and stored in -80 ^{0}C until used for in vitro transduction of cultured neurons. A representative titration of lentiviral supernatants on HEK293T cells can be seen in Figure 8.
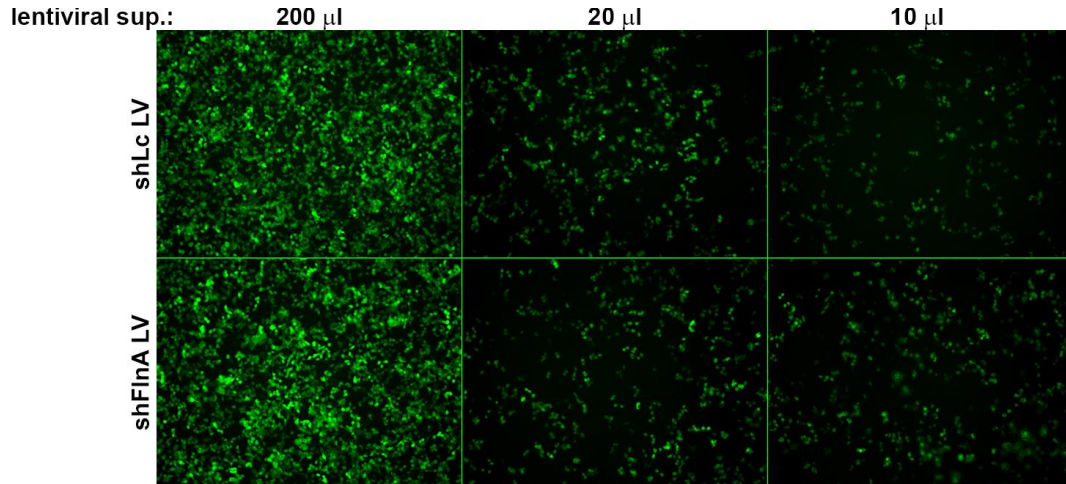
Figure 8: Representative images of control and shFlnA lentiviral supernatants on HEK293T cells.

1.6.2 *AAV production*

For AAV supernatant production, 1.5 million HEK239T cells were seeded in 2 ml viral packaging media into 6-well plates. Transfection of pAAV-backbone transfer, AAV2/1 packaging and AAV helper plasmids were done using Lipofectamine 3000 reagent according to manufacturer's instructions. 1:1:1 mixture of pAAV transfer backbone: pAAV2/1: pAdDeltaF6 plasmids in 250 µl of OptiMem media and mixed with 6 µl P3000 reagent. Once the Lipofectamine 3000 mixture (7 µl of Lipofectamine3000 in 250 µl OptiMem media) was added onto DNA mixture; DNA-lipid complexes were incubated in room temperature for 15 minutes. During this incubation time, half of the packaging media was removed from the 6-well plates and DNA-lipid complexes were then added dropwise onto the cells. Cells were placed back to incubator for 48 hours until the entire media is harvested. Collected supernatant was centrifuged 2000 rpm for 10 minutes to remove any cellular debris and finally filtered using a 0.45 µm filter. Cleared supernatants were then aliquoted and stored in -80 ^{0}C until used for in vitro transduction of cultured neurons. To qualitatively test

the unconcentrated viral titer, each produced viral supernatant was used to transduce HEK293T cells in 12-well plates and fluorescence signal was confirmed under microscope.

1.6.3　In vitro transduction of cells

To transduce mouse fibroblast cells (NIH3T3) with control and shNdr2 lentiviruses for FBS stimulation, 1×10^6 NIH3T3 cells were seeded in a 100mm dish. Next day, when cells were around 50% confluent, whole media was aspirated, 1ml fresh media (supplemented with 3 µg/ml Polybrene) with 2ml viral supernatant was added on the cells and dishes were gently swirled before returning to the incubator. 4-6 hours later, 9 ml fresh media was added onto each 10 cm dish and cells were placed back to the incubator. Two days after transduction, virus contained media was removed and transduced cells from 10 cm dishes were split into 12-well plates. Before lysis, cells were serum starved overnight and stimulated with 20% FBS in indicated time points (for pFlnA S2152 induction). GFP expression of the wells were confirmed before stimulation and lysis. When indicated, transduced fibroblasts were treated with 1 µM okadaic acid (Calbiochem, Merck) for 1 hour to stimulate Ndr activity (Devroe *et al.*, 2004; Waldt *et al.*, 2018).

Primary neurons were transduced based on the Ritter *et al.*, 2017 on DIV1. Briefly, half of the neuronal growth media from each well was collected and stored in a separate tube. Neurons were then transduced with 300 µl of lentiviral supernatant (or 200 µl AAV1 supernatant) per well for 3 hours. After three hours, virus-containing media was removed and replaced with 1:1 mixture of pre-transduction collected: fresh prewarmed neuronal growth media and neurons were placed back to incubator immediately. Next day, to stimulate CMV (cytomegalovirus) promoter in in vitro cultured neurons, neurons were supplemented with 20mM KCl (Wheeler and Cooper, 2001). Fluorescent signal was checked and confirmed from transduced neurons before lysis. Before acute

activation of integrins at DIV5, culturing media was replaced with neurobasal media without any supplements to synchronize the cells. 2 hours later, neurons were treated with 10 µg Fibronectin (#11-051-407-001, Roche) and 500 µM MnCl$_2$ in the same media before lysis for indicated time points.

1.7   Immunoblotting

1.7.1   Lysis of the cells

On the day of lysis, media was aspirated under laminar flow hood and cells were carefully washed with PBS (prewarmed HBSS for neuronal cultures). For 6 well plates, 200 µl of Lysis buffer (1% lauryl maltoside N-dodecyl-β-D-maltoside (Merck), 1% NP-40 (Sigma Aldrich), 1 mM Na-orthovanadate, 2 mM EDTA, 50 mM Tris-HCl, 150 mM NaCl, 0.5% deoxycholic acid, 1 mM 4-(2-Aminoethyl) benzene sulfonyl fluoride hydrochloride, 1 µM Pepstatin A, 1 mM NaF and protease inhibitor cocktail (one tablet per 50 ml, Pierce)) was added on each well and cells were incubated on ice for further 5 minutes. Next, 200 µl cell suspensions were pipetted into pre-cooled Eppendorf tubes which were then rotated for 30 minutes in cold room for sufficient lysis of the cells. Lastly, tubes were centrifuged for 30 minutes at 13,000 rpm in a pre-cooled (+4^{0}C) benchtop centrifuge, supernatants were transferred into a new tube and stored in -80 ^{0}C until further use. Cortical primary cultures and transduced cell lines that were stimulated were lysed directly with 1X Laemmli sample buffer (1-part 4x Laemmli buffer (252 mM Tris-HCl (pH 6.8), 8% SDS (w/v), 40% Glycerol (v/v), 0,04% Bromophenol blue (w/v), 20% β-mercaptoethanol) diluted in 3 parts of Lysis buffer) after the indicated times and kept on ice for 5 minutes. Lysates were heated for 10 minutes on 95 ^{0}C on a heat block for denaturation and stored in -20 ^{0}C until loading into SDS-PAGE gels.

1.7.2 Protein concentration quantification

For a standard protein curve, BSA protein standards in lysis buffer were prepared ranging from 0 to 8 µg/µl. Lysis buffer treated cell extracts were thawed on ice and their protein concentration was quantified using DC Protein Assay from Bio-Rad, which was based on the widely used Lowry method with some improvements (Lowry *et al.*, 1951). Briefly, 5 µl BSA standards and protein samples were loaded into a 96 well plate (BSA standards as triplicates and protein samples as duplicates). 25 µl of Reagent A (alkaline copper) and 200 µl Reagent B (folin) was added onto each well respectively. Samples were then incubated in dark for 15 minutes for color development and absorbance of each well was measured at 750 nm using a plate reader (Tecan M200). BSA standard values were used to plot a calibration curve and sample protein concentrations were calculated according to the linear regression line of the curve. Protein samples to load to SDS-PAGE gels were then prepared using 4x Laemmli sample buffer into equal concentrations and boiled at 95 ^{0}C for 10 minutes on a heat block for denaturation. These ready-to-load probes were stored in -20^{0}C until running in SDS-PAGE gels.

In case of directly 1X Laemmli sample buffer treated (containing β-mercaptoethanol and bromophenol blue already) and boiled cell lysates (such as cortical culture extracts), after a brief 1 minute 13000 rpm centrifugation, equal volumes of the lysate was directly loaded onto each well for SDS-PAGE.

1.7.3 SDS-PAGE and Western blotting

Mini-Trans-Blot Electrophoresis system (Bio-Rad) was used for separating the proteins in SDS-PAGE gels and consecutive transfer into PVDF membranes. Due to rather large size of the FlnA protein (280 kDA), 8% poly-acrylamide gels were used to run the protein samples (8.37 ml H2O;

4.77 30% Acrylamide 37.5:1; 4,5 ml 1.5M Tris-HCl (pH 8.8), 180 μl 10% SDS, 180 μl 10% APS and 18 μl TEMED for 2 mini-gels). These resolving gels were topped with 5% stacking gels (3.4 ml H2O; 0.83 30% Acrylamide 37.5:1; 0.63 ml 1.0M Tris-HCl (pH 6.8), 50 μl 10% SDS, 50 μl 10% APS and 5 μl TEMED for 2 mini-gels). These house-made polyacrylamide gels were put into the tanks filled with SDS-running buffer (25mM Tris (pH 8.3), 250 mM Glycine, 0.1% SDS in water) and equal volumes of samples were loaded onto each well along with 6 μl PageRuler Plus Prestained protein marker (ThermoFisher) for size determination and verify transfer efficiency. Empty wells were also loaded with a mixture of Laemmli buffer and lysis buffer to keep the stacked proteins as a straight-line during electrophoresis. Gels were run first at 80V until samples are stacked in a flat line through stacking gel and later voltage is increased to 120V until sufficient separation of the pre-stained protein bands are achieved. Gel was then removed from the glass plates, washed with distilled water and equilibrated in transfer buffer (25 mM Tris, 192 mM Glycine, %10 Methanol). At the same time, PVDF membranes were activated in methanol for 10 second, washed with water and equilibrated in transfer buffer. Protein transfers from gel to the membranes were done at constant 120 V for 1:15 hour at $+4\,^{0}C$. After transfer, gels were discarded and PVDF membranes were dried until further use. Transfer efficiency is confirmed qualitatively using the pre-stained protein marker. Once the PVDF membranes were re-activated using methanol, they were blocked with Intercept blocking buffer (in TBS, Licor) for 1 hour at room temperature; to prevent non-specific background signal.

1.7.4 *Antibodies used in the study*

Primary and secondary antibodies were also diluted in Intercept blocking buffer+ 0.2% Tween20 for blotting and incubated overnight at $+4\,^{0}C$ and 1 hour at room temperature, respectively. Primary antibodies used in immunoblotting is listed in Table 1 with their dilution factors and catalogue

numbers. As secondary antibodies for immunoblotting, 680nm/ 800nm fluorescently probed antibodies (1:15000-1:20000, Licor) or HRP-conjugated secondary antibodies (1:7500, Jackson ImmunoResearch) were used for fluorescent and ECL blots respectively. Membranes were washed 3 times for 10 minutes with TBS with 0.2% Tween20 after each antibody incubation.

Table 1: Primary antibodies used in this study for Western blotting and immunocytochemistry.

Antibody	Host Species	Company	Catalog #	Dilution
Filamin A	rabbit	Abcam	ab51217	1:1000 WB 1:200 ICC
p-Filamin A (Ser-2152)	rabbit	Cell Signaling	#4761	1:1000 WB
Integrin α_1	rabbit	Abcam	ab78479	1:1000 WB 1:200 ICC
Integrin β_1	rabbit	Abcam	ab52971	1:500 ICC
Tubulin	mouse	Sigma Aldrich	T6199	1:5000 WB
MAP2	mouse	Millipore	MAB3418	1:1000 ICC
HA tag	mouse	Bio Legend	#901501	1:1000 WB
FLAG tag	mouse	Santa Cruz	sc166355	1:200 ICC
Pan-Akt	mouse	Cell Signaling	#2920	1:2000 WB
pAkt (Thr 308)	rabbit	Cell Signaling	#2965	1:1000 WB
pAKT (Ser 473)	rabbit	Cell Signaling	#4060	1:1000 WB
FAK	rabbit	Cell Signaling	#3285	1:1000 WB
pFAK (Tyr397)	rabbit	Invitrogen	44-624G	1:1000 WB

After incubation with appropriate primary and secondary antibodies, membranes were imaged using Licor Odyssey Scanner for fluorescent and Licor FC imager for ECL imaging. For across membrane normalization, signals were normalized to the total signal of each antibody from the same membrane (each membrane contained a complete set of samples from a single experimental batch). Protein bands were quantified using ImageJ software and each signal was normalized against the tubulin of the same lane.

1.8 Immunocytochemistry

On the day of fixation, entire media was removed, and cells were washed once with pre-warmed PBS. Cells were then fixed in 4% PFA (paraformaldehyde)/ Sucrose solution (in 0.1M PBS) for 20 minutes under the fume hood. Following the fixation, dishes were washed two times with PBS for 5 minutes in room temperature. If the cells were used for fluorescent imaging for dendritic tracing/ Sholl analysis, coverslips were directly mounted on slides. For immunocytochemistry with antibodies, cells were first permeabilized using 0.3% TritonX in PBS at room temperature for 10 minutes, washed 3 times with PBS for 5 minutes and proceeded to blocking with 5% BSA in PBS for 1 hour at room temperature. Coverslips are then incubated with primary antibodies diluted in blocking buffer overnight at +4 ^{0}C (antibodies and their dilutions are listed in Table 1). Fluorescently probed secondary antibodies (1:1000, Invitrogen) or biotinylated-secondary antibodies (1:200, Vector Labs) were applied 1 hour at room temperature followed by 30 minutes incubation of fluorescently conjugated streptavidin (against biotin, 1:1000 in PBS, Jackson ImmunoResearch). Coverslips were washed 3 times for 10 minutes with PBS between antibody incubations. To stain actin filaments, 5 µl of rhodamine-phalloidin (Invitrogen) was diluted in 200 µl of PBS and added onto coverslips for 20 minutes. Lastly, coverslips were mounted on glass slides (brand!) using ImmunoMount (Thermo) mounting media and were stored at +4 ^{0}C until imaging. Images were taken using Leica DMI6000 epifluorescence microscope using the appropriate fluorescence filter cubes. All images used for side-by-side comparison of fluorescence signal were imaged with same light intensity and exposure time during microscopy and brightness/ contrast levels set to same values during image export.

1.9 Protein database analysis against phosphorylation motifs

Identified RxP(S/T) substrate motif (from Ndr2 positional peptide library scanning) was used in ScanProsite tool (https://prosite.expasy.org/scanprosite/). Option-2 of motif search (submit motifs

to scan them against a PROTEIN sequence database) was used and Swiss-Prot is selected as database (with Mus musculus filter (taxon ID:10090)). Identified Uniprot-IDs from this search then filtered for duplicates (mostly isoforms). This list was compared to the in-silico integrin adhesome components (http://adhesome.org/) for proteins that are involved in the adhesome complex. Common proteins were finally used in PhosphoSitePlus (https://www.phosphosite.org/homeAction.action) tool and in literature search for previously shown phosphorylation modifications on the Serine and Threonine residue of RxP(S/T) motif and their role in neuronal development regarding integrin receptors.

1.10 Sholl analysis of dendritic morphology

During microscopy, GFP and tdTom co-expressing neurons were selected with two main criteria: not being accompanied by any transfected neighboring cells to allow fine tracing of dendrites and to have a typical pyramidal morphology (being a multipolar cell with multiple thick dendrites with a clearly differentiated/extended axon) (Hanamura *et al.*, 2010). Texas Red channel of the pictures was exported as Tiff files and all images were pooled to randomize file names using the Fiji plugin. Dendrites of the randomized images were then traced blind to the genotypes and converted to binary pictures using Qwin software (Leica). Finally, these binary images were imported to ImageJ (NIH) and converted to 8-bit. To quantify the complexity of dendritic trees, Sholl analysis plug-in -which analyzes the number of dendritic intersections at various concentric circles drawn around the neuron soma at various intervals (Sholl, 1953)- was used on 8-bit skeleton images.

1.11 Statistical analysis

Statistical analysis and data representation (plots) were done using GraphPad Prism 8. The number of cells with long neurites (>100 µm) and short neurites (<100 µm) were compared using Chi-

square tests. Immunofluorescence data were log-transformed before statistical analysis. For Sholl analysis of dendrites, repeated two-way ANOVA using distance as repeating factor for each neuron is followed by Fisher Least Significant (LSD) test for multiple comparisons (in case of a significant interaction). One-way ANOVA was used in case of only one factor was present as an independent variable (such as total dendritic length across genotypes). Pairwise comparisons were done using Student's t-test when appropriate and a statistical threshold for significance was set at $p< 0.05$ in all the tests. While reporting post-hoc multiple comparison results (when significant interaction is present), instead of annotating each data point individually, portions of the line graphs were selected and noted with the least significance figure available in that portion; for better clarity and readability in the graphs.

RESULTS

1.1 Ndr2 modulates α_1 integrin distribution during neurite growth

Initial experiments with Ndr2 PC12 cells (in cooperation with Dr. Kati Rehberg, Figure 3, Figure 4, Demiray *et al.*, 2018) indicated a neurite growth deficiency specific to $\alpha_1\beta_1$ integrin function. Therefore, as the next step, α_1 integrin subunit distribution was examined during PC12 cells differentiation (Figure 9A-F). In fact, Ndr2 PC12 cells displayed significantly less labelling of α_1 integrin expression in their neurite tips compared to control cells (two-tailed Student's t-test, $p<$ 0.001). Unlike the α_1 integrin level, F-actin labelling in the growth cones did not differ between the genotypes (two-tailed Student's t-test, $p=$ 0.595; Figure 9G).
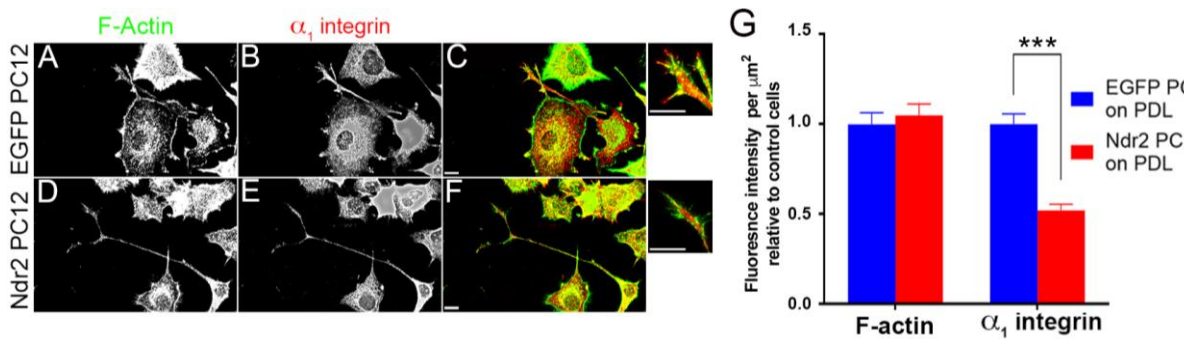
Figure 9: Localization of α_1 integrin in differentiating Ndr2 PC12 cells.
Microscopy images of 6 days NGF treated PC12 cells labelled for α_1 integrin and F-actin in **(A, B)** control and **(D, E)** Ndr2 PC12 cells. **(C, F)** Overlay images, Scale bars: 10 μm. (G) Quantification of labelling at neurite tips of differentiating PC12 cells (EGFP PC12 n= 46, Ndr2 PC12 n= 49 cells) revealed that Ndr2 PC12 cells have significantly less α_1 integrin labelling in their neurite tips compared to control cells (two-tailed Student's t-test, $p<$ 0.001), while F-actin levels did not differ between genotypes (two-tailed Student's t-test, $p=$ 0.595). Values are mean± SEM; ***$p<$ 0.001.

To distinguish whether Ndr2 regulates the overall α_1 integrin expression or its trafficking to neurite tips, total levels of α_1 integrin subunit in EGFP PC12 and Ndr2 PC12 cells were determined via

Western blotting. Cells were differentiated using NGF either for 3 days or 6 days which led to a profound increase of α_1 integrin expression (two-way ANOVA, treatment-days effect, on PDL: $F_{(2,18)}= 15.91$, $p< 0.001$ on Collagen IV: $F_{(2,18)}= 3.867$, $p= 0.0401$). However, this increase was very similar between EGFP PC12 and Ndr2 PC12 cells on both PDL (two-way ANOVA, genotype effect: $F_{(1,18)}= 0.2754$, $p= 0.6062$; Figure 10A) as well as Collagen IV (two-way ANOVA, genotype effect: $F_{(1,18)}= 1.74$, $p= 0.2036$; Figure 10B) substrates. These results suggest that the reduced levels of α_1 integrin in the growth tips of differentiating Ndr2 PC12 cells likely to result from a trafficking impairment, rather than an overall α_1 integrin expression deficiency.
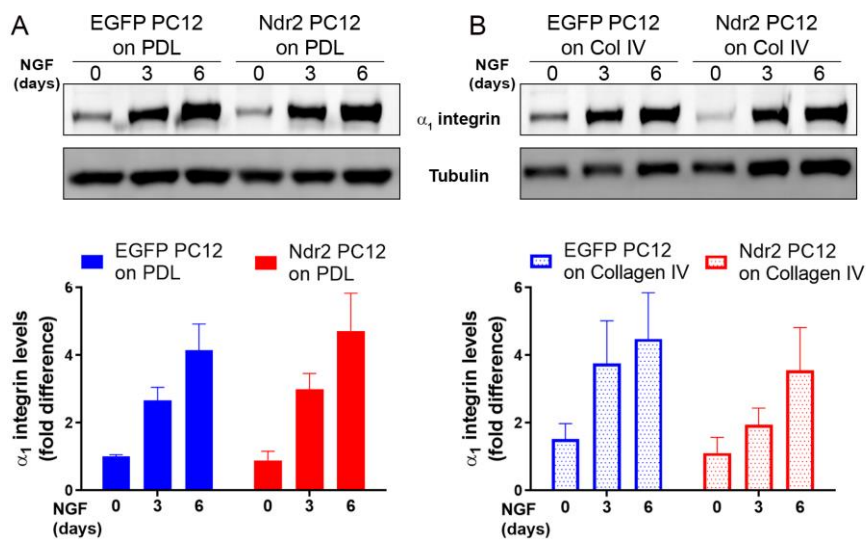
Figure 10: Total α_1 integrin expression level in Ndr2 PC12 cells during differentiation.
Immunoblotting shows no difference between induction of α_1 integrin expression in control and Ndr2 PC12 cells after NGF induction on both (**A**) PDL (two-way ANOVA, genotype effect: $F_{(1,18)}= 0.2754$, $p= 0.6062$) and (**B**) Collagen IV (two-way ANOVA, genotype effect: $F_{(1,18)}= 1.74$, $p= 0.2036$) substrates. Values are mean± SEM.

1.2   Ndr2 controls dendritic branching in primary neurons

Next, to transfer our insights from PC12 cells into neurons and investigate the role of Ndr2 in neuronal differentiation, hippocampal primary neuronal cultures (HPC) were prepared and acutely

transfected either with EGFP (EGFP HPC) or EGFP-Ndr2 (Ndr2 HPC) constructs. To check the interaction between $\alpha_1\beta_1$ integrins and dendritic growth, hippocampal neurons were plated either on PDL or Laminin-111 (LN111), a previously established ECM molecule of primary neurons and a known $\alpha_1\beta_1$ integrin substrate (Desban *et al.*, 2006; Tulla *et al.*, 2008). As expected, dendritic branching of control neurons (EGFP HPC) significantly increased on LN111 substrate compared to PDL (repeated two-way ANOVA substrate effect: $F_{(1,57)}= 12.59$, *p*= 0.0008; Figure 11A-C). However, Ndr2 HPC displayed significantly less dendritic branching on LN111 substrate compared to PDL (repeated two-way ANOVA substrate effect: $F_{(1,57)}= 15.46$, *p*= 0.0002; Figure 11D-F). These results re-iterate the impairment in α_1 integrin dependent growth in Ndr2 overexpressing cells, in line with previous experiments with PC12 cells. Furthermore, the total dendritic length of those acutely transfected neurons was analyzed. Although Ndr2 overexpression significantly increases the total dendritic length compared control neurons on PDL; it results to a significant reduction of dendritic length on LN111 substrate (one-way ANOVA: $F_{(3,115)}= 7.72$, *p*< 0.001, Fisher LSD; Figure 11G).
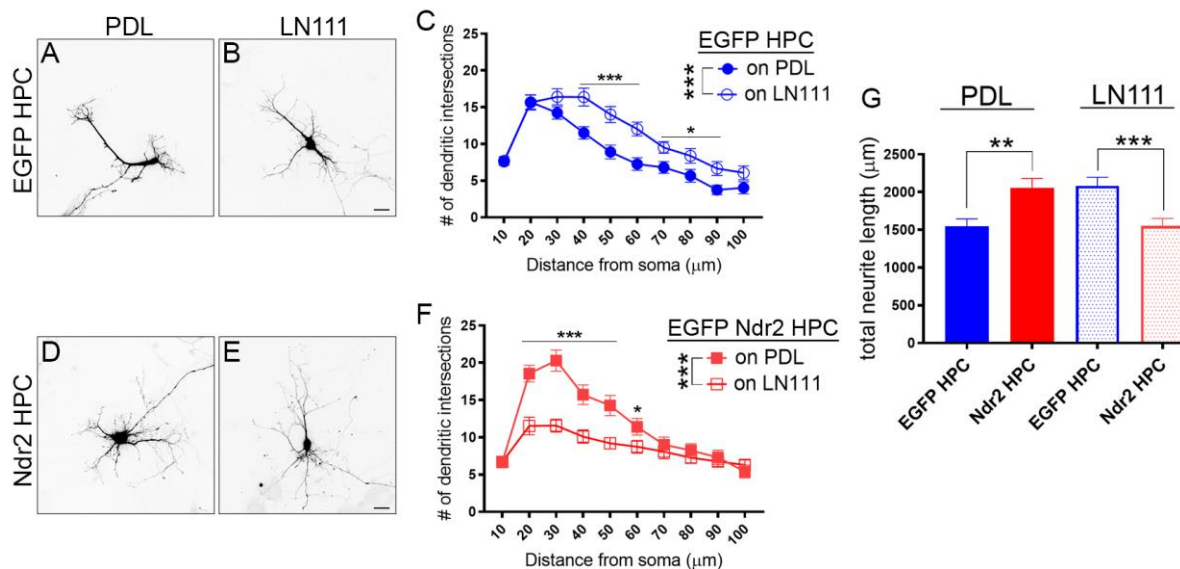
Figure 11: Ndr2 kinase overexpression impairs $\alpha_1\beta_1$ integrin dependent growth of hippocampal primary neurons.
Hippocampal neurons are transfected with EGFP plasmid either on **(A)** PDL or **(B)** Laminin-111 (LN111). **(C)** Sholl analysis of the dendrites demonstrated that LN111 substrate increases dendritic arborization compared to PDL only (repeated two-way ANOVA substrate effect: $F_{(1,57)}= 12.59$, $p= 0.0008$). **(D, E)** However, Ndr2 overexpressing neurons (Ndr2 HPC) displayed significantly less dendritic branching on LN111 substrate compared to PDL (repeated two-way ANOVA substrate effect: $F_{(1,57)}= 15.46$, $p= 0.0002$). **(E)** Total dendritic length of Ndr2 HPC is higher compared to control neurons on PDL, while significantly reduced on LN111 substrate (one-way ANOVA: $F_{(3,115)}= 7.72$, $p< 0.001$, Fisher LSD). Data presented as mean± SEM, N= 2, n= 30. Scale bars: 20 μm. **$p< 0.01$; ***$p< 0.001$.

Finally, to test how lack of Ndr2 affects the dendritic morphology in the same ECM setup, previously used shNdr2 plasmid (Rehberg *et al.*, 2014) is acutely transfected in hippocampal neurons. As control, an shRNA targeting firefly luciferase (shLuc, Paddison *et al.*, 2002) was used as previously (Rehberg *et al.*, 2014). Control neurons (shLuc HPC) increased their dendritic branching upon seeding on LN111 substrate as before (repeated two-way ANOVA substrate effect: $F_{(1,54)}= 12.16$, $p= 0.0010$; Figure 12A-C). On the other hand, Ndr2 knockdown neurons (shNdr2 HPC) entirely failed to increase their dendritic branching in response to LN111 coating (repeated two-way ANOVA substrate effect: $F_{(1,58)}= 1.262$, $p= 0.2660$; Figure 12D-F). Examining the total dendritic lengths of those neurons showed that shNdr2 neurons were significantly shorter than shLuc neurons on both PDL and LN111 substrates (one-way ANOVA: $F_{(3,113)}= 17.33$, $p< 0.0001$, Fisher LSD; Figure 12G).
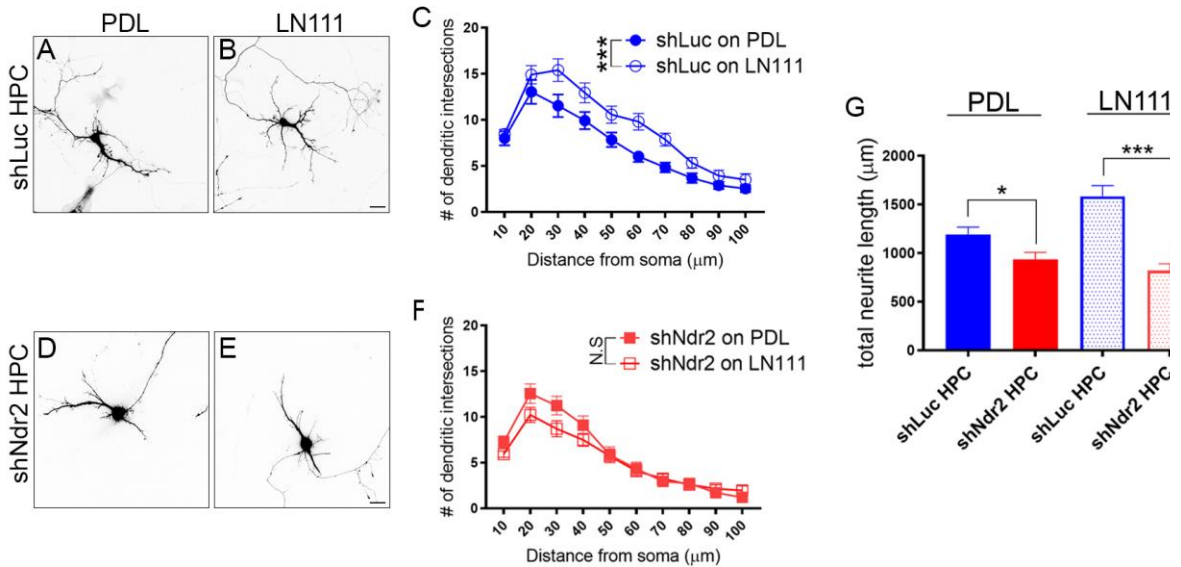
Figure 12: Ndr2 kinase is required for LN111 mediated dendritic growth of hippocampal neurons.
Hippocampal neurons are transfected with shLuc control plasmid either on **(A)** PDL or **(B)** Laminin-111 (LN111). **(C)** In line with previous observations, Sholl analysis of the dendrites demonstrated that LN111 substrate increases dendritic arborization of control neurons (repeated two-way ANOVA substrate effect: $F_{(1,54)}$= 12.16, p= 0.0010). **(D, E)** On the other hand, in shNdr2 transfected hippocampal neurons (shNdr2 HPC), dendritic branching between PDL and LN111 did not change (repeated two-way ANOVA substrate effect: $F_{(1,58)}$= 1.262, p= 0.2660). **(E)** In fact, shNdr2 HPC group displayed significantly less dendritic length on both PDL and LN111 substrate compared to control neurons, re-iterating its role in dendritic growth (one-way ANOVA: $F_{(3,113)}$= 17.33, p< 0.0001, Fisher LSD). Data presented as mean± SEM, N= 2, n= 30. Scale bars: 20 μm. *p< 0.05; ***p< 0.001.

1.3   Ndr2 kinase targets Filamin A as a downstream substrate

Previous work showed that Ndr2 can increase the phosphorylation (T788/T789) and surface expression of β_1 integrins (Rehberg *et al.*, 2014; Demiray *et al.*, 2018). However, neither okadaic acid stimulated nor an constitutively active form of Ndr2 could phosphorylate the cytoplasmic tail of β_1 integrins in an in vitro kinase assay (Rehberg *et al.*, 2014). This indicates an indirect effect on β_1 integrin activity by Ndr2 kinase rather than a direct phosphorylation. Therefore, as the next step, the question of which integrin-activity modulator might be the downstream target of Ndr2 was addressed. First, using purified WT Ndr2/Mob2 heterodimer, a positional peptide library scanning with radioactively labelled ATP identified the R-X-P-(S/T) motif as the optimal amino

acid substrate for Ndr2 kinase (in cooperation with Eric Devroe & Benjamin Turk, see 1.1.2 for details; Figure 13A, left; Waldt *et al.*, 2018). Normalized data from two independent runs were then averaged, log transformed, and heat maps were generated (Figure 13A, right). It should be noted that same reaction is also performed with catalytically inactive (K119A) Ndr2 mutant to confirm the labelling is not performed by contaminating kinase (personal communication, Eric Devroe & Benjamin Turk). Next, the identified RXP(S/T) motif was scanned in the mouse protein database using ScanProsite (Expasy tools); which resulted 3486 different proteins. This list is then aligned with an in-silico integrin adhesome network which consists of 221 proteins identified via biomedical literature and protein databases (Zaidel-Bar *et al.*, 2007; Winograd-Katz *et al.*, 2014). This approach has identified 28 different proteins in integrin adhesome containing the RXP(S/T) motif (Figure 13B, full list can be seen in Table 5). Of this 28 proteins, to distinguish previously observed posttranslational modifications on the phosphoacceptor residue from any non-specific RXP(S/T) motifs, PhosphoSitePlus tool (Cell Signaling) and further literature search has been used, which resulted into 3 possible downstream candidate of Ndr2 phosphorylation via this motif: protein tyrosine phosphatase receptor A (PTPRA-S204), heat shock binding protein 1 (HSBP-1-S15) and Filamin A (FlnA-S2152), which are listed with their interaction partners from integrin adhesome network in Figure 13C-E. Filamin A was the most interesting candidate among them by directly interacting with different integrin subunits in the adhesome network (Travis *et al.*, 2004; Kim *et al.*, 2008; Takala *et al.*, 2008) and with actin cytoskeleton (Nakamura *et al.*, 2002, 2005; Mammoto, Huang and Ingber, 2007).
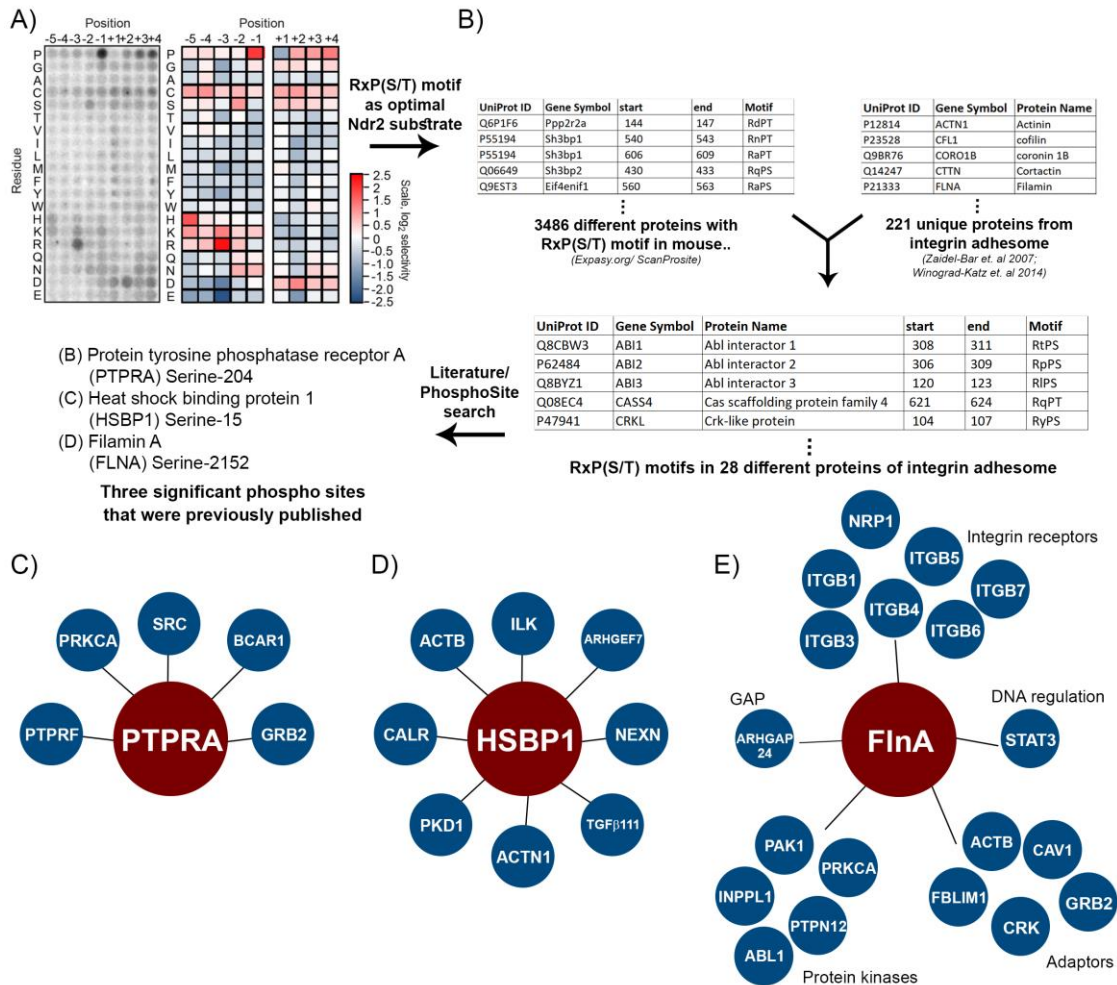
Figure 13: Identification of RXP(S/T) motif as Ndr2 substrate and integrin adhesome sequence search.

(A) Peptide library positional scanning is done using WT Ndr2/Mob2 heterodimer and radioactively labelled ATP used for tagging of possible substrates (from of Eric Devroe & Benjamin Turk; Waldt et al., 2018)). *(left)* Detection of the phosphorylated peptides by Ndr2 indicating the amino acid residue and its indicated position relative to phosphorylation residue. *(right)* Data was quantified, log2 transformed and used to generate a heat map (n= 2). R-X-P-(S/T) motif identified as an optimal motif for Ndr2 phosphorylation. **(B)** Aligning 3486 different proteins from mouse proteome containing the R-X-P-(S/T) motif (using ScanProsite) and 221 proteins from integrin adhesome database (Zaidel-Bar et al., 2007; Winograd-Katz et al., 2014) with further literature/PhosphoSite scanning resulted into 3 proteins; **(C)** protein tyrosine phosphatase receptor A (PTPRA-S204), **(D)** heat shock binding protein 1 (HSBP-1-S15) and **(E)** Filamin A (FlnA-S2152) is listed with their interaction partners in integrin adhesome network.

To further test whether Ndr2 can also phosphorylate FlnA, HEK293T cells are transfected with

wild type or catalytically dead (K119A) Ndr2 kinase and purified kinases is then tested in an in

vitro kinase assay using GST-FlnA fragment (repeats 19-24, containing Serine-2152 residue) as substrate (Figure 14A; in cooperation with Dr. Stefanie Kliche; Waldt *et al.* 2018). High levels of FlnA S2152 phosphorylation was detected specifically in wild type Ndr2 and not in K119A kinase-dead mutant elutes. It should also be noted that, S2152 phosphorylation of FlnA fragment by Ndr2 occurred specifically in okadaic acid (OA) pre-treated cells, which has previously shown to stimulate Ndr2 activity and inhibit phosphatases (Devroe *et al.*, 2004). Next, NIH3T3 fibroblast line were used to test how FlnA phosphorylation is controlled by Ndr2 kinase in mouse cells. To manipulate Ndr2 levels, unconcentrated lentiviral particles were produced in HEK293T cells using either a control (shLuc) or a Ndr2 shRNA (Rehberg *et al.*, 2014; Figure 14B). To stimulate FlnA phosphorylation in fibroblasts, cells were serum starved overnight and stimulated with FBS (Woo *et al.*, 2004; Zhang *et al.*, 2013) for indicated time points. Immunoblotting against phosphorylated FlnA at Serine-2152 residue showed that silencing Ndr2 significantly reduced FlnA phosphorylation levels upon FBS stimulation in untreated (Figure 14C; two-way ANOVA genotype effect: $F_{(1,80)}= 6.004$, *p*= 0.0165) and OA pre-treated cells (Figure 14D; two-way ANOVA genotype effect: $F_{(1,72)}= 7.442$, *p*= 0.0080). In parallel, using a more specific stimulation of Ndr2-FlnA axis other than FBS, it has been shown that T-cell receptor activation induces Ndr2 mediated S2152 phosphorylation. While control Jurkat T-cells displayed a significant increase of FlnA S2152 phosphorylation, shNdr2 or kinase-dead (K119A) Ndr2 transfected cells failed to respond to the CD3 stimulation did not phosphorylate FlnA S2152 (in cooperation with Dr. Stefanie Kliche; Appendix Figure 43; Waldt *et al.*, 2018).
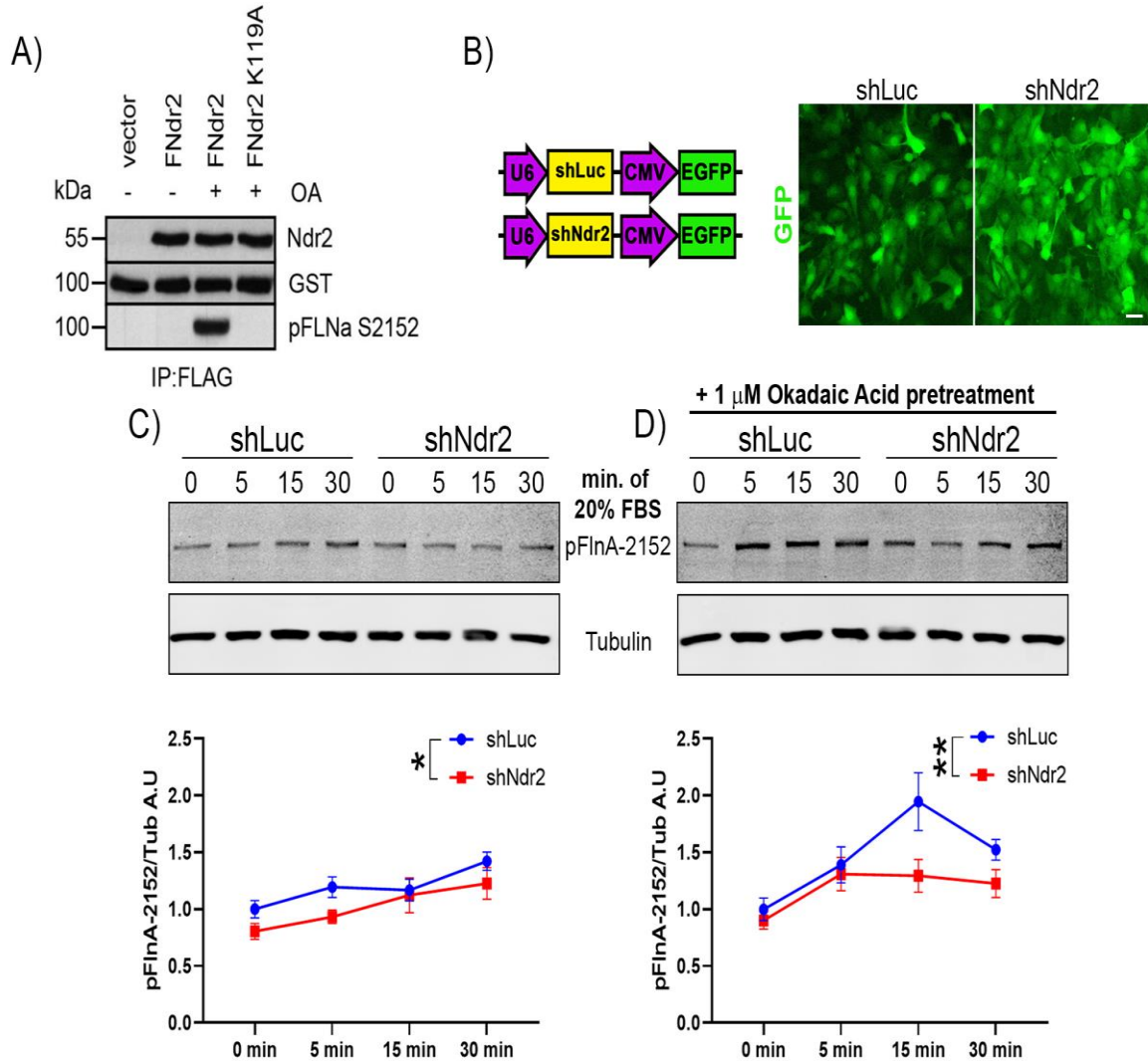
Figure 14: Ndr2 phosphorylates FlnA on S2152.
(A) HEK293T cells were transfected with empty backbone, Flag-Ndr2 or Flag-Ndr2K119A (kinase dead) mutant and left untreated or stimulated with okadaic acid (OA) before immunoprecipitation with FLAG antibodies. The purified FLAG constructs were used in an in vitro kinase assay using a GST-FlnA fragment (Ig19-24) which contains the S2152 residue. Western blotting against Ndr2 confirms the successful IP. Moreover, FlnA S2152 was strongly phosphorylated only after OA activation in Flag-Ndr2 kinase condition. **(B)** NIH3T3 mouse fibroblasts are transduced with control (shLuc) or shNdr2 lentiviral particles (Scale bars: 50 μm). Cells are serum starved overnight and stimulated with 20%FBS for indicated time points and immunoblotted against phosphor-Serine2152 FlnA either **(C)** directly (N= 6, n= 11 two-way ANOVA genotype effect: $F_{(1,80)}$= 6.004, p= 0.0165) or **(D)** with one hour of 1 μm OA pre-treatment (N= 5, n= 10 two-way ANOVA genotype effect: $F_{(1,72)}$= 7.442, p= 0.0080). To sum up, these results indicate that FlnA contains the RxP(S/T) substrate motif that can be targeted by Ndr2 kinase and indeed Ndr2 kinase can phosphorylate FlnA at Serine-2152. Although FlnA is widely studied in variety of cell lines regarding to its integrin and actin modulation, there has been limited attempts to investigate FlnA meditated dendritic mechanisms in neurons. The second half of this study aims to explore FlnA dependent modulation of dendritic

branching in hippocampal neurons and further investigate FlnA mediated molecular mechanisms that might be involved. Data presented as mean± SEM. *$p< 0.05$; **$p< 0.01$.

1.4 Filamin A levels control dendritic branching of hippocampal neurons

First, expression of FlnA and β_1 integrin proteins were monitored during differentiation of hippocampal primary neurons. Immunocytochemistry of the neurons at indicated time points revealed that both proteins are expressed early on with increasing expression throughout first two weeks of differentiation (Figure 15A). Furthermore, in a separate set of hippocampal neurons, total RNA was extracted during neuronal differentiation until DIV21 to check any transcriptional regulation of FlnA and β_1 integrin genes (in collaboration with Dr. Jan Teuber). In fact, qPCR analysis of these developing results revealed that both FlnA (n= 4; one-way ANOVA: $F_{(4,15)}=$ 5.798, $p= 0.0050$) and β_1 integrin (n= 4; one-way ANOVA: $F_{(4,15)}= 26.67$, $p< 0.0001$) mRNA expression is coordinated with dendritic development in primary hippocampal cultures, markedly reducing after DIV7 (Figure 15B; compared to DIV3, Fisher LSD).
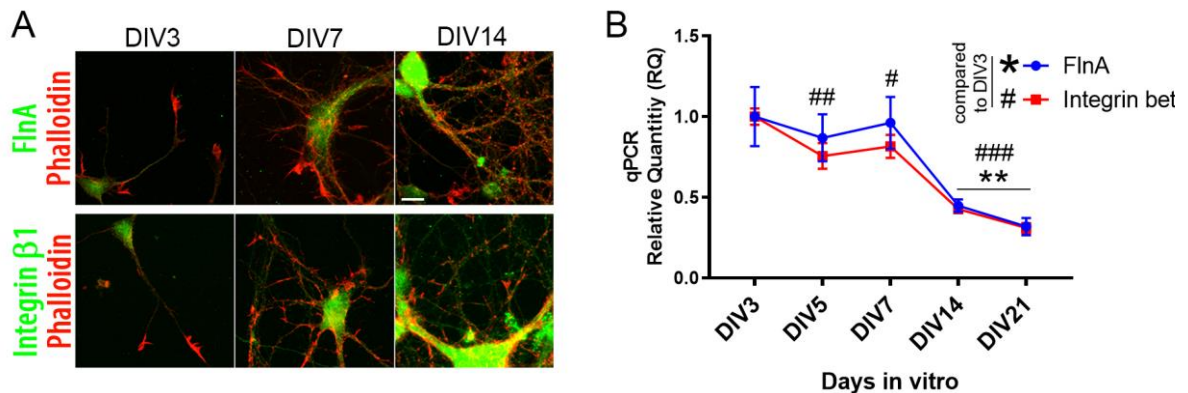
Figure 15: FlnA and integrin β_1 expression during hippocampal neuronal differentiation.
(**A**) Mouse hippocampal neurons are PFA fixed at indicated time points and stained for FlnA (above) and integrin β_1 (below). Phalloidin was also used to co-stain the actin cytoskeleton to outline the neuronal morphology. (Scale bars: 10 μm) (**B**) Total RNA is extracted from mouse hippocampal neurons at indicated time points. FlnA (n= 4, one-way ANOVA: $F_{(4,15)}= 5.798$, $p= 0.0050$) and

Integrin β_1 (n= 4, one-way ANOVA: $F_{(4,15)}$= 26.67, $p<$ 0.0001) gene expression levels are quantified using Taqman probes via qPCR. Fisher LSD multiple comparison tests were done against the DIV3 expression levels of the corresponding gene (*: FlnA; #: Integrin β_1). Data presented as mean± SEM. *$p<$ 0.05; **$p<$ 0.01; ***$p<$ 0.001.

Next, to manipulate the FlnA levels in mouse cells, a hairpin shRNA targeting mouse FlnA gene (NM_010227.3, 4321-4341) was used to interfere with FlnA expression in mouse cells. As control, an shRNA targeting firefly luciferase (shLuc) was used as previously (for detailed sequences of the inserts, see Table 2). Lentiviral backbone that is used to drive shRNAs also contains a GFP tag to confirm expression. Finally, a myc tagged human wild type FlnA construct is acquired (RRID:Addgene_8982, Woo *et al.*, 2004) for re-expression of FlnA in shRNA transfected cells (Figure 16A). These plasmids were then tested in NIH3T3 mouse fibroblasts with acute transfections. 48 hours after transfection, cells were fixed and subjected to immunocytochemistry. Staining for FlnA protein revealed that shFlnA expressing cells display markedly reduced levels of FlnA compared to both neighboring and shLuc transfected cells (Figure 16B). Moreover, when human WT FlnA is co-transfected with shFlnA, strong expression of FlnA can be observed in transfected cells due to CMV promoter in expression plasmid.
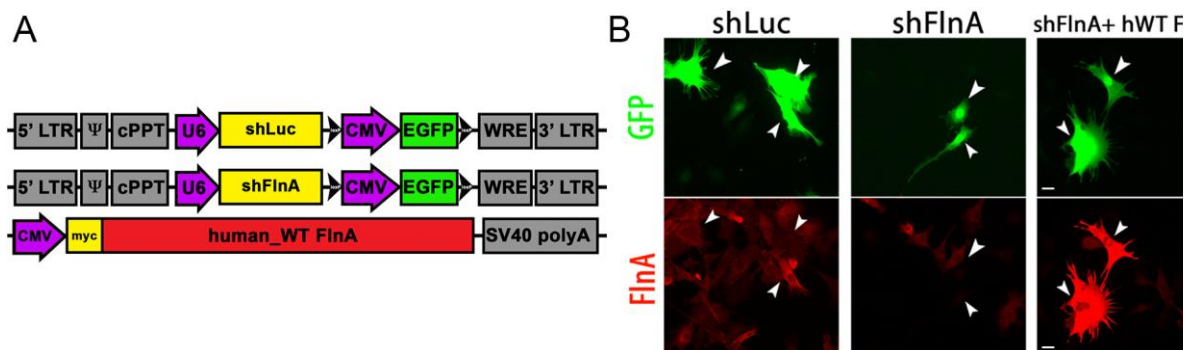
Figure 16: Silencing and re-expression of FlnA via acute transfections of fibroblasts.
(**A**) Scheme of control (against firefly luciferase, shLuc) and FlnA shRNAs in lentiviral backbones (with an EGFP tag to confirm the expression) and CMV driven human WT FlnA re-expression construct (Addgene ID #8982). (**B**) NIH3T3 mouse fibroblasts are transfected with control shRNA, shFlnA and shFlnA co-transfected with human WT FlnA expression plasmid. 2 days after, cells are

fixed and subjected to immunocytochemistry against FlnA, which shows efficient silencing and re-expression of FlnA protein. Scale bars: 20 μm.

Besides fibroblasts, strong reduction of endogenous FlnA protein upon shFlnA transduction (Figure 17B) as well as a robust increase of FlnA levels in shFlnA+ hWT FlnA co-transfection setup (Figure 40B) were detected in neurons. Overall, these plasmids (shFlnA and hWT FlnA) were used in further experiments to silence (shFlnA transfection) and overexpress FlnA protein (shFlnA+hWT FlnA co-transfection) in hippocampal neurons for the analysis of dendritic morphology.
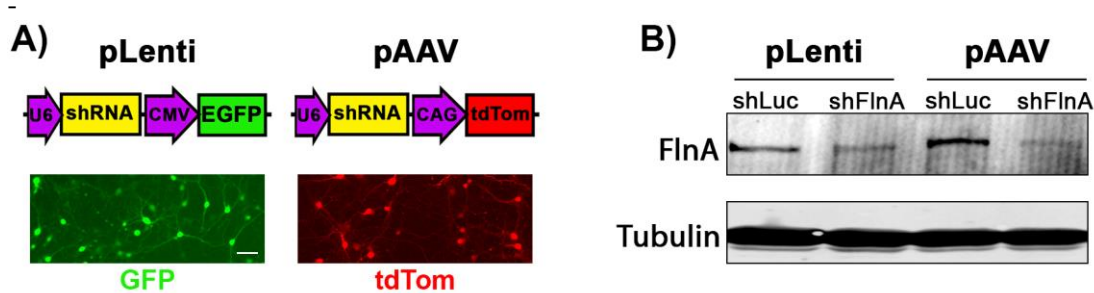
Figure 17: shFlnA can efficiently silence endogenous FlnA levels in cortical neurons.
(A) shFlnA used in further experiments were tested on cortical neurons either with lentiviral particles produced directly or subcloned into a AAV transfer plasmid that contains a tdTom as fluorescence reporter. Representative image of transduced DIV13 neurons before lysis can be seen below (Scale bar: 50 μm). **(B)** Western blotting of the lysates against FlnA reveals the strong silencing by shFlnA hairpin in cortical neurons.

In first set of experiments, hippocampal neurons are either seeded on poly-D-lysin (PDL) coated coverslips or on Fibronectin (FN) coated coverslips. While PDL is a widely used coverslip treatment as it increases general adhesion/growth of neurons due to its positive charge (Kim *et al.*, 2011), Fibronectin is an important member of brain ECM and supports neurite outgrowth via acting as a β1 integrin ligand (Tonge *et al.*, 2012). To investigate the role of FlnA in neuronal differentiation, primary hippocampal neurons are acutely transfected at DIV3 with either control (shLuc) or shFlnA plasmid to silence endogenous FlnA gene. Besides, human WT FlnA is co-

transfected with mouse shFlnA construct to further examine FlnA overexpression effects (called as hWT FlnA from now on). Neurons were then fixed at DIV7 to analyze dendritic tree with respect to FlnA manipulation and the extracellular coated substrate. Control neurons showed a significant overall increase of dendritic branching on FN compared to PDL (repeated two-way ANOVA substrate effect: $F_{(1,90)}= 7.434$, $p= 0.0077$). Besides, a significant interaction between substrate and distance was also observed which revealed that FN markedly increased the dendritic branching between 30-80 µm away from soma (repeated two-way ANOVA substrate x distance interaction: $F_{(39,3510)}= 2.451$, $p< 0.0001$; Fisher LSD; Figure 18A). Interestingly, silencing of FlnA occluded the FN mediated dendritic growth, in fact, a significant decrease in overall dendritic branching was observed (repeated two-way ANOVA substrate effect: $F_{(1,96)}= 3.944$, $p= 0.0499$; Figure 18B). Finally, hWT FlnA mediated dendritic branching was independent of the extracellular substrate and did not change on FN (repeated two-way ANOVA substrate effect: $F_{(1,90)}= 2.036$, $p= 0.1571$; Figure 18C).

To analyze the direct effects of the FlnA genotypes compared to control neurons, this data is then pooled and re-plotted as "on PDL" and "on FN" sets. Here, it could be seen that both silencing and overexpressing of FlnA caused a robust increase of the dendritic branching, especially in proximal radiuses, on PDL (repeated two-way ANOVA genotype x distance interaction: $F_{(78, 5265)}= 6.774$, $p< 0.0001$; Fisher LSD; Figure 18D). On the other hand, when coverslips were coated with fibronectin substrate prior to seeding of neurons, both silencing and overexpressing of FlnA resulted to reduction of overall dendritic branching (repeated two-way ANOVA genotype effect: $F_{(2,141)}= 6.499$, $p= 0.0020$). Despite this overall decrease on FN, hWT FlnA expressing neurons still persisted the dendritic hypertrophy compared to control neurons especially in proximal areas and

displayed significantly increased dendritic arborization (repeated two-way ANOVA genotype x distance interaction: $F_{(78, 5499)}= 7.137$, $p< 0.0001$; Fisher LSD; Figure 18E).
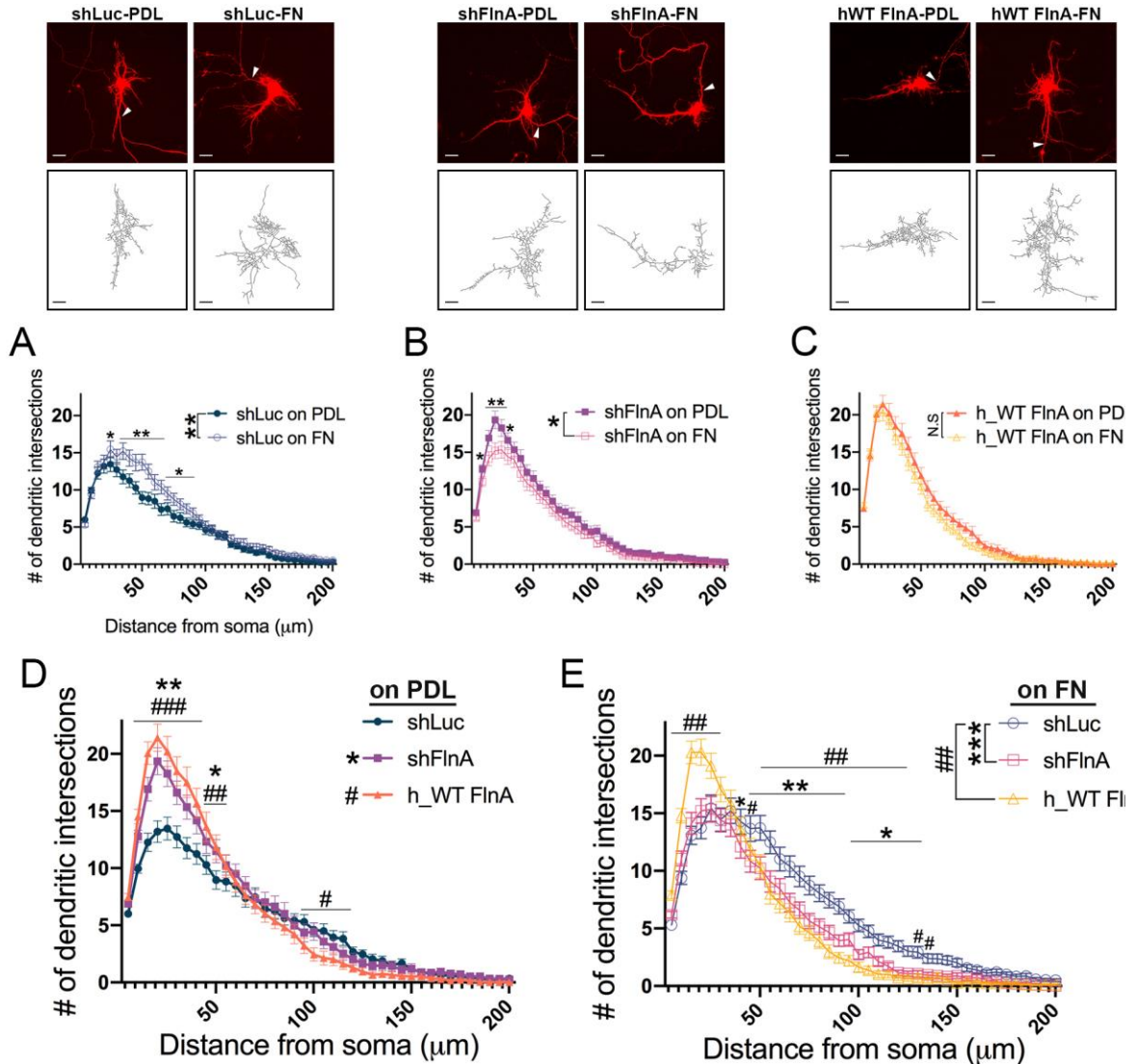
Figure 18: Manipulation of FlnA expression in hippocampal neurons affect dendrite morphology.

Hippocampal neurons are seeded on PDL or FN coverslips, transfected with shLuc, shFlnA or shFlnA+ hWT FlnA constructs, fixed at DIV7 and dendrites were traced using tdTom signal of transfected neurons. Scale bars: 20 μm (N= 3, n= 45 per group) **(A)** Control neurons showed a significant increase in their overall dendritic branching on FN substrate (repeated two-way ANOVA substrate effect: $F_{(1,90)}= 7.434$, $p= 0.0077$) **(B)** However, silencing the endogenous FlnA occluded the FN mediated branching and in fact resulted to reduction of overall branching on FN in shFlnA neurons compared to PDL (repeated two-way ANOVA substrate effect: $F_{(1,96)}= 3.944$, $p= 0.0499$) **(C)** Finally, in hWT FlnA expressing neurons, there was no difference in dendritic morphology between PDL and

FN substrata (repeated two-way ANOVA substrate effect: $F_{(1,90)}= 2.036$, $p= 0.1571$). **(D)** When data were pooled per substrate, it could be seen that both silencing and overexpressing of FlnA results to dendritic hypertrophy in proximal parts of the neuron on PDL (repeated two-way ANOVA genotype x distance interaction: $F_{(78, 5265)}= 6.774$, $p< 0.0001$; Fisher LSD). **(E)** However, despite an overall decrease of dendritic branching compared to control neurons in both genotypes, hWT FlnA expressing neurons persisted the increased branching in proximal parts. Data presented as mean± SEM. * is shLuc vs shFlnA, # is shLuc vs hWT FlnA.

Finally, besides dendritic arborization throughout 200 μm from soma via Sholl analysis, total dendritic length spanning this dendritic subfield of each traced skeleton was also calculated and analyzed (two-way ANOVA genotype x substrate interaction: $F_{(2,275)}= 3.747$, $p= 0.0248$). Compared to PDL, FN substrate did not increase total length significantly of shLuc and hWT FlnA dendritic trees (although a strong trend can be observed on shLuc neurons, $p= 0.0877$; Fisher LSD). However, shFlnA neurons displayed significantly shorter total dendritic length on FN substrate compared to PDL-only coverslips ($p= 0.0452$; Fisher LSD; Figure 19).
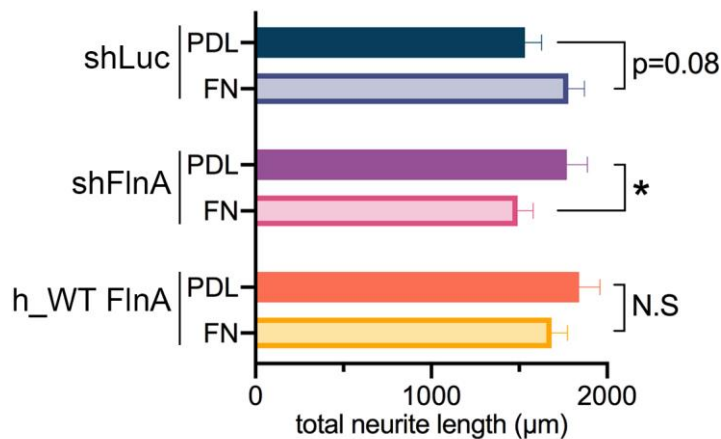
Figure 19: FlnA levels alter the dendritic length depending on the coating substrate.
Total dendritic lengths of the neurons on different coating coverslips were also analyzed (two-way ANOVA genotype x substrate interaction $F_{(2,275)}= 3.747$, $p= 0.0248$). A strong but not statistically significant increase of dendritic length can be observed in control neurons on FN substrate ($p= 0.0877$; Fisher LSD). On the other hand, shFlnA neurons displayed shorter dendrites on FN ($p=$

0.0452; Fisher LSD) while hWT FlnA neurons did not change between the substrates ($p= 0.2760$; Fisher LSD; repeated-measures two-way ANOVA substrate effect: $F_{(1,90)}= 7.434$, $p= 0.0077$).

Moreover, an alternative small hairpin RNA targeting mouse FlnA transcript (Figure 20A, named as shFlnA_v2) is further used to confirm the observed dendritic morphology. Transfection of shFlnA_v2 into mouse fibroblasts demonstrated the silencing of the endogenous mouse FlnA similar to original shFlnA hairpin (Figure 20B). shFlnA_v2 also caused a dendritic hypertrophy compared to control neurons (repeated two-way ANOVA substrate effect: $F_{(1,86)}= 11.47$, $p= 0.0011$; Figure 20C-D). Moreover, shFlnA_v2 also caused a significant increase in total dendritic length compared to control neurons on PDL (two-tailed Student's t-test, $p< 0.0001$; Figure 20E).
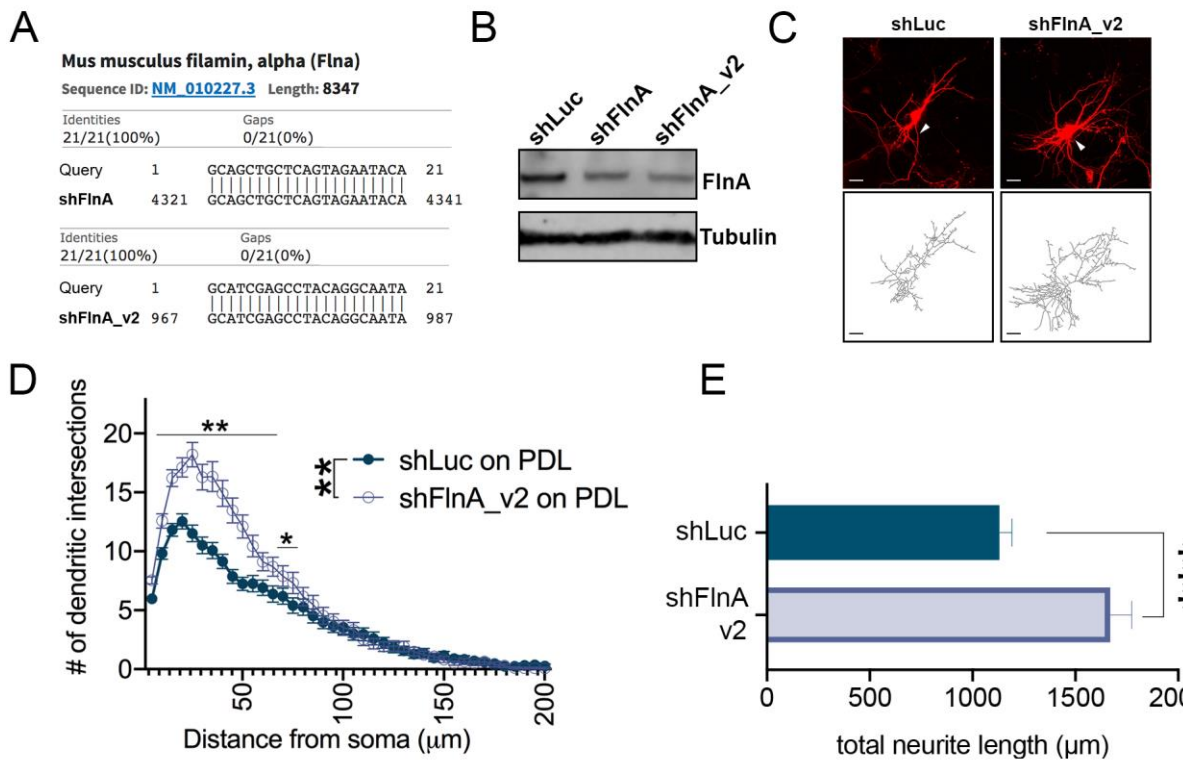
Figure 20: Silencing of FlnA with a second small hairpin RNA (shFlnA_v2) produces a similar dendritic hypertrophy.
(**A**) BLAST search of previously used shFlnA and the alternative shFlnA_v2 in mouse RefSeq transcript database. (**B**) NIH3T3 cells are transfected with control, shFlnA or shFlnA_v2 plasmids and lysed 48 hours later. Western blotting of the lysates demonstrates the efficient silencing of the endogenous FlnA by both FlnA shRNAs. (**C**) Hippocampal neurons are transfected with shLuc and

shFlnA_v2 shRNAs at DIV3, fixed at DIV7 and dendrites were traced using tdTom signal of transfected neurons. Scale bars: 20 μm (N= 3, n= 45 per group). **(D)** shFlnA_v2 hairpin also resulted increased dendritic arborization (repeated two-way ANOVA substrate effect: $F_{(1,86)}$= 11.47, *p*= 0.0011). **(E)** Moreover, shFlnA_v2 also caused a significant increase in total dendritic length compared to control neurons on PDL (two-tailed Student's t-test, *p*< 0.0001). Data presented as mean± SEM.

To conclude, both silencing and overexpression of FlnA increases the dendritic branching of hippocampal neurons during development. Furthermore, shFlnA mediated effects interact with the β1 integrin ligand fibronectin on the extracellular space while hWT FlnA mediated hypertrophy might be independent of β1 integrins thus does not alter between ECM substrates.

1.5 β1 integrin levels are crucial for dendritic branching

To further examine the interaction between FlnA mediated dendritic morphology and β1 integrin receptors, hippocampal neurons are transfected either with a β1 integrin shRNA (shItgb1) (Lei *et al.*, 2012; Rehberg *et al.*, 2014) only or co-transfected with FlnA plasmids (shItgb1+shFlnA and shItgb1+hWT FlnA). Neurons that were seeded and transfected on PDL coverslips were fixed on DIV7 to analyze their dendritic arborization (repeated two-way ANOVA genotype x distance interaction: $F_{(117,\ 9126)}$= 7.917, *p*< 0.0001). Silencing of endogenous β1 integrin receptor significantly reduced overall dendritic branching compared to control neurons (*p*< 0.0001, Fisher LSD). Co-transfection of shFlnA to simultaneously reduce endogenous FlnA rescues this phenotype and stimulates dendritic branching similar to the control cells (*p*= 0.9622, Fisher LSD). However, expression of hWT FlnA in shItgb1 neurons did not recover the dendritic tree and displayed markedly reduced overall dendritic branching compared to control cells (*p*= 0.0025, Fisher LSD), apart from few radiuses proximal to the soma (Figure 21A).

In addition to arborization, total dendritic lengths of the neurons revealed a similar interaction between endogenous β1 integrin and FlnA levels (ordinary one-way ANOVA: $F_{(3,234)}$= 12.78, *p*<

0.0001). The strong reduction of dendritic length caused by shItgb1 ($p < 0.0001$, Fisher LSD) could be reversed by simultaneous FlnA silencing ($p = 0.6566$, Fisher LSD) while hWT FlnA expression in shItgb1 neurons still resulted to significantly shorter dendrites compared to control ($p = 0.0050$, Fisher LSD; Figure 21B).
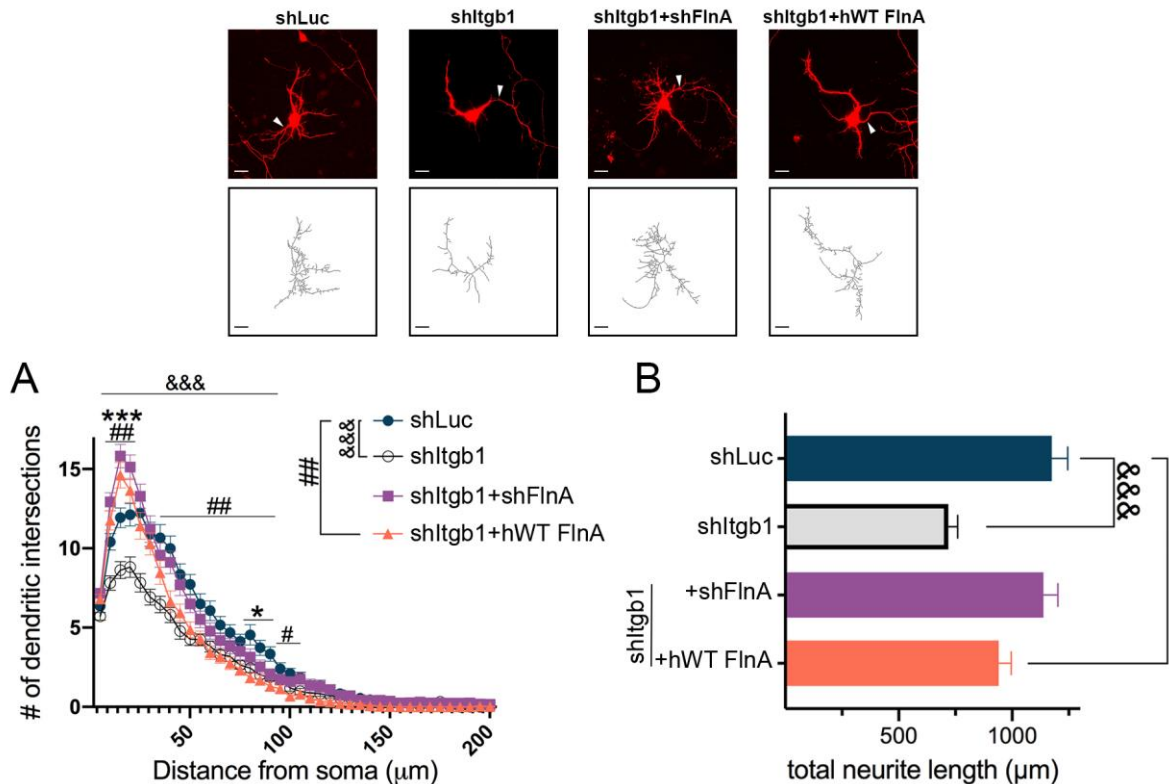
Figure 21: Reduced β_1 integrin levels impair dendritic growth and this morphology can be rescued by FlnA reduction.
Hippocampal neurons are transfected with shLuc, shItgb1, shItgb1+shFlnA or shItgb1+h_WT FlnA constructs, fixed at DIV7 and dendrites were traced using tdTom signal of transfected neurons. Scale bars: 20 μm (N= 4, n= 59 per group) (**A**) Reducing β_1 integrin expression strongly impairs overall dendritic branching of neurons (repeated two-way ANOVA genotype effect: $F_{(3,234)} = 11.36$, $^{\&\&\&}p < 0.0001$, Fisher LSD). While simultaneous reduction of FlnA (shItgb1+shFlnA) stimulates the dendritic branching similar to control levels ($p = 0.9622$), overexpressing of WT FlnA (shItgb1+h_WT FlnA) could not rescue the shItgb1-mediated reduction of overall dendritic arborization ($^{\#\#}p = 0.0025$). (**B**) Similar changes were also reflected in total dendritic lengths with respect to FlnA and β_1 integrin levels (ordinary one-way ANOVA: $F_{(3,234)} = 12.78$, $p < 0.0001$). Data

To sum up, these results suggest that WT FlnA mediated dendritic hypertrophy requires β_1 integrin receptor expression, at least for overall dendritic branching. Conversely, silencing endogenous FlnA in shItgb1 neurons can still stimulate dendritic growth further. This could be via increasing the activity states of remaining β_1 integrins, due to role of FlnA as an integrin activity modulator (Kiema *et al.*, 2006; Ithychanda *et al.*, 2009; Nieves *et al.*, 2010). Therefore, as a next step, FlnA-dependent morphology changes were tested under β_1 integrin receptor inhibiting conditions.

1.6 shFlnA mediated dendritic hypertrophy is dependent on β_1 integrin activity

To test whether FlnA mediated dendritic hypertrophy requires β_1 integrin activity, hippocampal neurons were acutely transfected as previously to manipulate FlnA levels and then treated with integrin inhibiting antibodies specific to β_1 integrin (clone Ha2/5) (Chavis and Westbrook, 2001; Jongbloets *et al.*, 2017) from DIV4 on for 2 days. Cells were fixed at DIV6 and to analyze dendritic tree with respect to FlnA manipulation and β_1 integrin activity. As expected, Ha2/5 antibody significantly reduced overall dendritic branching of control neurons (repeated two-way ANOVA antibody effect: $F_{(1,88)}= 5.799, p= 0.0181$) especially in proximal areas between 10-55 µm (repeated two-way ANOVA antibody x distance interaction: $F_{(39,\ 3432)}= 4.653, p< 0.0001$, Fisher LSD; Figure 22A). Furthermore, shFlnA mediated dendritic hypertrophy was drastically reduced when β_1 integrin receptor activation is blocked specifically with Ha2/5 (repeated two-way ANOVA antibody effect: $F_{(1,87)}= 13.98, p= 0.0003$; Figure 22B). Finally, hWT FlnA mediated dendritic hypertrophy was also impaired under Ha2/5 antibody (repeated two-way ANOVA antibody effect: $F_{(1,88)}= 5.632, p= 0.0198$), but to a much lesser extend compared to decrease in shFlnA neurons

(Figure 22C). When data plotted together per treatment, the dendritic hypertrophy caused by FlnA silencing and overexpression could be observed as previously (repeated two-way ANOVA genotype effect: $F_{(2,132)}= 9.751$, $p< 0.0001$; Figure 22D). WT FlnA mediated increase in dendritic branching still persisted even under Ha2/5 antibody treatment (repeated two-way ANOVA genotype effect: $F_{(2,131)}= 4.463$, $p= 0.0133$, Fisher LSD $p= 0.0038$), while shFlnA neurons did not significantly differ, albeit still markedly higher, compared to control neurons treated with Ha2/5 antibody (Fisher LSD $p= 0.0601$; Figure 22E).
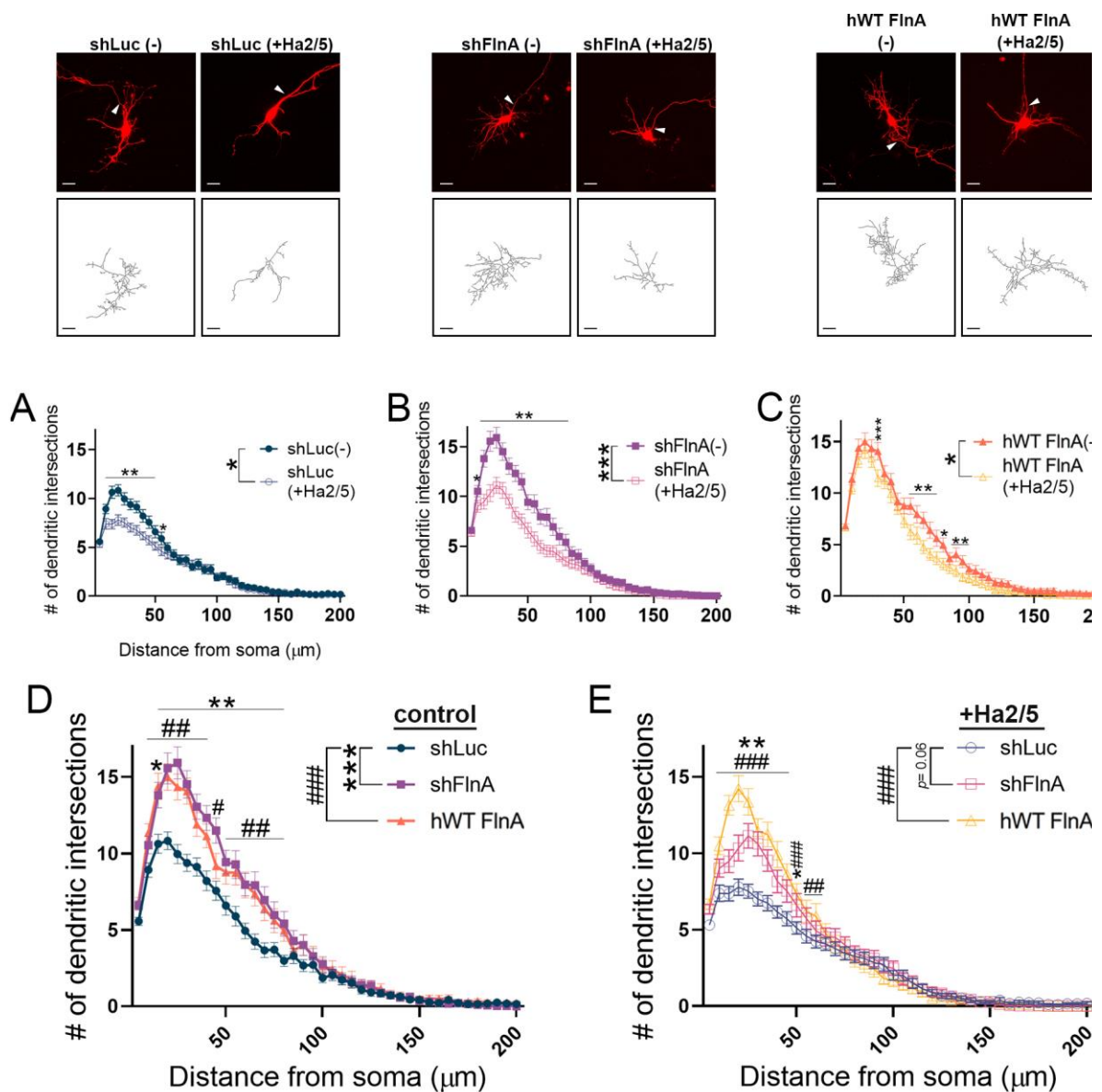
Figure 22: β₁ integrin activity is required for shFlnA mediated dendritic hypertrophy.
Hippocampal neurons are seeded on PDL coverslips, transfected with shLuc, shFlnA or shFlnA+ hWT FlnA constructs, treated with β₁ integrin blocking antibody (clone Ha2/5, 25 μg/ml), fixed at DIV6 and dendrites were traced using tdTom signal of transfected neurons. Scale bars: 20 μm (N= 3, n= 45 per group) **(A)** Control neurons showed a significant decrease in their overall dendritic branching upon treatment with Ha2/5 antibody (repeated two-way ANOVA antibody effect: $F_{(1,88)}=$ 5.799, $p=$ 0.0181) **(B)** Furthermore, shFlnA mediated dendritic arborization is drastically reduced when β₁ integrin receptors are blocked with Ha2/5 antibody (repeated two-way ANOVA antibody effect: $F_{(1,87)}=$ 13.98, $p=$ 0.0003). **(C)** While there was a significant decrease of dendritic branching compared to control conditions in hWT FlnA expressing neurons (repeated two-way ANOVA antibody effect: $F_{(1,88)}=$ 5.632, $p=$ 0.0198), the reduction was still milder compared to shFlnA neurons. **(D)** In line with previous observations, both silencing and overexpressing of FlnA results to a very similar pattern of dendritic hypertrophy on PDL compared to control neurons (repeated two-way ANOVA genotype effect: $F_{(2,132)}=$ 9.751, $p<$ 0.0001; Fisher LSD). **(E)** Finally, under Ha2/5 antibody, only hWT FlnA overexpression could significantly increase overall dendritic branching compared to control neurons (repeated two-way ANOVA genotype effect: $F_{(2,131)}=$ 4.463, $p=$ 0.0133, Fisher LSD $p=$ 0.0038). Data presented as mean± SEM, post-hoc comparison: * is shLuc vs shFlnA, # is shLuc vs hWT FlnA.

Besides altering the dendritic arborization, total dendritic length of the neurons is significantly reduced when treated with β₁ integrin inhibiting Ha2/5 antibodies (two-way ANOVA Ha2/5 antibody effect: $F_{(1,263)}=$ 32.36, $p<$ 0.0001), independent of the FlnA manipulations (two-way ANOVA genotype x antibody interaction: $F_{(2,263)}=$ 2.016, $p=$ 0.1353; Figure 23).
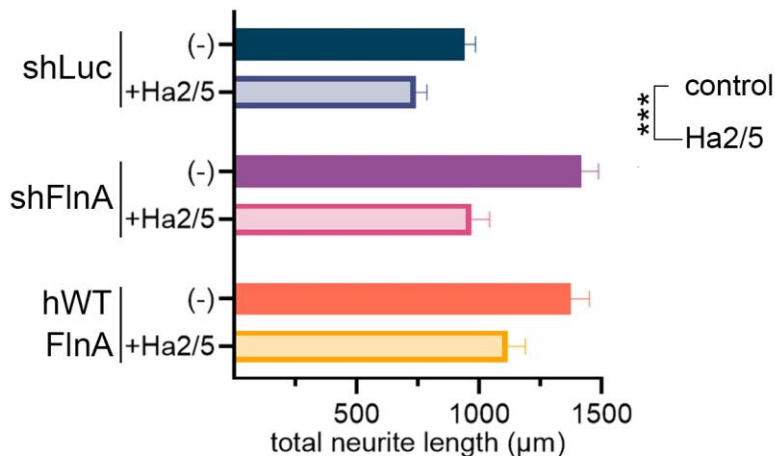
Figure 23: β₁ integrin activity controls the total dendritic length of hippocampal neurons.
Total dendritic lengths of the neurons under control or β₁ integrin blockage was also analyzed. Treatment of neurons with Ha2/5 antibody significantly reduced dendritic length in all genotypes (two-way ANOVA Ha2/5 antibody effect: $F_{(1,263)}=$ 32.36, $p<$ 0.0001), independent of FlnA

manipulations (two-way ANOVA genotype x antibody interaction: $F_{(2,263)}= 2.016$, $p= 0.1353$). Data presented as mean± SEM.

Next, as one of the first immediate downstream effector of β_1 integrin pathway, focal adhesion kinase (FAK) activity was inhibited in hippocampal neurons with a similar experimental setup (Ivankovic-Dikic *et al.*, 2000). This will allow for further examination of the interaction between FlnA mediated dendritic morphology and β_1 integrin mediated downstream cascade.

1.7 WT FlnA mediated dendritic hypertrophy can persist under FAK inhibition

To pharmacologically inhibit FAK activity during dendritic branching, acutely transfected hippocampal neurons were treated with 1μM Y15 (also known as 1,2,4,5-benzenetetraamine tetrahydrochloride), a specific FAK inhibitor (Monje *et al.*, 2012) from DIV4 for 2 days and fixed at DIV6 for dendritic tracing as previously. Since FAK activity is crucial for dendritic development, 48 hours of Y15 treatment impaired the overall dendritic arborization in neurons (repeated two-way ANOVA inhibitor effect: $F_{(1,56)}= 18.36$, $p< 0.0001$; Figure 24A). Similarly, a strong decrease in shFlnA mediated dendritic hypertrophy can be observed when FAK is inhibited (repeated two-way ANOVA inhibitor effect: $F_{(1,58)}= 44.04$, $p< 0.0001$; Figure 24B). In human WT FlnA expressing neurons, Y15 inhibitor again disrupted the overall dendritic arborization, while this reduction was not notable throughout all measured distances and as profound as in control and shFlnA neurons (repeated two-way ANOVA inhibitor effect: $F_{(1,58)}= 8.705$, $p= 0.0046$; Figure 24C). To distinguish the FlnA genotype-specific interactions to the FAK activity, data is further analyzed per treatment. In control treatment group (DMSO only), while there were not an overall change in dendritic branching between genotypes (repeated two-way ANOVA genotype effect: $F_{(2,85)}= 1.352$, $p= 0.2643$), both FlnA silencing and overexpression led to an increased arborization

in proximal (until around 60 μm) regions (repeated two-way ANOVA genotype x distance interaction: $F_{(78, 3315)}= 2.310$, $p< 0.0001$; Figure 24D). On the other hand, as WT FlnA expressing neurons still display increased dendritic branching compared to shLuc neurons (repeated two-way ANOVA genotype effect: $F_{(2,87)}= 6.907$, $p= 0.0016$; Fisher LSD, $p= 0.0017$), FAK inhibition completely abolished shFlnA mediated dendritic hypertrophy (Fisher LSD, $p= 0.9695$; Figure 24E).
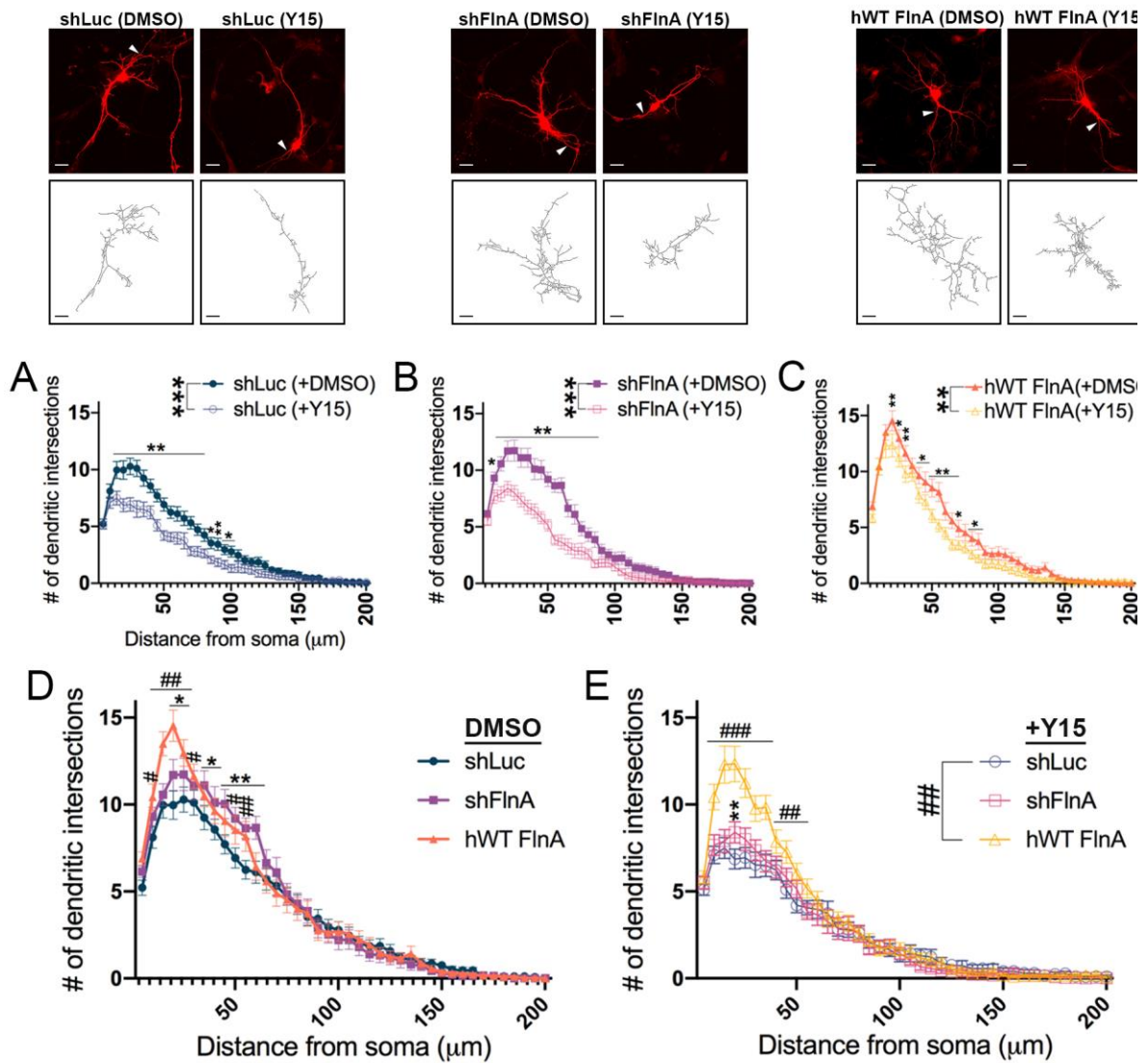
Figure 24: WT FlnA mediated dendritic arborization does not depend on FAK activity.
Hippocampal neurons are seeded on PDL coverslips, transfected with shLuc, shFlnA or shFlnA hWT FlnA constructs, treated FAK inhibitor (Y15, 1 μM), fixed at DIV6 and dendrites were traced using tdTom signal of transfected neurons. Scale bars: 20 μm (N= 2, n= 30 per group) **(A)** FAK inhibition from DIV4 to DIV6 significantly reduced arborization of control neurons (repeated two-way ANOVA inhibitor effect: $F_{(1,56)}$= 18.36, $p<$ 0.0001). **(B)** A drastic decrease in shFlnA mediated dendritic hypertrophy was observed when FAK is inhibited (repeated two-way ANOVA inhibitor effect: $F_{(1,58)}$= 44.04, $p<$ 0.0001). **(C)** In human WT FlnA expressing neurons, Y15 inhibitor also disrupted the overall dendritic arborization, while this reduction was not notable throughout all measured distances as in control and shFlnA neurons (repeated two-way ANOVA inhibitor effect: $F_{(1,58)}$= 8.705, $p=$ 0.0046). **(D)** Both FlnA silencing and overexpression lead to increased arborization in proximal (until around 60 μm) regions (repeated two-way ANOVA genotype x distance interaction: $F_{(78, 3315)}$= 2.310, $p<$ 0.0001), although no overall change in dendritic branching between genotypes was observed (repeated two-way ANOVA genotype effect: $F_{(2,85)}$= 1.352, $p=$ 0.2643). **(E)** On the other hand, hWT FlnA expressing neurons still display increased dendritic branching compared to shLuc neurons (repeated two-way ANOVA genotype effect: $F_{(2,87)}$= 6.907, $p=$ 0.0016; Fisher LSD, $p=$ 0.0017), while FAK inhibition completely abolished shFlnA mediated dendritic hypertrophy (Fisher LSD, $p=$ 0. 9695). Data presented as mean± SEM, post-hoc comparison: * is shLuc vs shFlnA, # is shLuc vs hWT FlnA.

Inhibition of FAK activity in neurons from DIV4 to DIV6 significantly decreased total dendritic length in all genotypes (two-way ANOVA inhibitor effect: $F_{(1,272)}$= 66.87, $p<$ 0.001) independent of FlnA manipulations (two-way ANOVA genotype x inhibitor interaction: $F_{(2,172)}$= 2.420, $p=$ 0.0919); re-iterating the crucial role of FAK activity for neurite extension (Figure 25).
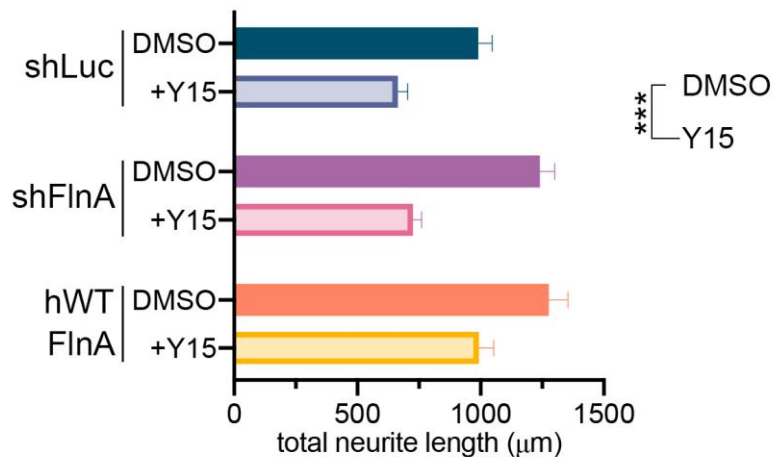
Figure 25: Focal adhesion kinase is indispensable for dendritic growth of hippocampal neurons.
Total dendritic lengths of the neurons under DMSO and FAK inhibitor Y15 were also analyzed Treatment of neurons with FAK inhibitor significantly reduced dendritic length in all genotypes (two-way ANOVA inhibitor effect: $F_{(1,272)}$= 66.87, $p<$ 0.001), independent from FlnA manipulations (two-

way ANOVA genotype x inhibitor interaction: $F_{(2,172)}= 2.420$, $p= 0.0919$). Data presented as mean$\pm$ SEM.

1.8 Efficient transduction neuronal cultures with lentiviral particles

In summary, numerous transfection and pharmacological assays have been conducted to analyze dendritic morphology via Sholl analysis of fluorescently filled hippocampal neurons. Results indicating the potential of role of FlnA in dendritic arborization have been observed throughout these experiments. However, biochemical aspects of the FlnA mediated dendritic hypertrophy, regarding to intracellular pathways, remained unexplored. Compared to calcium phosphate transfection method used before, which resulted into sparse transfection of neurons thus allowing tracing of morphology, higher gene transfer efficiency into confluent neurons is required for biochemical analysis via Western blotting. Lentiviral systems are often used for such experiments (Ritter *et al.*, 2017). However, in our hands, using lentiviral particles in vitro often resulted fluorescent labelling glial cells rather than differentiating neurons in culture (Figure 26C). This could be due to CMV promoter present in the transfer plasmids, which contains cAMP-response elements and can be upregulated with neuronal activity (Wheeler and Cooper, 2001). Accordingly, this approach is tested with a routinely used control lentivirus (shRandom) on primary hippocampal neurons (Figure 26A). Cells were transduced at DIV2, depolarization of neurons were induced by increasing K^+ in media (20 mM KCl wash-in DIV6-7) and they were fixed at DIV8 for fluorescent analysis (Figure 26B). GFP labelling from the lentivirus could exclusively detected in non-neuronal (MAP2 negative) cells under basal conditions. Nevertheless, depolarization caused by 20 mM KCl treatment of cells induced the CMV promoter and GFP expression also in neurons (Figure 26C), without obvious effects on neuronal growth and differentiation (Wheeler and Cooper, 2001). This approach is further employed for high efficiency lentiviral transduction of neurons to silence FlnA and consequent biochemical analysis of intracellular kinases.
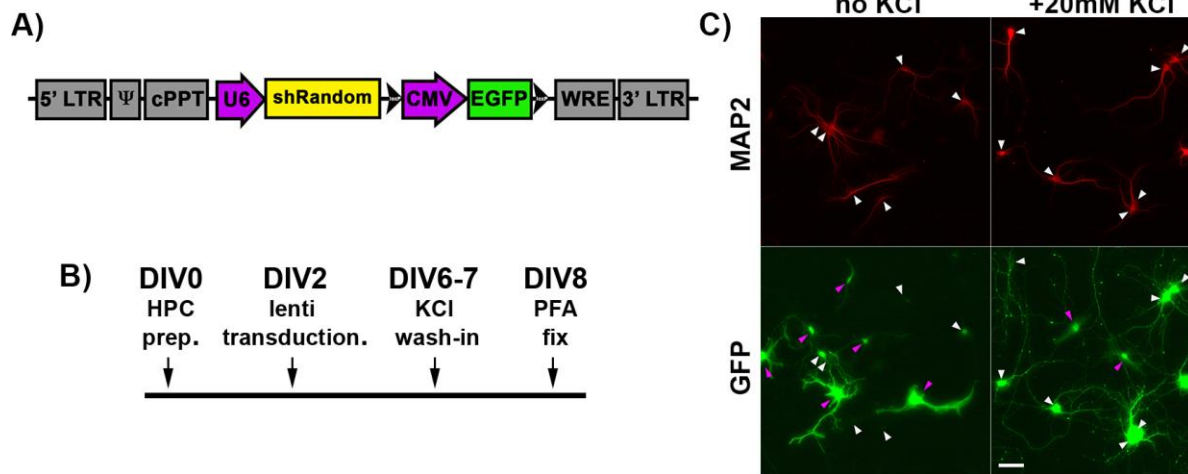
Figure 26: CMV promoter activity in developing neurons is induced by neuronal activity.
(A) A non-targeting shRNA hairpin in the same lentiviral shRNA backbone as in shLuc and shFlnA plasmids. **(B)** Hippocampal neurons were transduced at DIV2, neuronal activity was induced with 20mM KCl at DIV6 and cells were fixed at DIV8. **(C)** MAP2 to distinguish neurons and GFP for viral labelling were visualized (white arrows show the MAP2 positive neurons, while purple arrows point the MAP2 negative glial cells). Results show that only non-neuronal cells show the GFP expression under basal conditions, while 20 mM KCl increases the neuronal expression of the lentiviral marker. Scale bars: 50 μm.

1.9 Lack of FlnA causes abnormal Akt phosphorylation after integrin receptor stimulation

Once the morphological effects of FlnA manipulation in hippocampal neurons was demonstrated, next, intracellular pathways that causes this hypertrophy was investigated. For this reason, two important mediators of dendritic growth, FAK (Schlomann *et al.*, 2009) and Akt signaling pathway (Jaworski *et al.*, 2005; Kumar *et al.*, 2005) was examined in FlnA knockdown cortical neurons using the highly efficient lentiviral system (Figure 27A). First, neurons were transduced at DIV2 with control and shFlnA lentiviruses and directly lysed at DIV5. Western blotting of these probes (Figure 27B) demonstrated a significant decrease only in FlnA levels in shFlnA neurons (n= 4, two-tailed Student's t-test, *p*= 0.0263). Moreover, pAkt308/Akt and pAkt473/Akt measures

showed a very minor increase in FlnA silenced neurons rather than any significant change, mostly due to high variability of the signals (Figure 27C).

To synchronize all the neurons in basal conditions, next, neurons were serum starved for 2 hours and then stimulated with 10 μg/ml Fibronectin and 500 μM MnCl2 (ligand and co-factor respectively) for controlled activation of integrin receptor mediated intracellular pathways (Tan *et al.*, 2011; Yousif, 2014). As expected, FlnA levels stayed significantly lower in shFlnA virus transduced cells throughout the stimulation (two-way ANOVA genotype effect: $F_{(1,24)}$= 39.30, *p*< 0.0001, Figure 27D). As before, pFAK397/FAK ratio did not differ neither over time nor between genotypes (two-way ANOVA treatment effect: $F_{(3,24)}$= 0.9988, *p*= 0.4104, genotype effect: $F_{(1,24)}$= 0.0944, *p*= 0.7613; Figure 27E). Finally, pAkt308 and pAkt473 to total Akt levels were analyzed after integrin receptor stimulation. First, integrin stimulation significantly increased the phosphorylation of both pAkt308 (two-way ANOVA treatment effect: $F_{(3,24)}$= 33.92, *p*< 0.0001) and pAkt473 (two-way ANOVA treatment effect: $F_{(3,24)}$= 19.54, *p*< 0.0001) over time and integrin mediated pAkt increase significantly interacted with FlnA genotype (two-way ANOVA genotype x time interaction: $F_{(3,24)}$= 3.410, *p*= 0.0337 and $F_{(3,24)}$= 12.79, *p*< 0.0001 for pAkt308/Akt and pAkt473/Akt respectively). 30 minutes after stimulation, shFlnA neurons display significantly enhanced pAkt308 phosphorylation compared to control neurons (Fisher LSD, *p*= 0.0032; Figure 27F). Although control neurons have increased pAkt473/Akt levels at 15 minutes (Fisher LSD, *p*= 0.0169), shFlnA neurons again showed an abrupt 5-fold increase pf Akt-473 phosphorylation at 30 minutes (Fisher LSD, *p*< 0.0001) after acute integrin stimulation (Figure 27G).
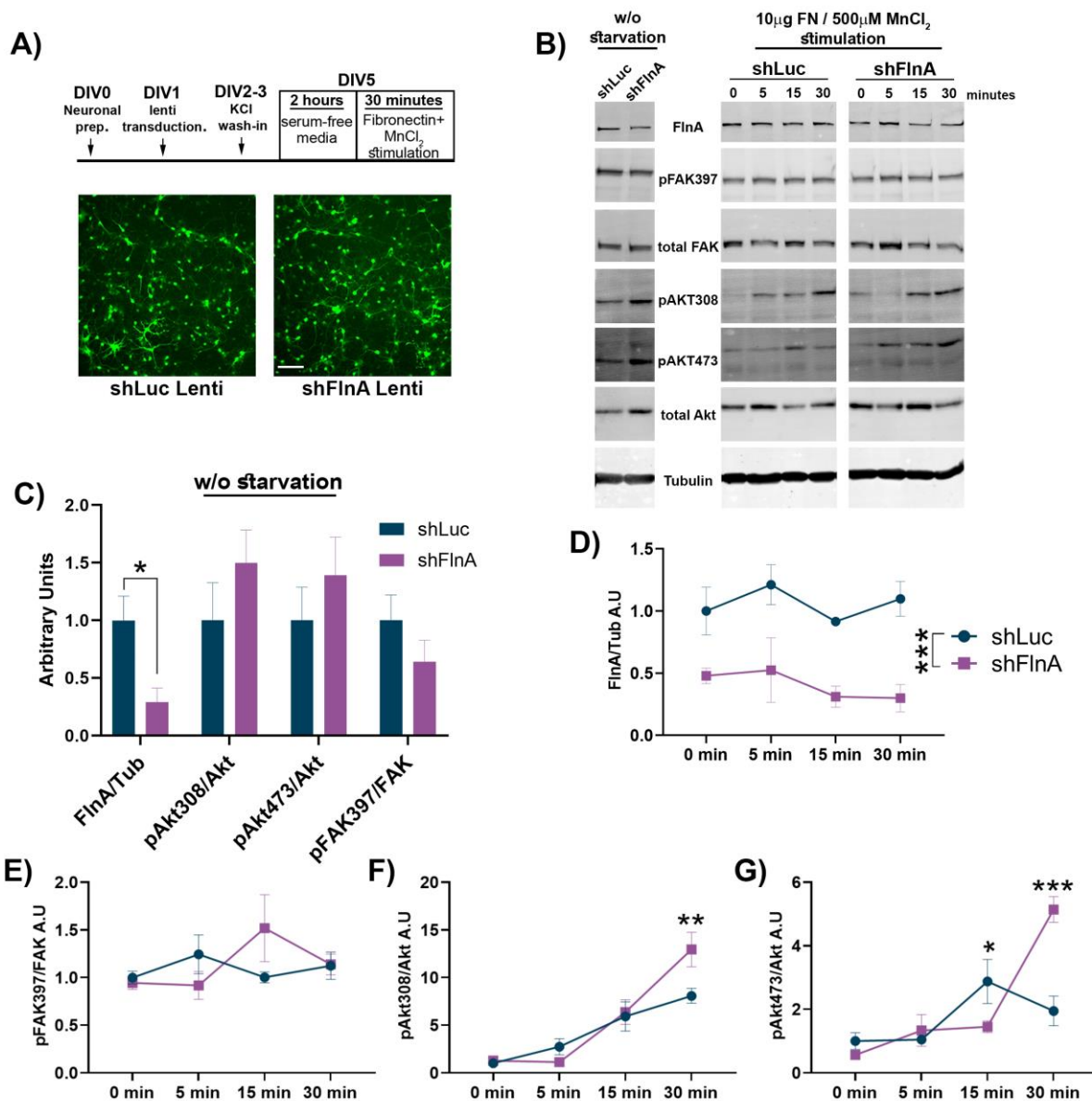
Figure 27: shFlnA neurons display significantly increased Akt activation upon integrin receptor stimulation.

(**A**) Cortical neurons were transduced at DIV1 with control or shFlnA lentiviruses (representative GFP labelling below, Scale bar: 100μm). At DIV5, neurons are serum-starved for 2 hours then integrin receptors are stimulated with Fibronectin and MnCl₂ indicated time points. (**B**) Similarly, one set of neurons are lysed directly without any starvation and samples are used for Western blotting. (**C**) In the cells that were lysed directly without any starvation/stimulation, FlnA signal was significantly less in shFlnA transduced cells (two-tailed Student's t-test, *p*= 0.0263). However, there were only trends of increase in the other measures. (**D**) As FlnA levels were also markedly reduced in shFlnA neurons that went under stimulation (two-way ANOVA genotype effect: $F_{(1,24)}$= 39.30, *p*< 0.0001), (**E**) pFAK397/FAK ratio was not changed over time (two-way ANOVA genotype effect: $F_{(1,24)}$= 0.0944, *p*= 0.7613). Finally, shFlnA neurons displayed increased levels of (**F**) pAkt308/Akt and (**G**) pAkt473/Akt ratios 30 minutes after integrin receptor stimulation (two-way ANOVA

genotype x time interaction: $F_{(3,24)}= 3.410$, $p= 0.0337$ and $F_{(3,24)}= 12.79$, $p< 0.0001$ respectively, Fisher LSD). Data presented as mean± SEM.

1.10 WT FlnA and dendritic branching

Using a lentiviral approach, acute integrin stimulations of shFlnA transduced neurons displayed an abrupt Akt activation, which could cause the shFlnA mediated dendritic hypertrophy in neurons. On the other hand, actin crosslinking by FlnA is a possible mechanism that mediates hWT FlnA mediated dendritic growth that was observed previously. Before examining the actin crosslinking by FlnA, first, pure overexpression of hWT FlnA is tested in neurons for its morphology effects. As control, pcDNA3, the empty backbone of FlnA expression construct, was used. While mouse shFlnA+human WT FlnA co-transfection again resulted to a dendritic hypertrophy; pure hWT FlnA expression resulted a more pronounced effect on dendrites (repeated two-way ANOVA genotype effect: $F_{(2,132)}= 19.66$, $p< 0.0001$, Fisher LSD; Figure 28A). When total dendritic length of these neurons was quantified, similar increase compared to control condition was observed (one-way ANOVA: $F_{(2,132)}= 21.93$, $p< 0.0001$, Fisher LSD). These results demonstrate that hWT FlnA can affect the dendritic growth independent of the co-introduced shRNA to silence endogenous mouse FlnA (Figure 28B).
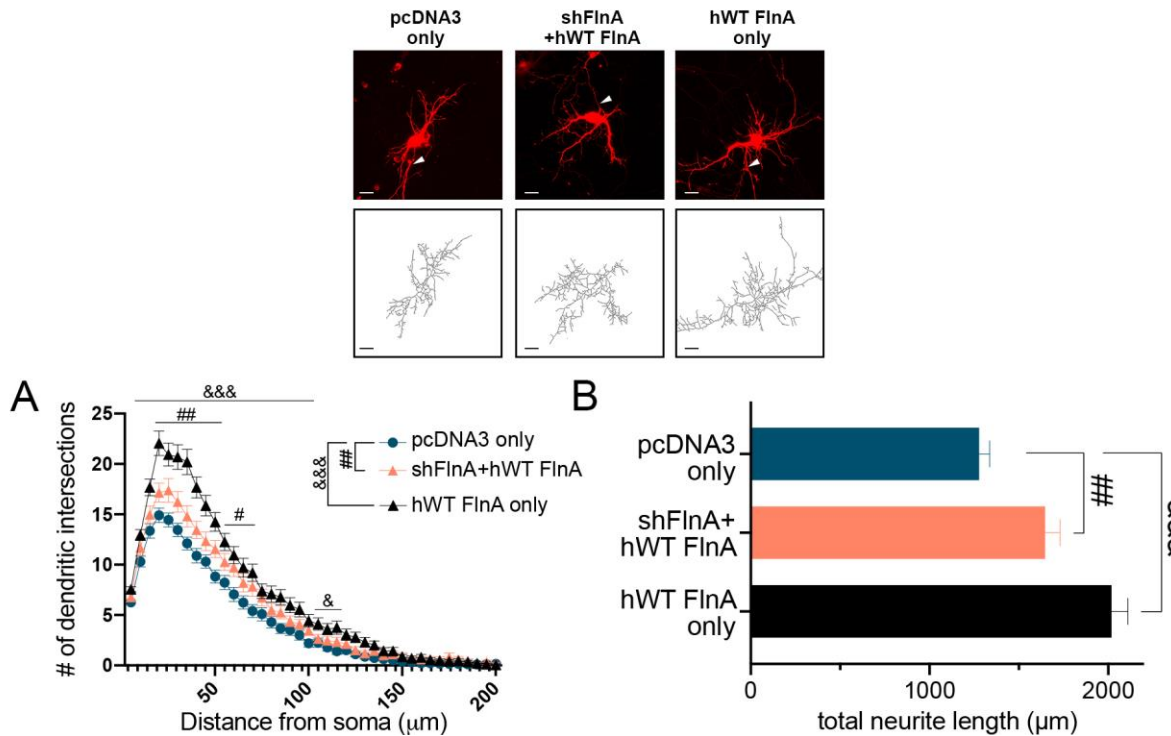
Figure 28: Pure overexpression of hWT FlnA in mouse hippocampal neurons enhances dendritic arborization and extension.
Hippocampal neurons are transfected with pcDNA3 empty backbone, shFlnA hWT FlnA or hWT FlnA only and fixed at DIV7. Dendrites were traced using tdTom signal of transfected neurons. Scale bars: 20 μm (N= 3, n= 45 per group). **(A)** While the previously used shFlnA hWT FlnA transfection setup caused a significant increase in dendritic arborization, pure hWT FlnA expression without any shRNA resulted the maximal arborization (repeated two-way ANOVA genotype effect: $F_{(2,132)}=$ 19.66, $p< 0.0001$, Fisher LSD). **(B)** Similar growth enhancement was observed when total dendritic length of the neurons is analyzed (one-way ANOVA: $F_{(2,132)}= 21.93$, $p< 0.0001$, Fisher LSD). # is pcDNA3 vs shFlnA hWT FlnA; & is pcDNA vs hWT FlnA only. Data presented as mean± SEM.

Next, role of actin crosslinking by FlnA in hippocampal dendritic growth is tested. To do so, a mutant FlnA construct is acquired in which the dimerization domain (Ig24) is missing (kindly provided by Dr. Fumihiko Nakamura, (Nakamura *et al.*, 2007)). This ΔIg24 mutant cannot form the FlnA V-shape structure and crosslink the actin cytoskeleton as the wild type form (Figure 29A). Hippocampal neurons are transfected with the pcDNA3 empty backbone, hWT FlnA only or ΔIg24 mutant forms at DIV3 and fixed at DIV7 to trace their dendrites (Figure 29B). hWT FlnA expression in hippocampal neurons caused an overall increase of dendritic arborization (repeated

two-way ANOVA genotype effect: $F_{(2,131)}= 7.577$, $p< 0.0008$, Fisher LSD). More importantly, the ΔIg24 mutant failed to induce such dendritic hypertrophy compared to control neurons ($p= 0.1320$; Figure 29C). Like dendritic branching, ΔIg24 FlnA was incapable of enhancing total dendritic length compared to control cells, while hWT FlnA significantly stimulated dendritic growth (one-way ANOVA: $F_{(2,131)}= 14.26$, $p< 0.0001$, Fisher LSD; Figure 29D).
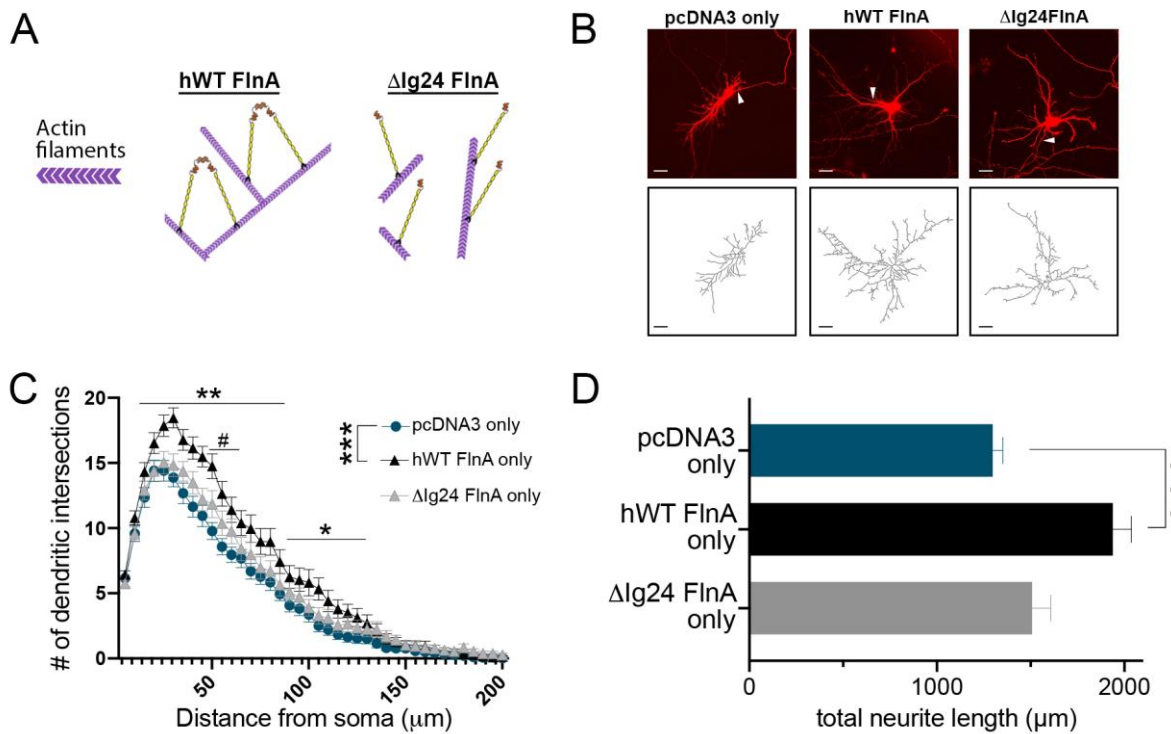
Figure 29: Efficient actin crosslinking by FlnA is required for hWT FlnA mediated dendritic growth.
(A) ΔIg24 mutant of FlnA does not contain the 24 Ig repeat which is the dimerization domain of the FlnA homodimer. Thus, this mutant cannot crosslink the actin microfilaments as its wild type of isoform. **(B)** Hippocampal neurons are transfected with empty pcDNA3, hWT FlnA and ΔIg24 FlnA constructs, fixed at DIV7 and dendrites were traced using tdTom signal of transfected neurons. Scale bars: 20 μm (N= 3, n= 45 per group). **(C)** While hWT FlnA can cause dendritic hypertrophy (repeated two-way ANOVA genotype effect: $F_{(2,131)}= 7.577$, $p= 0.0008$, Fisher LSD); ΔIg24 FlnA cannot significantly increase the dendritic arborization compared to control neurons ($p= 0.1320$). **(D)** Similar to dendritic branching, ΔIg24 FlnA failed to increase total dendritic length of neurons as in WT form

(one-way ANOVA: $F_{(2,132)}= 14.26$, $p< 0.0001$, Fisher LSD). * is pcDNA3 vs hWT FlnA only; # is pcDNA3 vs ΔIg24 FlnA only. Data presented as mean± SEM.

Lastly, role of Serine 2152 phosphorylation of FlnA was tested during dendritic branching of hippocampal neurons. To this end, we have acquired the phosphodeficient mutant of human WT FlnA, in which the conserved Serine-2152 residue is converted to Alanine (S2152A) via site-directed mutagenesis (Woo *et al.*, 2004; Figure 30A). Hippocampal neurons are then transfected with shFlnA targeting endogenous mouse FlnA and co-transfected either with WT or S2152A FlnA constructs at DIV3. Besides PDL, S2152A FlnA transfected neurons were also tested on Fibronectin substrate to further explore the interaction between S2152 phosphorylation and integrin activation (Figure 30B). Analysis of transfected neurons on DIV7 revealed no significant difference between genotypes neither in dendritic branching (repeated two-way ANOVA genotype effect: $F_{(2,84)}= 0.6574$, $p= 0.5208$; Figure 30C) nor in total dendritic length (one-way ANOVA: $F_{(2,84)}= 1.405$, $p= 0.2510$; Figure 30D).
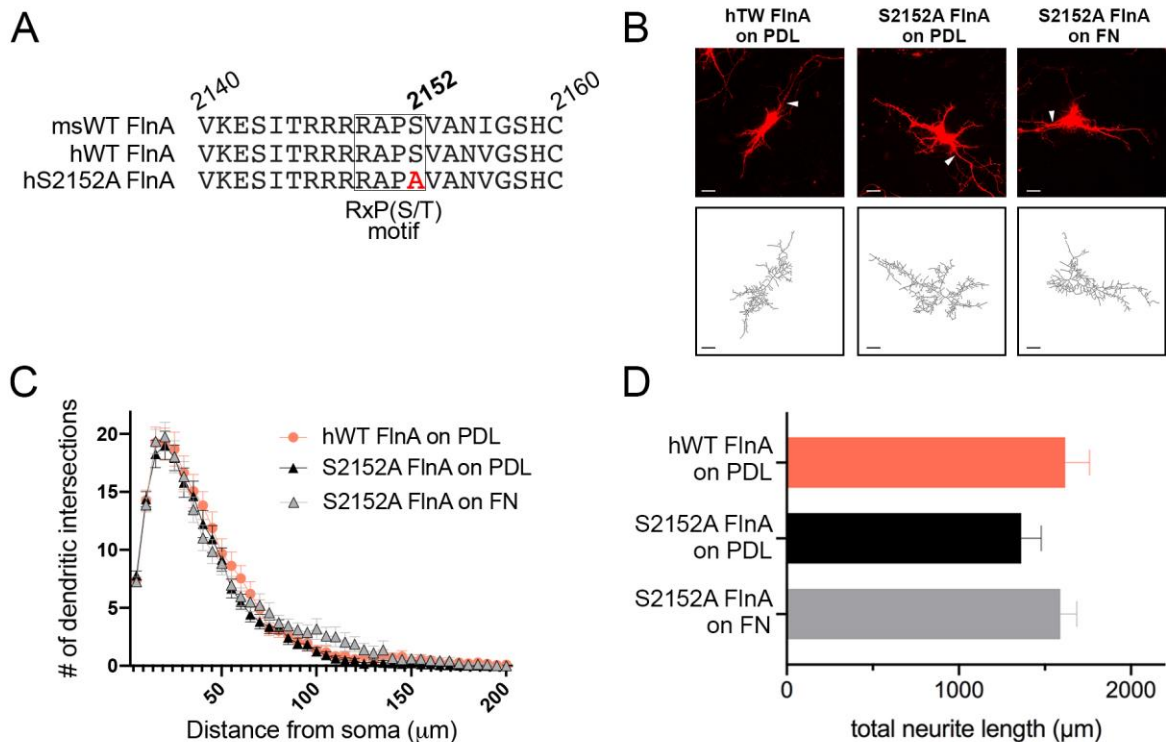
Figure 30: Serine 2152 phosphorylation of FlnA does not play an important role during dendritic branching.
(A) Alignment of wild type mouse, wild type human and phosphodeficient (S2152A) human FlnA protein sequences. Serine-2152 residue can be seen in the previously identified RxP(S/T) motif of Ndr2 kinase. **(B)** Hippocampal neurons are transfected with empty shFlnA and co transfected with either hWT or S2152A FlnA constructs, fixed at DIV7 and dendrites were traced using tdTom signal of transfected neurons. Scale bars: 20 μm (N= 2, n= 30 per group). **(C)** Quantification of dendritic arborization showed no significant difference between groups (repeated two-way ANOVA genotype effect: $F_{(2,84)}$= 0.6574, p= 0.5208). **(D)** Similar to dendritic branching, S2152A FlnA did not cause any significant difference in total dendritic length compared to WT FlnA expressing neurons (one-way ANOVA: $F_{(2,84)}$= 1.405, p= 0.2510). Data presented as mean± SEM.

1.11 Developing new tools for manipulation of endogenous FlnA

Finally, to efficiently silence or overexpress FlnA protein in mouse brains in vivo, series of experiments were conducted to establish a state-of-the-art CRISPR/Cas9 system. First, a conventional Cas9 is used to target FlnA gene to ablate the FlnA protein expression. Later, different systems using catalytically dead Cas9 mutants (dCas9) that are fused to transcriptional activators were targeted to promoter region to enhance FlnA gene expression.

1.11.1 CRISPR knockout of FlnA via Cas9 editing system

The Cas9 nuclease from bacteria, when targeted to a specific location in the genome by guide RNAs (gRNA), creates a double stranded break on the DNA. This break then undergoes non-homologous end joining repair, which often results to mutations that cause loss of function with in the target exon (Joung *et al.*, 2017). GFP tagged Cas9 nuclease from Streptococcus pyogenes (Cas9-EGFP, Chen *et al.*, 2015) and a U6 driven gRNA plasmid that has a mCherry tag (Savell *et al.*, 2019) were acquired in lentiviral backbones (Figure 31A). Four different gRNAs targeting mouse endogenous FlnA gene was designed using the Broad Institute-Genetic Perturbation Platform and cloned into the gRNA-mCherry backbone (Figure 31B). To test this CRISPR/Cas9 system for FlnA silencing, mouse fibroblasts were co-transduced with lentiviruses of these constructs. Before lysis, both GFP from Cas9 and mCherry from gRNA backbone were detected

to confirm the transduction (Figure 31C). However, both 10 and 15 days of incubation after viral

infusion did not cause any reduction in FlnA protein levels (Figure 31D-E).
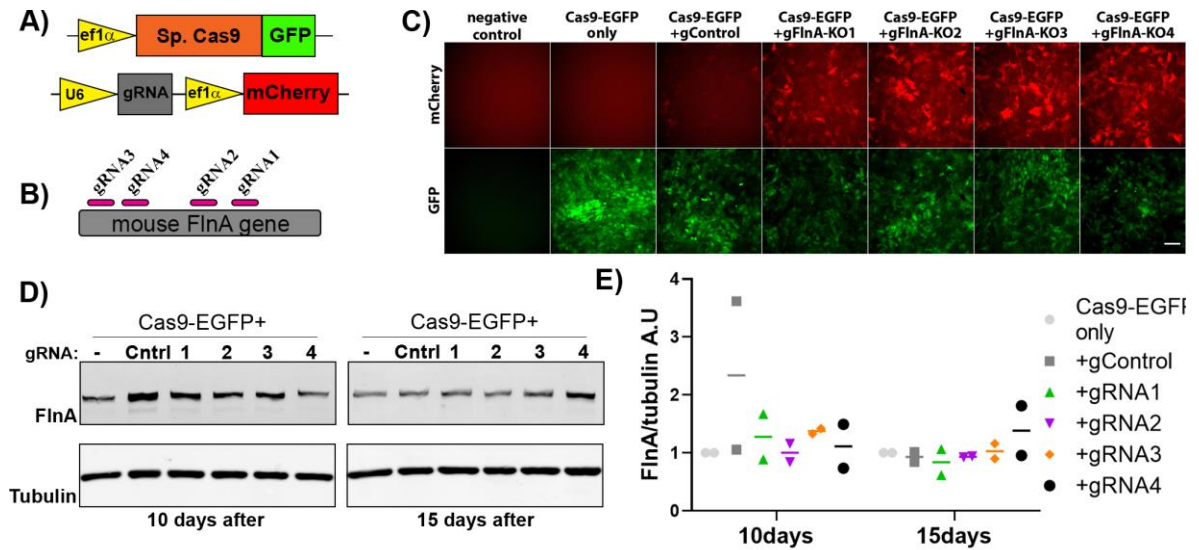
Figure 31: Lentiviral delivery of Cas9-GFP and gRNA-mCherry to disturb FlnA gene in NIH3T3 cells.
(A) Lentiviral particles were produced using ef1α-Cas9-GFP and U6-gRNA(mCherry) targeting (B) mouse FlnA gene for genome editing. (C) NIH3T3 fibroblasts are transduced with both viruses and transduction of both cassettes is confirmed with GFP/ mCherry expression (Scale bar: 100 μm). (D) Cells were lysed at indicated time points and lysates were used in Western blotting against FlnA. (E) Quantification of the FlnA signal did not reveal any robust change in FlnA protein levels compared to control cells (n= 2).

Next, a single-AAV system that contains a shorter Cas9 homolog (from Staphylococcus aureus)

and a U6-driven gRNA (which still stays below the AAV packaging limit) was used for to target

mouse FlnA gene (Figure 32A; Ran *et al.*, 2015). Same four gRNAs that were used in the lentiviral

system similarly cloned into this pAAV backbone under the U6 promoter (Figure 32B). Cortical

neurons were transduced using these AAVs at DIV1 and cells were lysed at DIV13. Since there

were no fluorescent tag in this AAV, to confirm viral production/transduction, a CAG-driven

tdTom AAV is produced and transduced in parallel (Figure 32C, right panel). Western blotting

against FlnA demonstrated a strong decrease of protein levels in FlnA targeting guide RNAs

compared to non-targeting control gRNA. HA-tag of the Cas9 AAV was also detected in transduced neurons, except for the fluorescence control pAAV-CAG-tdTom, which HA tag is not present (Figure 32C).
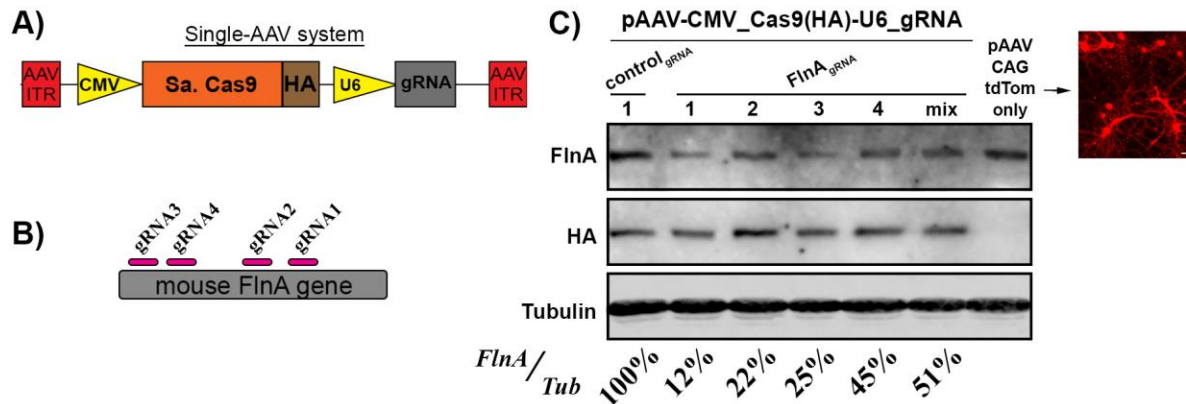
Figure 32: Single-AAV system to deliver Cas9 and gRNA for FlnA genome editing.
(**A**) AAV transfer plasmid containing HA-tagged Sa. Cas9 and U6 driven gRNA cassette targeting (**B**) mouse FlnA gene for genome editing. (**C**) Mouse cortical neurons are transduced with the single Cas9-AAV, along with a simultaneously produced CAG-tdTom AAV to confirm virus production/transduction (right panel, Scale bar: 20 μm). Neurons were lysed at 12 days after transduction (DIV13) and Western blotting against FlnA demonstrate notable decrease in FlnA levels with different guide RNAs targeting FlnA gene.

Finally, FlnA gRNAs were systematically tested in neurons to evaluate the different Cas9/gRNA AAVs, before the in-vivo grade production. To this end, each gRNA virus (including non-targeting control guide RNA) were made in three independent AAV production without ultracentrifugation. Cortical neurons were then transduced at DIV1 with 200 or 400 μl AAV containing supernatant at DIV1 and incubated for 12 further days. Neurons were lysed at DIV13 for protein extraction and Western blotting of the probes demonstrated a statistically significant reduction of FlnA protein using FlnA gRNAs compared to control gRNA, with FlnA gRNA2 displaying the most robust effect with least variation (Figure 33).
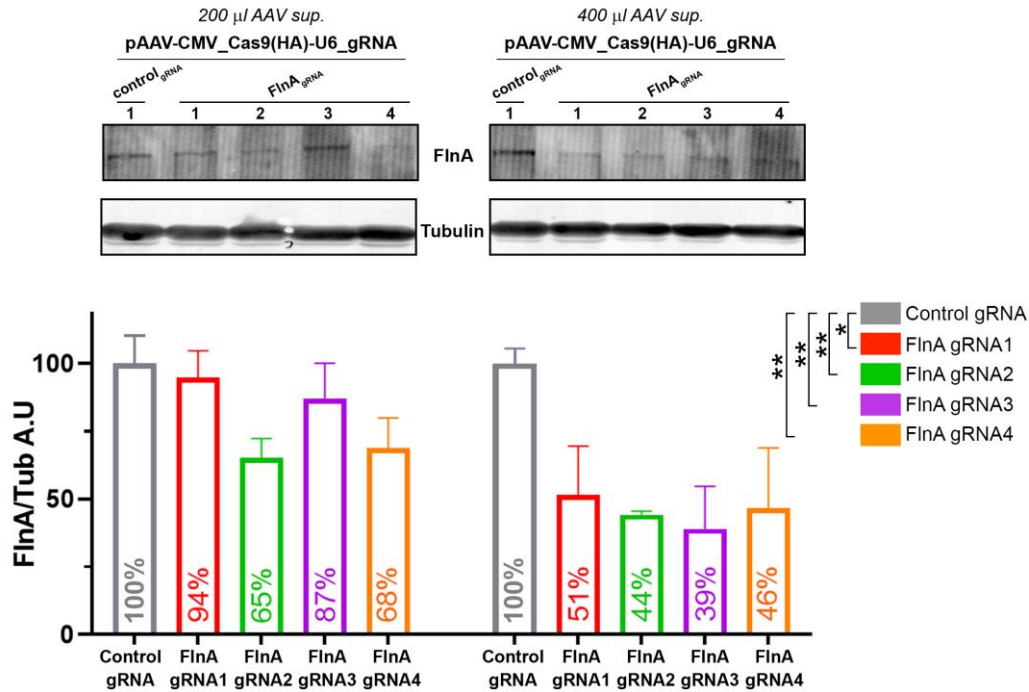
Figure 33: Cas9-AAV particles targeting FlnA gene significantly reduces FlnA protein in cortical neurons.
Three different batches of Cas9-gRNA AAVs (as in Figure 32**Error! Reference source not found.**) were produced in HEK293T cells and either 200 µl or 400 µl AAV supernatant used on cortical neurons at DIV1 (N= 3). 12 days after transduction, neurons were lysed directly, and probes used in Western blotting against FlnA. Although to different extends, each gRNA targeting the FlnA gene caused significant decrease in FlnA protein level in cortical neurons (two-way ANOVA genotype effect: $F_{(4,20)}= 4.067$, $p= 0.0143$; Fisher LSD). Data presented as mean± SEM.

1.11.2 Transcriptional activation FlnA expression via catalytically defective Cas9

Next, a transcriptional activation system was sought to be established in which catalytically defective Cas9 (dCas9) nucleases are directly fused to transcriptional activators are targeted to the promoter of mouse FlnA gene. Different dCas9 transcriptional activator systems have been tested with a tdTom fluorescent reporter system as a proof of principle experiment. tdTom fluorescent reporter is driven by a minimal CMV promoter (miniCMV) that has a very low basal activity and its expression can be achieved only upon targeting dCas9-fused transcriptional activators via promoter targeting guide RNAs.

First system that was tested contains a dCas9 fused to a VP64 activation domain (Joung *et al.*, 2017). Besides, the gRNA backbone that targets the dCas9-VP64 to the promoter contains MS2 loops which can further recruit the heterelougsly expressed p65-HSF1 activation domains for enhancement of transcription (Figure 34A-B). To test the system, a guide RNA targeting the promoter of tdTom (-100 of transcription start site) is cloned into the gRNA backbone for controlled activation of tdTom fluorescence via dCas9-VP64 (Figure 34C). HEK293T cells were transfected with the miniCMV_tdTom reporter along with either MS2-p65-HSF1 only, dCas9-VP64+gRNA$_{CMV}$ together or all three components together (Figure 34D). MS2-65-HSF1 transfection had no effect on tdTom expression (Figure 34D*1*), while dCas9-VP64/gRNA$_{CMV}$ co-transfection resulted a minimal increase in the fluorescence (Figure 34D*2*). Finally, combining the VP64 fused dCas9, miniCMV promoter targeting gRNA and p65-HSF1 transcriptional activators caused a very strong increase in tdTom fluorescence, indicating successful transcriptional activation (Figure 34D*3*).

87
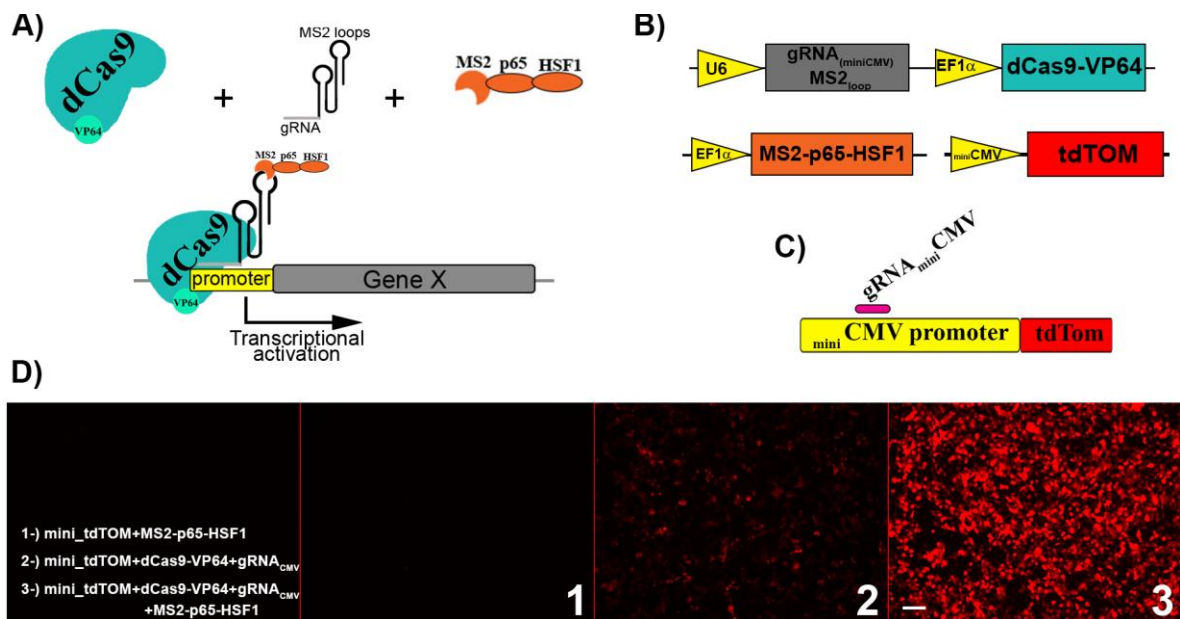
Figure 34: Transcriptional activation with dCas9-VP64 /MS2-p65-HSF1 system in HEK293T cells.
(A) General scheme of the transcriptional activation (adapted from Joung *et al.*, 2017). dCas9 fused to VP64 activation domain is guided to target promoter with guide RNA (sgRNA). Two different activation domains (p65 and HSF1) are further recruited via the MS2 loops. **(B)** U6-gRNA_ef1α-dCas9VP64 and ef1α-MS2-p65-HSF1 constructs used for transcriptional activation. **(C)** A minimal CMV promoter (miniCMV) driven tdTom is targeted with a gRNA as a reporter for dCas9 mediated activation. **(D)** HEK293T cells are transfected with mini_tdTom reporter plasmid and either with *(1)* MS2-p65-HSF1 alone, *(2)* dCas9-VP64_gRNA$_{CMV}$ alone or *(3)* dCas9-VP64_gRNA$_{CMV}$ and MS2-p65-HSF1 together (Scale bar: 100µm). A strong increase of tdTom fluorescence was observed upon co-transfection both gRNA and transcriptional activators.

Next, same gRNA backbone is used to clone in four different guide RNAs targeting upstream of mouse FlnA gene (-113, -159, -79 and -58 of transcription start site respectively) (Figure 35A-B). Mouse fibroblasts were transfected with the combination of dCas9/gRNA and p65-HSF1 plasmids and cells were lysed at indicated time points for Western blotting (Figure 35C). However, compared to non-targeting control guide RNAs, none of the FlnA gRNAs caused any transcriptional activation at 2 or 4 days after transfection (Figure 35D).
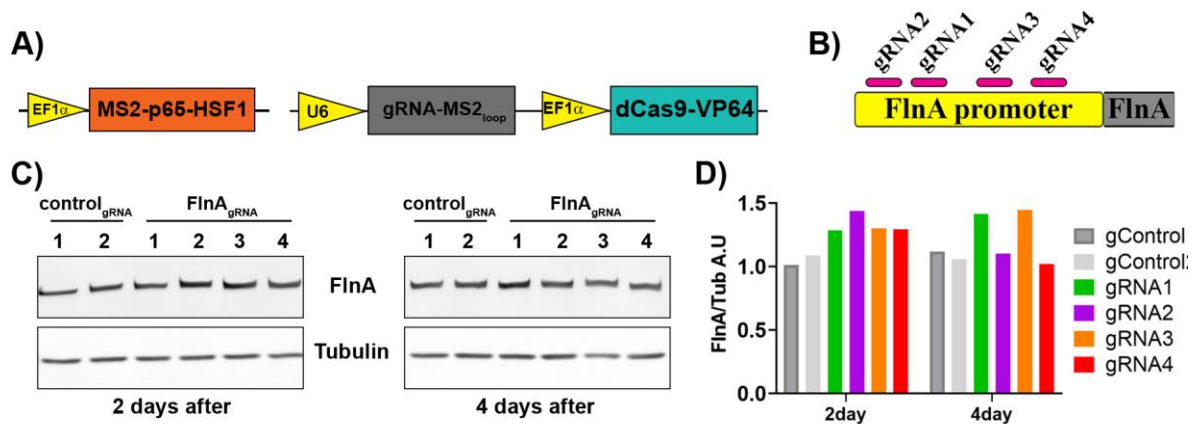
Figure 35: Targeting FlnA gene in NIH3T3 cells using dCas9-VP64 and MS2-p65-HSF1.
(A) ef1α-MS2-p65-HSF1 and U6-gRNA_ef1α-dCas9VP64 constructs used for transcriptional activation along with **(B)** 4 different guide RNAs targeting FlnA promoter. **(C)** Mouse NIH3T3 cells are transfected either with 2 control (non-targeting) or 4 different FlnA guide RNAs (along with MS2-p65-HSF1 activator plasmid). Cells were lysed at indicated timepoints after transfection and lysed for

western blotting. (D) Quantification of the FlnA signal did not reveal any robust change in FlnA protein levels compared to control cells.

There have been reports demonstrating that pooling of multiple gRNAs targeting same gene significantly increases Cas9 mediated modulation (Seki and Rutz, 2018; Savell *et al.*, 2019). Therefore, in a similar setup as before, multiple gRNAs that are targeting FlnA upstream are combined to increase FlnA gene expression. However, 3 days after transfection, different combinations of FlnA gRNAs did not result a significant change of FlnA expression in mouse fibroblasts (one-way ANOVA: $F_{(3,8)}=$ 0.1788, *p*= 0.9078, Fisher LSD; Figure 36).
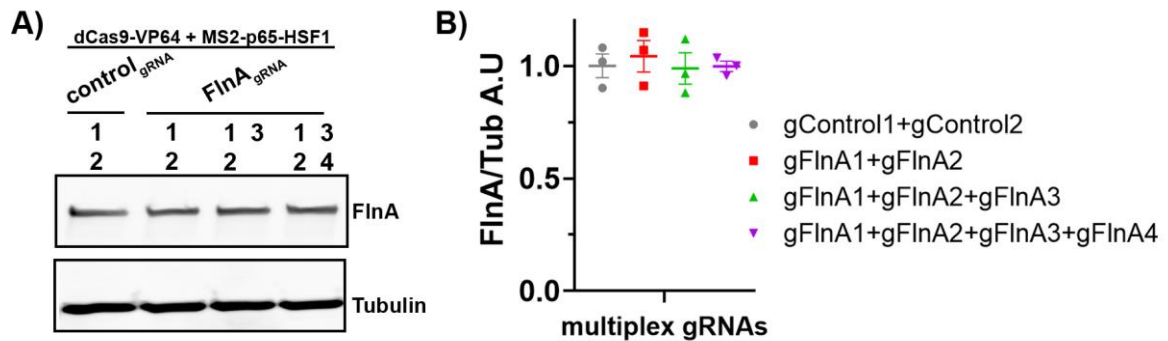
Figure 36: Targeting FlnA gene in NIH3T3 cells with multiplex gRNA sets.
(**A**) Mouse NIH3T3 cells are transfected with ef1α-MS2-p65-HSF1 and combination of FlnA targeting U6-gRNA_ef1α-dCas9VP64 constructs and lysates are used in Western blotting against FlnA. (**B**) Quantification of the FlnA signal did not reveal any change in FlnA protein levels compared to control cells (n= 3). Data presented as mean± SEM.

After observing that dCas9-VP64/gRNA/p65-HSF1 combination did not modulate the FlnA transcription, another, and simpler, dCas9 system in lentivirus backbone is acquired to test. In this setup, heterologous expression p65-HSF1 is not needed since dCas9 is already fused to VP64, p65 and Rta (VPR) activators (Figure 37A). This new dCas9 activator is used with tdTom reporter assay using a U6 driven gRNA plasmid (without MS2 loops) targeting miniCMV promoter (Figure 37B). When transfected in HEK293T cells without any guide RNA, both ef1α and synapsin driven dCas9-VPR did not show any nonspecific transcriptional modulation (Figure 37 C*1,2,3*). On the

other hand, when gRNA$_{CMV}$ is co-transfected, very robust induction of tdTom fluorescence can be detected in both dCas9-VPR constructs (Figure 37C*4,5*). Similar tdTom fluorescence induction upon miniCMV gRNA transfection was also observed in mouse NIH3T3 fibroblasts, confirming the efficiency of the dCas9-VPR mediated transcriptional activation (Figure 37D).
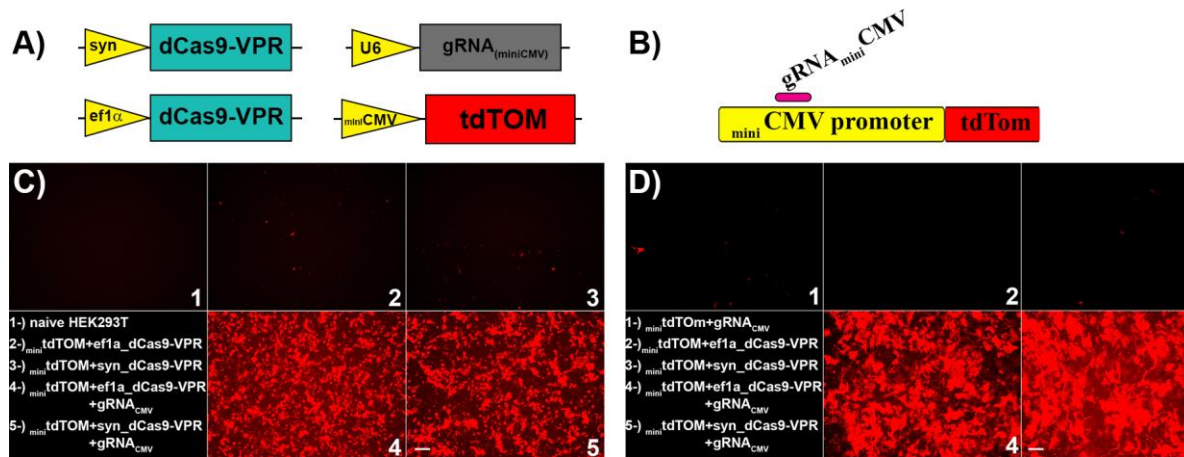
Figure 37: Transcriptional activation with two-vector dCas9-VPR / U6-gRNA system.
(**A**) Plasmids used in this assay (based on Savell *et al.*, 2019). dCas9-VPR either driven with synapsin or ef1α promoter and (**B**) a U6-gRNA targeting mini-CMV promoter. (**C**) *(1)* HEK293T cells are transfected with mini_tdTom reporter plasmid and co-transfected with *(2)* ef1α_dCas9-VPR only, *(3)* syn_dCas9-VPR only, *(4)* ef1α_dCas9-VPR + gRNA$_{CMV}$, *(5)* syn_dCas9-VPR + gRNA$_{CMV}$ plasmids. (**D**) NIH3t3 cells are transfected *(1)* tdTom reporter only, or co-transfected with *(2)* ef1α_dCas9-VPR only, *(3)* syn_dCas9-VPR only, *(4)* ef1α_dCas9-VPR + gRNA$_{CMV}$, *(5)* syn_dCas9-VPR + gRNA$_{CMV}$ plasmids. A robust increase in tdTom fluorescence can be observed upon co-transfection of gRNA and indicated Cas9 (Scale bars: 100μm).

For the delivery of dCas9-VPR and FlnA gRNAs, instead of previously used liposome mediated transient transfection, a lentiviral transduction approach is employed to have a stable integration of CRISPR components in the genome which would allow for much longer incubation times. Lentiviruses containing dCas9-VPR and FlnA gRNA/mCherry constructs (Figure 38A-B) are used on mouse fibroblasts and mCherry expression were detected before lysis, showing successful viral integration of at least the gRNA plasmid (Figure 38C). Cells were lysed at indicated time points

for Western blotting (Figure 38D). However, FlnA expression again did not change notably compared to control guide RNAs in neither 10 or 15 days after lentiviral transduction.
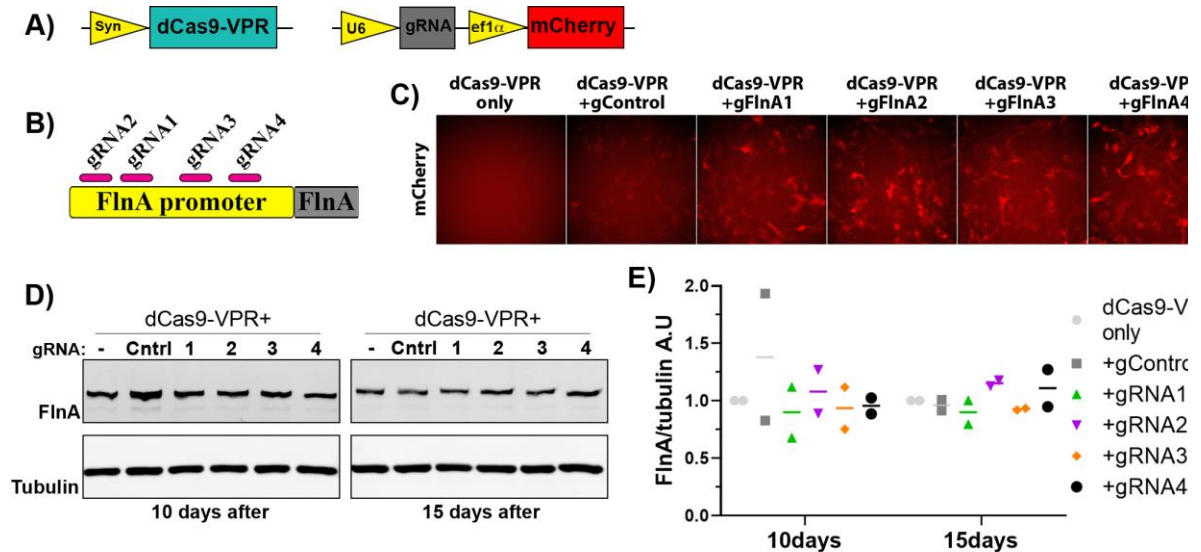
Figure 38: Lentiviral delivery of dCas9-VPR and U6-gRNA in NIH3T3 cells.
(**A**) Lentiviral particles were produced using synapsin-dCas9-VPR and U6-gRNA(mCherry) targeting (**B**) mouse FlnA promoter. (**C**) NIH3T3 fibroblasts are transduced with both viruses and transduction is confirmed with mCherry expression (Scale bar: 100 μm). (**D**) Cells were lysed at indicated time points and lysates were used in Western blotting against FlnA. (**E**) Quantification of the FlnA signal did not reveal any robust change in FlnA protein levels compared to control cells (n= 2).

Since dCas9 mediated transcriptional activation can be affected by basal expression level of the target gene in the tissue (Chavez *et al.*, 2015; Konermann *et al.*, 2015), dCas9-VPR lentiviral particles were finally tested in cortical neurons. Neurons were transduced at DIV1 and lysed at DIV13 for protein extraction and Western blotting (Figure 39A-B). Although nuclei-targeted mCherry signal can be detected in neurons before lysis, FlnA levels did not notably increase compared to control Grna (Figure 39C).
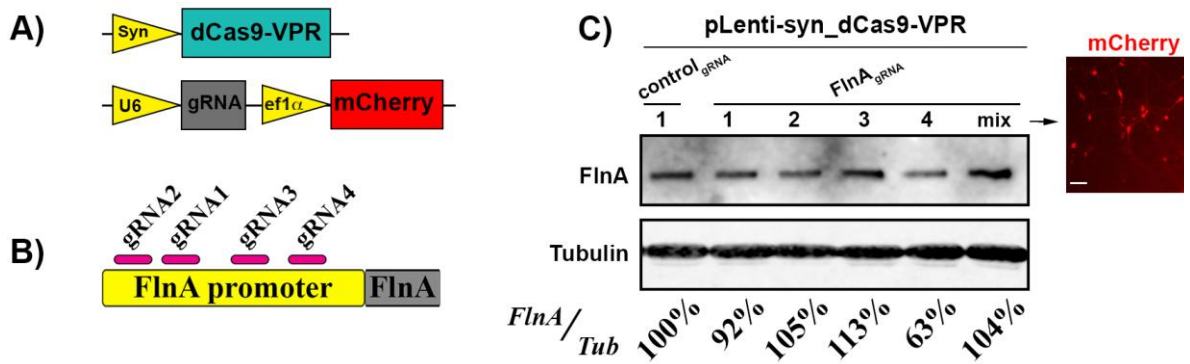
Figure 39: Lentiviral delivery of syn-dCas9-VPR and U6-gRNA to mouse cortical neurons.
(A) Lentiviral particles were produced using synapsin-dCas9-VPR and U6-gRNA(mCherry) targeting **(B)** mouse FlnA promoter. **(C)** Mouse cortical neurons are transduced with both viruses at DIV1 and proteins were extracted at DIV13 for western blotting, However, as in case of mouse fibroblast, FlnA signal did not show any notable change compared to control gRNA. Viral transduction is confirmed with mCherry expression before lysis (Scale bar: 50 μm).

While gRNA expression can be detected due to its mCherry tag, co-expression of the dCas9-VPR cassette within the same cell could not be confirmed before lysis due to lack of a live-fluorescent tag. Finally, to check the FlnA levels in a double positive cell (expressing both gRNA and dCas9-VPR), neurons were transfected with the same constructs at DIV3 and fixed at DIV7 for staining. Immunocytochemistry against FlnA demonstrated no change of FlnA levels in a dCas9-VPR/gRNA expressing neurons compared to any neighboring untransfected cells (Figure 40A). As a positive control of FlnA overexpression, neurons were transfected with control or shFlnA+hWT FlnA combination as previously and stained for total FlnA. Here, a very robust increase in FlnA signal can be observed after introduction of human WT form, which also confirms the inefficiency of the FlnA targeting of dCas9 approach so far for the transcriptional activation (Figure 40B).
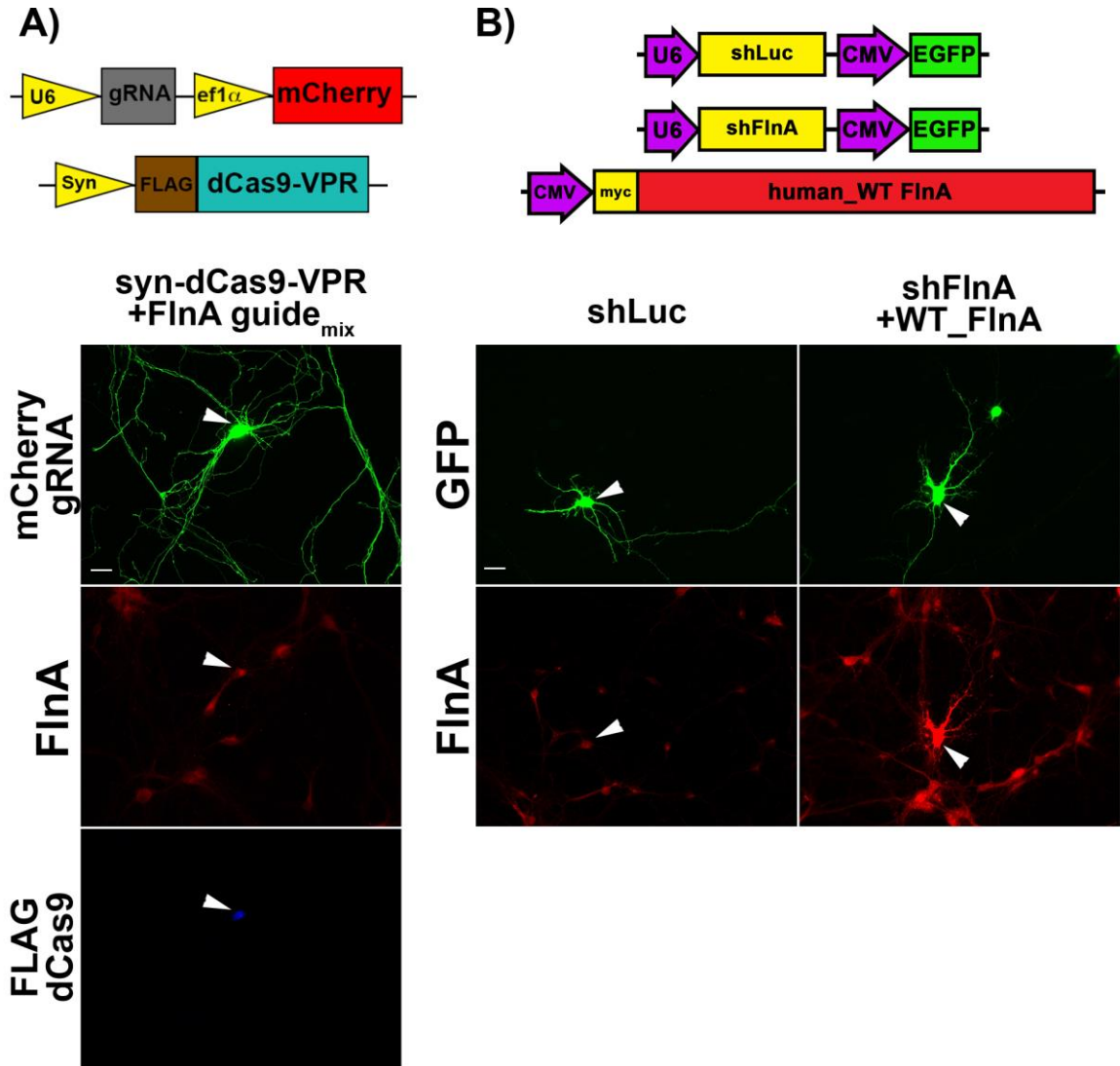
Figure 40: Hippocampal neurons co-transfected with dCas9-VPR and FlnA-gRNA mix.
(**A**) Neurons were immunostained against FlnA and FLAG tag after co-transfection of dCas9-VPR and FlnA gRNA mix. Representative co-transfected neurons can be seen with white arrow (positive for both mCherry and FLAG tag), which does not show a transcriptional over activation of FlnA levels. (**B**) When previously used control and shFlnA FlnA transfection setups were applied as positive control, a robust overexpression caused by human FlnA plasmid can be observed. Scale bar: 20 μm.

DISCUSSION

Integrins form an important signaling hub on the membrane that controls the neuronal development. They signal bidirectionally where both extracellular and intracellular components can act on. The latter comprise of signaling proteins that can bind to intracellular tail of integrin receptors and contribute to tight regulation of integrin activity, called as inside-out signaling. In this study, two intracellular proteins, Ndr2 kinase, a target of Hippo pathway in brain; and its recently described downstream substrate, Filamin A, were investigated for their role in integrin inside-out signaling. Experiments were designed to test their critical function in dendritic arborization regarding ECM specificity, integrin engagement and actin cytoskeleton. Findings from PC12 cultures and hippocampal neurons suggest that Ndr2 determines the substrate specificity of neurite extension via surface expression of $\alpha_1\beta_1$ integrins. Moreover, results from various genetical and pharmacological manipulations indicated that its substrate FlnA plays a crucial role during dendritic arborization of neurons downstream of integrin signaling and via actin crosslinking.

1.1 ECM and neurite growth

Neurite growth and dendritic branching are shaped not only by the intracellular neural signaling but also by the signals from their microenvironment, namely ECM. ECM in brain is a heterogeneous mixture of proteins and proteoglycans surrounding the neurons and astrocytes varying in a temporal (developmental) manner (Barros, Franco and Müller, 2011). Although once seen as a simple physical scaffold, studies have increasingly revealed its important role in regulating neuronal differentiation and neurite growth. Several studies showed that members of the ECM proteins or their combinations improve the survival/neurite growth of differentiating neurons

(O'Connor *et al.*, 2001; Fusaoka-Nishioka *et al.*, 2011; Tonge *et al.*, 2012). ECM specificity of neurite growth is obtained via different ligand affinities of integrin subtypes that reside on the membrane. Among the integrin receptors, β_1 containing heterodimers are the main receptor type for neurite growth mechanisms in neurons, while α subunits provide the ligand specificity for ECM (Denda and Reichardt, 2007; Wu and Reddy, 2012). Since the role of Ndr2 in neurons regarding β_1 integrin function was previously described (Rehberg *et al.*, 2014), I further explored whether Ndr2 plays any role in ECM substrate specificity of neurite growth.

To do so, stably transfected PC12 cells were employed, due to their ease of culturing and ability to differentiate/extend neurites upon acute NGF stimulation. Although ECM is a heterogenous mixture of different glycoproteins and proteoglycans, ECM substrates can be classified into 3 major groups depending on their integrin recognition sequences: laminins, fibronectins (RGD sequence containing) and collagens (GFOGER sequence containing) (Barczyk, Carracedo and Gullberg, 2010). On an array of these substrates, Ndr2 overexpressing PC12 cells displayed more neurite initiation compared to control cells (Figure 3A). This is likely to be caused by increased β_1 integrin activation via Ndr2 (Rehberg *et al.*, 2014; Demiray *et al.*, 2018) as β_1 integrins have a major role in recognition of each ECM substrate subtypes that were used (Hynes, 2002). It should also be noted that, even in the absence of NGF, Ndr2 PC12 cells displayed short, but noticeable neurites during routine passaging in flasks (data not shown). These culture flasks were not coated with any specific ECM and control PC12 cells appeared round in the same conditions. This further indicates an NGF-independent *neurite initiation* by Ndr2 overexpression, possibly via overactivation of the PI3K (phosphoinositide 3-kinase) pathway components. PI3K axis have been shown to be a positive regulator of PC12 neurite extension (Jackson *et al.*, 1996; Kim *et al.*, 2004) and, two of is important members, Akt and Tuberin, displayed significantly increased phosphorylation in

95

unstimulated Ndr2 PC12 cells (Daniel Lang & Oliver Stork, unpublished data), which could underlie those short neurites in basal conditions.

To examine a substrate-specific interaction of neurite growth and Ndr2 kinase, EGFP and Ndr2 PC12 cells grown were further analyzed for their neurite length (in cooperation with Dr. Kati Rehberg, Demiray *et al.*, 2018). PDL, laminin and collagen IV substrates were used for this approach since they caused maximal neurite initiation in both the control and Ndr2 PC12 cells without any genotype difference (Figure 3A). In this analysis, collagen IV caused a striking contrast to the overall morphology effects caused by Ndr2. Compared to control cells, significantly less number of Ndr2 PC12 cells were induced by collagen IV substrate to extend long neurites (Figure 3B-C). On the other hand, the previously reported Ndr2 mediated increase of PC12 neurite extension was also observed on PDL (Stork *et al.*, 2004). On laminin substrate, there were no differences between genotypes, possibly due to its high efficiency of neurite extension also in control cells. Thus, neurite growth of Ndr2 PC12 cells on PDL and collagen IV substrates were tested further to address potential mechanisms that may cause the unresponsiveness of Ndr2 overexpressing cells to collagen IV signaling.

Twenty-eight different collagen subtypes have been identified so far and among them, collagen subtypes I, II, III and IV were shown to induce neurite extension of PC12 cells in a Mg^{2+} dependent manner (Turner, Flier and Carbonetto, 1987). Control PC12 cells already displayed a significant boost in neurite extension on collagen IV after NGF, via mediating the collagen IV-integrin receptor interactions (Tomaselli, Damsky and Reichardt, 1987; Ali, Pappas and Parnavelas, 1998). On the other hand, Ndr2 PC12 cells did not alter in their neurite morphology between PDL and collagen IV, underscoring the lack of collagen IV response (Figure 4). Divalent ions such as Mg^{2+} or Mn^{2+} prime the integrins to their activation state by binding to metal ion dependent adhesion

sites (Zhang and Chen, 2012). Accordingly, the observed moderate enhancement of neurite growth of the Ndr2 PC12 cells on both PDL and collagen IV substrates by Mg^{2+} (Figure 4) could result from the combination of the divalent ion mediated priming and Ndr2 mediated intracellular activation of β_1 integrin receptors (β_1 $^{pThr788/789}$) at neurite tips (Rehberg *et al.*, 2014; Demiray *et al.*, 2018).

1.2   Integrins and substrate selectivity

One possible explanation of unresponsiveness to collagen IV could be a disturbance of collagen IV induced integrin signaling in Ndr2 PC12 cells. Due to the redundancy of integrin-ligand interactions, collagen IV substrate was first reported to be recognized by both $\alpha_1\beta_1$ and $\alpha_2\beta_1$ integrin heterodimers (Vandenberg *et al.*, 1991). However, previous studies suggest that $\alpha_1\beta_1$ integrin heterodimer has higher affinity and mainly interacts with collagen IV (Knight *et al.*, 2000; Becker *et al.*, 2013). This was indeed quantitatively shown using purified integrin receptors and ligands in which $\alpha_1\beta_1$ integrins displayed 4-fold higher affinity to Collagen IV compared to $\alpha_2\beta_1$ integrins in the presence of divalent ions (Kern *et al.*, 1993). Moreover, T-cells, which use integrin receptors for adhesion, display a differential distribution along the lung tissue depending on the collagen subtype of the basement membrane. In the same study, it has been shown that $\alpha_1\beta_1$ integrin expressing T-cells enriched on collagen IV rich surfaces where $\alpha_2\beta_1$ expressing cells rather localize on collagen I enriched spaces (Richter *et al.*, 2007). Differential affinity of the two closely related α integrin to collagen subtypes can be explained via existence of the I domain in their integrin N terminus. This I domain is a common feature in collagen subtypes and it has been shown that α_1I domain has the highest affinity to the collagen IV while α_2-I domain to the collagen types I-III (Tulla *et al.*, 2001).

To specifically address this question, a diffusible ligand that mimics collagen IV mediated binding to integrin receptors was tested on Ndr2 PC12 cells. KTS ligand peptide (CW**KTS**LTSHYC) which derived from the larger disintegrin obtustatin and has shown to specifically bind $\alpha_1\beta_1$ integrin dimer was utilized for this purpose (Moreno-Murciano *et al.*, 2003). Although higher concentration of this disintegrin is used as an antagonist for the $\alpha_1\beta_1$ function, at the concentration used in the experiments described here (140 µM; based on Marcinkiewicz *et al.*, 2003), the synthetic KTS ligand did not induce any change in the flattening of the cells that would indicate a generally altered adhesion (data not shown). More importantly, control cells did not show any difference and could successfully reach their maximal levels in the neurite extension between the PDL and Collagen IV substrate under 140 µM KTS ligand (Figure 4). This corroborates the notion that the concentration used in experiments did not cause any inhibition of the $\alpha_1\beta_1$ integrin-Collagen IV interaction. Strikingly, in spite of the increased β_1 integrin phosphorylation (pThr$^{788/799}$) via Ndr2 (Rehberg *et al.*, 2014; Demiray *et al.*, 2018), the KTS ligand failed to induce any neurite extension in the Ndr2 PC12 cells. The failure of the KTS stimulation in Ndr2 PC12 cells was evident both on the PDL and Collagen IV, which strongly indicates a disturbance specifically in the $\alpha_1\beta_1$ integrin mechanism. In line with morphology, immunocytochemistry of those cells demonstrated that Ndr2 PC12 cells expressed significantly less α_1 integrin in their neurite tips (Figure 9). Moreover, when total α_1 integrin levels were investigated during NGF stimulation, no significant differences were observed between the genotypes on both substrates (Figure 10). It is important to note that α_1 integrin protein levels increased up to 5-fold in 6 days of NGF treatment compared to day 0 in both genotypes (Figure 10). This is in line with earlier reports that α_1 integrin mRNA expression markedly increases with NGF treatment and correlates with level of adhesion on collagen substrates and neurite extension of PC12 cells (Zhang, Tarone and Turner, 1993). The observed

null difference in neurite initiation between the genotypes on collagen IV (Figure 3A) may arise from the low dependence on α_1 integrin expression during early phases of differentiation of PC12 cells.

Given the role of Ndr2 in control of β_1 integrin trafficking to the membrane (Rehberg *et al.*, 2014), it is no surprise that Ndr2 can modulate the localization of another integrin subunit, α_1. It has been shown that α integrin subunits are internalized and can be recycled via Rab-mediated pathways via their conserved Rab-interacting domains (Pellinen *et al.*, 2008; Caswell, Vadrevu and Norman, 2009). Since the association of Ndr2 to Rab5/Rab11 positive early/late endosomes in neurons was previously demonstrated (Rehberg *et al.*, 2014), it is highly likely that Ndr2 also regulates the α integrin trafficking in differentiating PC12 cells via aforementioned Rab-dependent mechanisms. Moreover, Rabin8, a Rab-8 guanine exchange factor, has been identified as a substrate for Ndr2 kinase (Ultanir *et al.*, 2012). Rabin8 plays an important role in neurite outgrowth as it controls the Rab-dependent endosomal trafficking in PC12 cells (Homma and Fukuda, 2016).

To translate these observed effects of from PC12 cells in a neuron-like environment, mouse hippocampal neurons were transfected with Ndr2 overexpression or silencing vectors. Here, LN111 coating was used as an extracellular substrate, since it has been previously shown bind $\alpha_1\beta_1$ integrins during neuronal development in vitro (Desban *et al.*, 2006; Tulla *et al.*, 2008). Similar to EGFP PC12 cells on collagen IV, control neurons on LN111 displayed enhanced dendritic growth. $\alpha_1\beta_1$ substrate LN111 again failed to stimulate dendritic growth in Ndr2 overexpressing hippocampal neurons, which indicates the persistence of α_1 integrin disturbance (Figure 11). The differential trafficking of α_1 subunit may be mediated by clathrin dependent vesicular endocytosis, which is an important aspect of integrin trafficking (Bridgewater, Norman and Caswell, 2012). For

example, α_{1-3} but not α_5 or α_V integrin subunits are regulated by Dab2 adaptor protein which interacts with clathrin coated vesicles, which can cause such differential sorting mechanisms (Teckchandani *et al.*, 2009). Adapter-protein-2 (AP2) is another crucial scaffold for clathrin-dependent endocytosis and redistributed in the PC12 cells membrane after NGF treatment (Beattie *et al.*, 2000). Likewise, α_2 and α_6, but not α_1 integrin receptors incorporate the binding domain for AP2 (De Franceschi *et al.*, 2016). Intriguingly, AP2 associated kinase (AAK1), which can regulate AP2 binding affinity. is a previously shown downstream target of Ndr kinase in the brain (Ultanir *et al.*, 2012). It is plausible to assume that Ndr2 interacts with such adaptor proteins which warrants further investigation of Ndr2 kinase in vesicular trafficking of integrin receptor subtypes. Silencing of Nd2, however, inhibited proper dendritic branching on both PDL and LN111 (Figure 12). The overall decrease of dendritic branching could be caused by the reduced β_1 integrin activity in shNdr2 neurons as β_1 containing heterodimers are responsible for overall neurite differentiation in neurons (Marrs *et al.*, 2006; Warren *et al.*, 2012).

1.3 A drawbridge between Ndr2 and integrin receptors: FlnA

Ndr2 sits downstream of Mst kinases as a target of hippo pathway and exact mechanisms of how it can mediate β_1 integrin activity was still unclear up to this point. $Thr^{788/789}$ site on the β_1 integrin tail is an important regulator for its activation state (Nilsson *et al.*, 2006) and has been shown to be targeted by CamKII and PKCε (Suzuki and Takahashi, 2003; Stawowy *et al.*, 2005). Indeed, activated Ndr2 can also induce $Thr^{788/789}$ phosphorylation, and this action is sensitive to CamKII and PKCε inhibitors. However, the $Thr^{788/789}$ phosphorylation was not direct since activated Ndr2 did not phosphorylate the cytoplasmic tail of β_1 integrins in an in vitro kinase assay (Rehberg *et al.*, 2014). This prompted us to investigate whether there is an adaptor protein downstream of Ndr2

that may mediate its effects on β_1 integrin (in cooperation with Eric Devroe & Benjamin Turk, Waldt *et al.*, 2018; Figure 13A). As a side note, kinase regulator Mob2 was also present during radioactive phosphorylation labelling as it has been shown to drastically stimulate Ndr catalytic activity (Devroe *et al.*, 2004).

Determining R-X-P-(S/T) as the optimal Ndr2 target motif led to identification of three significant phosphorylation substrates in the integrin adhesome containing this motif (Figure 13). Next to the prominent integrin association by FlnA, R-X-P-(S/T) motif in the HSBP- S15 and protein tyrosine phosphatase receptor A at S204 are worth taking note. Although it has only shown by high throughput mass spectrometry (Ewing *et al.*, 2007), interaction between HSBP1 and integrin linked kinase (ILK) can be critical as ILK is one of the downstream effector of integrin receptors and can regulate dendritic initiation and growth (Naska *et al.*, 2006). Heat-shock activated chaperone proteins including HSBP1 are linked to peripheral neuropathies and S15 phosphorylation of HSBP1 affects its structure and chaperone activity (Rogalla *et al.*, 1999; Weeks *et al.*, 2018). Besides HSBP1, phosphorylation of S204 on PTPRA has been shown to enhance its phosphatase activity and substrate specificity. Activation of PTPRA is important tyrosine phosphatase since it targets variety of downstream kinases such as Src and thereby modulates their activity (Zheng, Resnick and David, 2002). This may then also play an important role due to involvement of Src in dendritic morphogenesis and spinogenesis (Kotani *et al.*, 2007). Given these evidence, potential Ndr2 mediated PTPRA-Src pathway warrants further investigation in the context of neuronal growth.

In the present study, S2152 phosphor acceptor residue on FlnA was focused primarily, and has been shown to directly phosphorylated by active Ndr2 (Figure 14A). Ndr2 mediated FlnA phosphorylation was further tested and silencing of Ndr2 disturbed the FlnA phosphorylation in

both mouse fibroblast (NIH3T3) and human Jurkat T-cell lines (Figure 14, Appendix Figure 43). Results obtained from T-cells using CD3 stimulation demonstrated a much stronger difference in Ndr2-mediated FlnA 2152 phosphorylation compared to FBS treated NIH3T3 cells. It is important to underline that mouse NIH3T3 cells have relatively similar Ndr2 and Ndr1 expression levels (Cornils *et al.*, 2010) and both isoforms are known to be activated with okadaic acid (Devroe *et al.*, 2004). The effects of shNdr2 thus can be diluted to some extend by Ndr1 mediated RxP(S/T) phosphorylation on FlnA in mouse NIH3T3 cells. On the other hand, Jurkat T cells that were used in CD3 stimulation express much higher Ndr2 relative to Ndr1 isoform, therefore providing a more suitable environment to quantify Ndr2-FlnAS2152 axis under shNdr2 manipulation (Waldt *et al.*, 2018). Most importantly, differential expression of Ndr1 and Ndr2 isoforms have been demonstrated throughout different mouse tissues. As opposed to rat brain, Ndr1 protein was not detected in mouse brain tissue while Ndr2 was profoundly expressed both in mouse cortex and hippocampus (Cornils *et al.*, 2010; Rehberg *et al.*, 2014). Together, these findings indicate that Ndr2 phosphorylates FlnA on S2152 and is the primary Ndr kinase in the brain. It is worth noting that in Ndr2 KO mouse neurons, Ndr1 protein expression was not upregulated (Kul Madencioglu, 2019- Doctoral Thesis). Due to this lack of compensation, neuronal cultures are valuable tools to study Ndr2 mediated S2152 FlnA phosphorylation and its effects in vitro in future. Cells expressing an activated or kinase-dead Ndr2 and different FlnA phosphomutants (S2152A and S2152E) might further reveal any Ndr2 targeted FlnA-S2152 specific effects in dendritic morphology. Aside from that, by analyzing a developmental profile of FlnA phosphorylation compared to wild type mice, Ndr2 KO mouse model that is available (Rehberg *et al.*, 2014) will be a particularly useful tool for first in vivo Ndr2 mediated FlnA S2152 description from the brain.

Another reason for the pronounced FlnA phosphorylation effect in CD3 stimulated Jurkat T cells compared to mouse fibroblasts could be the heterogenous nature of FBS stimulation, which may also activate Ndr independent phosphorylation of FlnA via other previously reported upstream kinases such as PKA, PKC or RSK (Jay, García and de la Luz Ibarra, 2004; Woo *et al.*, 2004; Muriel *et al.*, 2011). More importantly, FlnA S2152 phosphorylation in Jurkat T cells induces its release from LFA1 integrins, which allow activators such as talin and kindlin to associate to the receptors intracellular tail (Waldt *et al.*, 2018). Therefore, FlnA may act as an on/off switch on the intracellular side of the integrins depending on its physical association with the receptor.

FlnA is critically positioned beneath the neuronal membrane where it connects the integrin mediated signaling to intracellular actin dynamics. Therefore, it is of particular interest when it comes to exploring mechanisms of dendritic growth. However, since the loss of FlnA function in humans is the most frequent cause of PH (accumulation of neurons that fail to properly migrate into cerebral cortex) (Lange *et al.*, 2015), the research to date mostly focused on how FlnA controls neuronal migration. Thus, the knowledge about FlnA effects on dendritic growth was limited. Accordingly, first, the role of FlnA expression on dendritic growth were tested in hippocampal neurons. Considering the downregulation of FlnA mRNA after DIV7 (Figure 15), likely due to the maturation of dendritic tree, neurons were transfected at DIV3 and analyzed at DIV7 to manipulate FlnA during this critical developmental stage.

1.4 Precise levels of FlnA: less is more

Intriguingly, both under and overexpression of FlnA in hippocampal neurons displayed dendritic hypertrophy (Figure 18D). Moreover, another shRNA targeting FlnA transcript (Figure 20) and pure overexpression of FlnA (Figure 28) verify that it is the main effect of FlnA manipulation and

is not caused e.g. by a side effect of the hairpin or co-transfections. This was not surprising since there have been several studies reporting similar consequences of FlnA manipulation. For instance, although comprising of a very distinct neuronal population compared to hippocampus, olfactory bulb neurons also display an increase in dendritic arbor numbers after silencing as well as overexpression of FlnA (Zhang *et al.*, 2014). In more mature hippocampal neurons (DIV14), both increase and silencing of FlnA caused similar immature spine phenotype on dendrites (Segura *et al.*, 2016). Increased expression or S2152 phosphorylation of FlnA, as well as its loss via transgenic mouse model, exhibited similar impairments in neuronal migration (Zhang *et al.*, 2012, 2013). Lastly, in *Drosophila*, two different mutant fly lines that shows aberrant FlnA expression were described in a behavioral screen (Cher and Joy mutants, decreased and increased FlnA expression levels respectively). Accordingly, both mutant lines displayed disturbance in long term memory after one-day spaced training (Bolduc *et al.*, 2010). In summary, these results, including the hippocampal neurons morphology from experiments reported here, suggest that precise regulation of FlnA is needed in neurons for proper neuronal migration, dendritic/spine development, and synaptic functioning.

Given the role of FlnA in modulation of integrin activity, we then tested how the FlnA silenced and overexpressed neurons would grow on Fibronectin, a known β_1 integrin ligand that supports neurite growth (Tonge *et al.*, 2012; Nieuwenhuis *et al.*, 2018). On Fibronectin, the FlnA effects were dissociated in such that the proximal dendritic hypertrophy still persisted in hWT FlnA expressing neurons, while shFlnA mediated arborization were disturbed significantly (Figure 18E). As a negative regulator of integrin activity, silencing FlnA may cause an increased β_1 activity on the growing neurite tips and this mild increase can be advantageous for branching on PDL only. On the other hand, on the fibronectin-precoated coverslip, this increased activation may cause a

hyper adhesion state that disturbs the dendritic arborization. It is worth noting that ECM is collectively synthesized by both neurons and glia (Dzyubenko, Gottschling and Faissner, 2016). Hippocampal neurons used in dendritic morphology experiments were fed with a media that was conditioned on confluent astrocytes for 72 hours. Thus, on PDL only coverslips, there is an accumulated basal amount of ECM to which shFlnA neurons can respond and branch efficiently. The integrin dependent growth on PDL only coverslips were further observed as growth impairments after β_1 integrin silencing (Figure 21) or after β_1 integrin activity blocking (Figure 23). On the other hand, fibronectin coated coverslips contain a high density of immobilized RGD ligands on the ECM, whereby disturbing of the integrin activation dynamics by shFlnA impairs the arborization. Even more striking result that was evident from this experiment was the fact that hWT FlnA mediated dendritic hypertrophy persisted as it did not change between PDL and fibronectin substrates (Figure 18C). This finding suggests that hWT FlnA induced arborization might be independent of integrin receptor modulation. A possible mechanism that may mediate the observed effects is its actin crosslinking.

If the effects of FlnA under and overexpression are distinguished by integrin activity, then β_1 integrin level, as the main integrin receptor in neurons, should play a pivotal role in this mechanism. Therefore, as the next step, whether the detrimental effects of β_1 integrin reduction can be rescued by either FlnA genotype was tested. Co-transfection of shFlnA with shItgb1 rescued the overall deficiency in dendritic branching length and enhanced it to similar levels as control neurons, consistent with the notion of augmented β integrin activation upon FlnA silencing. However, hWT FlnA co-expression did not rescue the growth impairment caused by β_1 integrin reduction. Despite prior evidence showing hWT FlnA could increase the dendritic branching independent of ECM-integrin interaction (possibly via direct actin cytoskeleton association), these results suggest that

FlnA induced actin crosslinking still relies on the presence of integrin receptors to stimulate branching. It has been shown that FlnA can bind to intracellular tail of β_1 integrins (Gehler *et al.*, 2009; Nieves *et al.*, 2010). This binding may serve as a docking station for the heterologous expressed hWT FlnA and may be crucial for its actin-mediated stimulation of dendritic arborization.

1.5   Targeting the middleman: β_1 integrin, FAK and actin

Moreover, to test whether activity of β_1 integrins is required for FlnA genotype effects, neuronal cultures were then treated with a β_1 specific blocking antibody Ha2/5 (Chavis and Westbrook, 2001). The previously observed dendritic hypertrophy caused by FlnA manipulation could still be observed in untreated neurons (Figure 22D). Ha2/5 treatment significantly reduced dendritic branching in all genotypes to different extent and shFlnA neurons displayed the most drastic decrease (Figure 22A-C). The Ha2/5 treatment showed a more coherent disassociation of FlnA mediated effects on dendritic growth and their integrin receptor activity dependency. Nevertheless, hWT FlnA expressing neurons also displayed a mild but significant decrease of dendritic branching under Ha2/5 antibody. This decrease was also anticipated as β_1 integrin activity is a big component of growth mechanisms and actin crosslinking might not compensate for the whole disturbance. Nevertheless, the significant hypertrophy mediated by hWT FlnA expression persisted in comparison to control and shFlnA neurons under Ha2/5 antibody. Interestingly, total length of the dendritic tree was significantly reduced overall in all genotypes (**Error! Reference source not found.**), suggesting that the FlnA mediated enhancements are arborization-specific rather than increasing the overall growth rate.

FAK has been highly associated with integrin signaling since its discovery (Kornberg *et al.*, 1992),

and is widely implicated with neuronal development, with a prominent role of first downstream effector of integrin-ECM interactions (Navarro and Rico, 2014). FAK serves as a docking station below the membrane after integrin engagement and orchestrates downstream signals that eventually remodels local cytoskeleton via effector proteins such as Src, RhoA and Rac (Parsons, 2003). As a highly enriched kinase in neural growth cones and given its crucial position 'below of' integrin receptor and 'above from' actin cytoskeleton, FAK was targeted pharmacologically in shFlnA and hWT FlnA genotypes. The findings from FAK inhibitor Y15 experiments highlighted a clear distinction between the dendritic arborization effects: hWT FlnA expression could still enhance branching, since its actin crosslinking function could serve as a downstream compensation. Remarkably, as with β_1 integrin blocking experiments, total dendritic length was significantly disturbed in each genotype, confirming the arborization-specificity of the FlnA effects.

The notion that actin crosslinking is the main reason behind the hWT FlnA branching effects was only hypothesized up to this point and required direct evidence. To test this, a mutant FlnA that cannot dimerize, thus cannot crosslink actin filaments as in WT form, was expressed in hippocampal neurons. And indeed, dimerization mutant FlnA failed to stimulate dendritic branching compared to control neurons (Figure 29). An earlier study using a similar dominant negative FlnA, which lacks the ABD but retains its V-shape, demonstrated results akin to here. This actin binding mutant failed to rescue the cortical radial migration disturbances in mouse in contrast to the WT FlnA form (Kurabayashi *et al.*, 2018). These observations together indicate that efficient actin crosslinking by FlnA is crucial for significant FlnA effects in neurons. The importance of actin branching and cross linking for neuronal development and memory formation has become more evident in respect to a more recognized actin branching factor: Arp2/3 (Kim *et*

al., 2013; Spence *et al.*, 2016). Arp2/3 has been implicated in controlling dendritic arborization during neuronal development and its overactivation was reported to increase dendritic branching in hippocampal neurons (Rocca *et al.*, 2008). Interestingly, Arp2/3 mediated dendritic arborization was also more prominent in the proximal parts as revealed by the Sholl analysis of transfected hippocampal neurons (Rocca *et al.*, 2008), similar to hWT FlnA results presented in the current work. Studies comparing FlnA and Arp2/3 showed that FlnA- and Arp2/3-mediated actin crosslinking are complementary and both necessary for proper actin dynamics and maintenance of filament stability (Flanagan *et al.*, 2001; Nakamura *et al.*, 2002). Lastly, most of the hWT FlnA genotype effects were reflected in the dendritic arborization while the total length of the dendritic tree is reduced similar to control neurons (Figure 23, Figure 25). Interestingly, in a very recent preprint, researchers systematically analyzed microtubule and microfilament distributions from live Drosophila sensory neurons and found that local microtubule and microfilament levels are associated with dendritic elongation and branching respectively (Nanda *et al.*, 2020). In light of this new evidence, a better understanding of how actin cytoskeleton is differentially regulated in hWT FlnA neurons needs be investigated in future research. This could be carried out by combining FlnA manipulation and staining of actin filaments (i.e., phalloidin followed by high resolution microscopy) or following their dynamics with tracking methods such as LifeAct.

1.6 A possible shift in the RhoA/Rac1 balance

The contribution of shFlnA on dendritic branching is well demonstrated throughout this study regarding their dependency on integrin activity and FAK. Finally, the influence of FlnA silencing on intracellular pathways, primarily on PI3K-Akt signaling, was explored to gain a better insight on its downstream action in neurons. Akt activity has been shown to be critical for neuronal survival and differentiation. Akt converges different growth signals (such as ECM ligands-β_1 integrin

engagement or neurotrophin signaling) as an important downstream effector (Kaplan and Miller, 2000; Rodgers and Theibert, 2002; Velling *et al.*, 2004). Similar to its role in hippocampal neurons, Akt also regulates dendrite morphology of cortical neurons (Dijkhuizen and Ghosh, 2005). For high throughput biochemistry assays, mouse cortical neurons were used in the present study for the lentiviral transduction and subsequent Western blotting experiments. Cortical neurons displayed a strong induction of Akt phosphorylation at Thr308 and Ser473 after stimulation of integrin receptors. Interestingly, as the Akt induction tapers down over time in control neurons, aberrant activation of Akt was observed in shFlnA neurons 30 minutes after acute integrin stimulation (Figure 27). Increased dendritic arborization via shFlnA may be attributed to abnormal Akt phosphorylation during neurite growth. It has been shown that expression of constitutively active Akt or its pharmacological inhibition significantly enhanced and disturbed hippocampal dendritic branching respectively (Jaworski *et al.*, 2005). Moreover, a recent paper reported a negative correlation between FlnA levels and Akt activity upon growth factor signaling in colorectal cancer cell lines (Wang, Zhu and Zhao, 2019), in line with integrin mediated aberrant Akt phosphorylation in shFlnA neurons.

The mechanisms behind controlled activation of Akt is an extensively studied topic as it plays a central role in growth dynamics. Three members of the Rho family of GTPases; RhoA, Rac1 and Cdc42, are among the most extensively studied organizers of actin cytoskeleton dynamics and can control dendritic branching in opposite directions in neurons (Stankiewicz and Linseman, 2014). For instance, silencing of Rac1 in hippocampal neurons significantly impairs dendritic growth (Gualdoni *et al.*, 2007). Overactivation of RhoA results in a significant simplification of dendritic tree and disturbs arborization in hippocampal neurons (Nakayama, Harms and Luo, 2000). Moreover, RhoA can affect dendritic arbor stability downstream of integrin mediated activation of

Abelson and Abelson-related-gene kinases (Moresco *et al.*, 2005; Lin, Yeckel and Koleske, 2013). Besides their distinct effects on dendritic tree, crosstalk between Rac1 and RhoA cascades converge on Akt and control its activation in opposite directions: while Rac1 increases Akt activity via PI3K, RhoA activity inhibits Akt through ROCK (Rho associated protein kinase) and PTEN (phosphatase and tensin homolog) (Stankiewicz and Linseman, 2014). Therefore, the balance between Rac1 and RhoA activation during adhesion is crucial for accurate growth dynamics. Rac1 activation and RhoA inhibition is associated with early adhesion upon integrin engagement and induces actin nucleation/polymerization beneath growing tips. Consecutively, as nascent adhesion complex matures and RhoA becomes activated, it signals down its effectors such as ROCK and limits further growth (Govek, Newey and Aelst, 2005; Lawson and Burridge, 2014). Interestingly, fibronectin binding to the cells significantly reduces RhoA activation at first (nascent adhesion phase), which is then recovered after 30 minutes of stimulation; indicating its role in integrin mediated growth dynamics. It should be also noted that this temporal regulation of RhoA activity is highly dependent on FAK and does not take place in FAK KO cells (Lim *et al.*, 2008). FAK Tyr397 phosphorylation, as a readout for its activity, was also examined in Fibronectin/Mn^{2+} treated neurons. However, no significant change was detected under acute integrin stimulations (Figure 27E). Although an increase in the FAK activation was expected upon integrin stimulation, it could be that immunoblotting of whole cell lysates might have diluted the expected increase in FAK pTry397, as it is primarily localized in active adhesion sites for autophosphorylation (Parsons, 2003).

It has been shown that RhoA silencing or RhoA dominant-negative mutant in fact causes an increase in Akt phosphorylation, since Akt activity is negatively regulated by RhoA-ROCK-PTEN pathway (Yang and Kim, 2012). It is plausible to consider that silencing of FlnA disturbs this on-

off balance, impairs the late RhoA activation and therefore leads to an aberrant phosphorylation of Akt after acute stimulation. It has been further shown that FlnA can physically interact with RhoA GTPase and loss of FlnA caused a dysregulation in RhoA activation in neural progenitor cells (Lian *et al.*, 2019). RhoA activity can be suppressed by another GTPase, p190RhoGAP, which has been shown to interact with FlnA. The same study demonstrates that the interaction between FlnA and p190RhoGAP prevents p190RhoGAP from blocking RhoA activity in round cells. However, during cell spreading, FlnA levels are reduced via calpain cleavage, which allows p190RhoGAP localization in growing lipid raft and block local Rho activity (Mammoto, Huang and Ingber, 2007). It could be that in shFlnA neurons, RhoA inhibition was augmented due to the lack of FlnA and increased p190RhoGAP suppression on RhoA. Next to RhoA, its mutual antagonist, Rac1, can also be modulated by FlnA. A FlnA associated RhoGTPase activating protein, FilGAP, targets and inhibits Rac1 upon binding to FlnA (Ohta, Hartwig and Stossel, 2006). It is worth noting that FilGAP can also be phosphorylated by ROCK, and thereby can mediate the antagonist crosstalk between RhoA and Rac1 dynamics. Considering the findings of the current study and observations from the literature, the suggested overall scheme of FlnA-Akt mediated dendritic hypertrophy can be seen below (Figure 41). Further experiments are necessary to demonstrate role of FlnA in dendritic branching with respect to RhoA/Rac1 balance by quantifying their activity levels in FlnA manipulated neurons and needs to be further confirmed with RhoA/Rac1 pharmacological interventions.
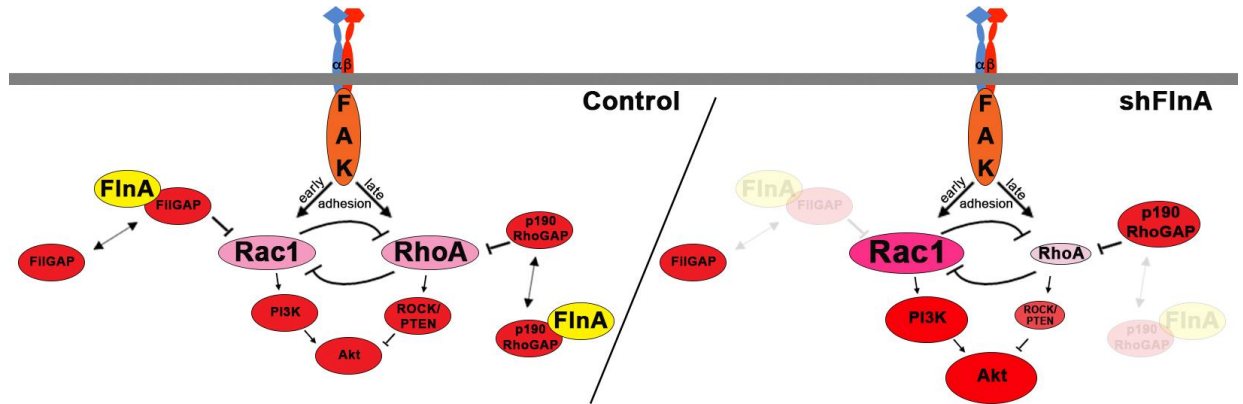
Figure 41: Suggested model for shFlnA mediated dendritic remodelling.
(left) FAK orchestrates the integrin mediated activation of actin organizers temporally (via Src-p190RhoGEF interactions, not depicted here) (Lim *et al.*, 2008). While Rac1-PI3K pathway stimulates Akt phosphorylation, RhoA-ROCK-PTEN cascade inhibits AKT activity (Stankiewicz and Linseman, 2014). Rac1 can be inhibited via GTPase activity of FilGAP upon FilGAP-FlnA binding (Ohta, Hartwig and Stossel, 2006). Moreover, Rac1 antagonist RhoA can be inhibited by p190RhoGAP, which is prevented by FlnA binding (Mammoto, Huang and Ingber, 2007). *(right)* Lack of FlnA might cause an imbalance in Rac1-RhoA dynamics, therefore augments the downstream Akt phosphorylation upon integrin ligand binding which can cause aberrant neurite outgrowth phenotypes.

1.7 Development of new and more specific intervention tools

Cell culture assays are helpful to dissect the FlnA-mediated mechanisms and detect signals that are involved in dendritic growth. However, these in vitro conditions do not provide the heterogenous extracellular matrix that is critical for the hippocampal dendritic architecture in vivo. Furthermore, in vivo models are crucial for the subsequent physiological characterization and behavioral analysis. Therefore, future in vivo investigations are necessary to validate and translate the current findings that can be drawn from FlnA effects in the present study. Almost all studies using FlnA knockdown animal models have been carried out in the context of muscular and vascular development, neuronal proliferation and migration (Feng *et al.*, 2006; Zhang *et al.*, 2013; Lian and Sheen, 2015; Retailleau *et al.*, 2016). In the present study, establishment of AAV-mediated CRISPR/Cas9 system against mouse FlnA gene was carried out to generate a brain specific FlnA

KO animal model. This approach has successfully disturbed mouse FlnA gene in cultured cortical neurons (Figure 32, Figure 33). This CRISPR approach will therefore be employed in future in vivo for testing FlnA loss-of-function in the brain. Interestingly, same gRNAs did not disturb the mouse FlnA gene when lentiviral vectors have been used for delivery in mouse fibroblasts (Figure 31). It should be noted that two lentiviral constructs were used simultaneously to utilize both canonical Streptococcus pyogenes and gRNAs. Their respective GFP and mCherry labels indicate that they might not completely overlap during the transduction phase (Figure 31C). This might hinder the Cas9 mediated genetic perturbation as it requires both components. Therefore, single AAV delivery of the CRISPR elements (Cas9 and gRNA) provided a more robust approach for targeting the FlnA gene for knockdown.

On the other hand, gain of function studies were classically accomplished using an expression construct from gene of interest. However, this limits the scope of the studies to the available cDNA libraries and the packaging size limits of the carrying vector. This limitation was apparent during biochemistry assays in the present study as well, in which ≈9 kb FlnA transcript was too large to be packaged in the available AAV or lentiviral transfer particles. Recent advances in CRISPR-Cas9 field allow researchers to regulate transcription of target genes without genome editing. These systems employ catalytically-death Cas9 (dCas9) fused with transcriptional activator to target promoters specifically via gRNAs. However, transcriptional activation of mouse FlnA gene failed in different dCas9 systems using both liposome mediated transfections for short and lentiviral delivery for longer incubation times (Figure 35, Figure 36, Figure 38, Figure 39, Figure 40). This could also be caused by previously reported inverse correlation between the basal expression level of the gene of interest and acquired transcriptional activation (Konermann *et al.*, 2015; Vora, Cheng, Xiao, VanDusen, *et al.*, 2018). Due to successful Cas9 mediated genome editing in a single-

AAV system, similar single-AAV transfer plasmid containing a short dCas9-VPR and gRNA cassette was recently acquired. Proof of principles assays demonstrated a successful induction of tdTom fluorescence reporter in HEK293T cells (Appendix Figure 45) and further testing needs to be done after cloning the FlnA promoter targeting gRNAs.

1.8   Limitations of the study

The present study contributes to our knowledge by addressing the crucial roles of Ndr2 kinase and its recently identified substrate FlnA in determining ECM specificity of neurite growth, integrin activation and downstream actin re-organization pathways, however with some limitations. First and foremost, all the dendritic branching quantifications were conducted on fixed neurons at DIV6-7, and therefore do not reflect the quantification of growth dynamics. Future experiments using live cell imaging are needed to assess whether dendritic arborization, stability or retraction are affected specifically by FlnA manipulations. Secondly, FlnA mediated-integrin dependent intracellular mechanisms are deeply examined throughout a classical PDL coated substrates containing a minimal ECM. However, FlnA mediated ECM remodeling has not been considered. It has been shown that FlnA controls the extracellular substrate abundance and organization via affecting ECM degradation pathways and secreted proteases such as matrix metalloproteinases (Baldassarre *et al.*, 2012; Mezawa *et al.*, 2016). Immunostaining of the ECM from these cultures needs to be done to test for any significant extracellular changes after FlnA manipulations. Future in vivo studies are also needed to test how FlnA mediated dendritic architecture will translate in brain where ECM is highly heterogenous and integrin receptor activity is tightly regulated.

One main FlnA manipulation that was used in the experiments was heterologous expression of human wild type FlnA (hWT FlnA genotype) rather than homologous overexpression of mouse

FlnA cDNA in mouse hippocampal neurons in vitro. Nevertheless, similar heterologous expression of human and rat FlnA in mouse olfactory bulbs could successfully affect dendritic morphology suggesting that it is still functional in mouse cells (Zhang *et al.*, 2014). Moreover, this heterologous expression system allowed neurons to overexpress human FlnA via strong CMV promoter since the used shRNA was mouse FlnA transcript specific (Figure 40B).

The exact role of Ndr2 mediated FlnA S2152 phosphorylation during dendritic branching remained unexplored up to this point. To address the principal role of FlnA Serine-2152 in FlnA mediated dendritic morphology, first, S2152A FlnA mutant was used in the same setup during dendritic arborization. However, even though S2152 residue has been shown to significantly regulate FlnA activity, no differences in dendritic development were observed between WT and phosphodeficient FlnA expressing neurons (Figure 30). It could be that FlnA phosphorylation during dendritic development in vitro were at its basal levels thus the introduced S2152A FlnA did not differ significantly from its WT isoform. Western blotting of forebrain and whole brain lysates also revealed profoundly low pS2152 FlnA levels in embryonic mice (E16.5, which corresponds to the developmental timeline of in vitro neuronal cultures) (Zhang *et al.*, 2012). To this end, S2152E FlnA (Muriel *et al.*, 2011) is also acquired which might overcome the low-phosphorylation issue via mimicking phosphorylated FlnA electrostatically.

Another challenge in the S2152A FlnA transfections was the altered total FlnA protein levels upon transfection, irrespective of Serine 2152 residue. Expression constructs of FlnA used in neurons cause an overshoot in the expression due to its strong CMV promoter (Figure 16B, Figure 40B). Based on results presented here and previous research suggesting precise level of FlnA is needed for proper neuronal differentiation, such synthetic promoters might prevent identifying any role of FlnA Serine-2152 residue in neuronal development. Upregulation of both WT and S2152A FlnA

proteins after the transfections thus might hinder the phosphorylation-specific effects.

An alternative genome modification approach based on CRISPR might solve the gene dosage issue: CRISPR toolbox is now widely used in neuronal and non-neuronal for ablation or transcriptionally activating target genes, expanding the available canonical intervention method. Cas9 mediated double stranded DNA breaks usually undergo non-homologous-end-joining which is prone to make error and create non-sense mutations within coding parts (hence the ablation of the target gene occurs such as FlnA in Figure 32, Figure 33). An alternative approach is providing a repair template with the Cas9/gRNA complex, which can be integrated to the target site via homology directed repair (HDR). As HDR is mainly restricted in G2 and S phase of dividing cells, alternative HDR independent approaches are developed to efficiently modify the genome in neurons (Gao *et al.*, 2019; Willems *et al.*, 2020). Moreover, precise single base edits can also be introduced with the developing cytosine and adenosine base editors fused to dCas9/gRNA complexes for single amino acid substitutions without double strand breaks (Yeh *et al.*, 2018). These recent advances in the CRISPR field might allow a more suitable intervention of Serine-2152 residue on endogenous FlnA gene, where S2152A and S2152E FlnA mutant neurons can be used to study the role of FlnA phosphorylation during dendritic growth in more natural gene expression dosage.

Besides its phosphorylation, intrinsic regulation of FlnA expression has not been considered in the present study since silencing/overexpression manipulations were present throughout experiments, which result in strong FlnA genotypes. Furthermore, as mentioned before, not enough attention has been paid to regulation of FlnA during learning and memory processes. In this line, as a relevant activation pathway that can translate in vitro FlnA findings to brain function, BDNF (brain derived neurotrophic factor) and NGF neurotrophin signaling were tested to collect preliminary data on

FlnA expression regulation. BDNF and NGF were selected as they are consistently associated with learning and memory events, LTP and associated structural changes in dendrites (Falkenberg *et al.*, 1992; Morimoto *et al.*, 1998; Hall, Thomas and Everitt, 2000; Mizuno *et al.*, 2000; Ji *et al.*, 2005; Lazo *et al.*, 2013), in which FlnA might be involved. Preliminary data gathered from acute treatments of neurons with neurotrophins indicated a time-dependent differential regulation of FlnA expression in vitro (Appendix Figure 44). In parallel, NGF receptor TrkA is temporally regulated in cultured neurons with high levels around DIV4 and declines significantly overtime, e.g. at DIV7 and later (Culmsee *et al.*, 2002), which might contribute to the observed FlnA regulation. Future experiments are needed to further confirm and develop these initial findings from neurotrophins-FlnA crosstalk how it might affect FlnA S2152 phosphorylation dynamics. Moreover, cultured neurons from Ndr2 KO mouse brain will also be useful to test contribution of Ndr2-FlnA axis in the neurotrophin signaling.

1.9 Concluding remarks

Disturbances in the dendritic architecture are prominent hallmarks of number of brain disorders ranging from autism-spectrum-disorders to schizophrenia (reviewed in Kulkarni and Firestein, 2012). FlnA, next to being the most common cause of inherited PH (Sheen, 2012), has also attracted much attention in the past years as an important protein mediating tau phosphorylation in Alzheimer's disease (Wang *et al.*, 2012; Burns and Wang, 2017) and causing abnormal dendritic complexity in Tuberous sclerosis (Zhang *et al.*, 2014). Further on, recent advances in FlnA research led to a discovery of small molecule drug PTI-125, which can bind and inhibit aberrant FlnA activity in neurons, and paved the way for launching therapeutical approaches in Alzheimer's disease and cortical malformation models such as Tuberous sclerosis and focal cortical dysplasia in mice (Wang *et al.*, 2017; Zhang *et al.*, 2020). These findings provide insights for future treatment

strategies to target FlnA pharmacologically in such neurological diseases in humans (clinicaltrial.gov # NCT04388254, Sumifilam (PTI-125) in Alzheimer's Disease patients).

The findings presented here add to a growing body of research that implicates FlnA with β_1 integrin activity and describe its effects on the downstream actin cytoskeleton remodeling during dendritic differentiation of neurons. Based on the important roles of integrin and actin cytoskeleton for neuronal transmission, future investigations are necessary to test the critical role of FlnA in vivo during development and plasticity of hippocampal dendrites and in the hippocampal circuits that mediate memory formation. Next to investigating basic mechanisms of FlnA effects in healthy conditions, future studies should also focus on the FlnA levels in diseases with abnormal dendritic architecture as its precise levels are needed for proper arborization.

REFERENCES

Ali, S. A., Pappas, I. S. and Parnavelas, J. G. (1998) 'Collagen type IV promotes the differentiation of neuronal progenitors and inhibits astroglial differentiation in cortical cell cultures', *Developmental Brain Research*, 110(1), pp. 31–38.

Ali, U. *et al.* (1977) 'Restoration of normal morphology, adhesion and cytoskeleton in transformed cells by addition of a transformation-sensitive surface protein', *Cell*, 11(May), pp. 115–126.

Anton, E. S., Kreidberg, J. A. and Rakic, P. (1999) 'Distinct functions of α3 and α(v) integrin receptors in neuronal migration and laminar organization of the cerebral cortex', *Neuron*, 22(2), pp. 277–289.

Askari, J. A. *et al.* (2009) 'Linking integrin conformation to function.', *Journal of cell science*, 122(Pt 2), pp. 165–170.

Baldassarre, M. *et al.* (2009) 'Filamins regulate cell spreading and initiation of cell migration', *PLoS ONE*, 4(11).

Baldassarre, M. *et al.* (2012) 'Filamin A controls matrix metalloproteinase activity and regulates cell invasion in human fibrosarcoma cells', *Journal of Cell Science*, 125(16), pp. 3858–3869.

Baldassarre, M. and Calderwood, D. A. (2018) 'Filamin A', in Choi, S. (ed.) *Encyclopedia of Signaling Molecules*. Cham: Springer International Publishing, pp. 1731–1737.

Barczyk, M., Carracedo, S. and Gullberg, D. (2010) 'Integrins', *Cell and Tissue Research*, 339(1), pp. 269–280.

Barros, C. S., Franco, S. J. and Müller, U. (2011) 'Extracellular Matrix: Functions in the nervous system', *Cold Spring Harbor Perspectives in Biology*, 3(1), pp. 1–24.

Baum, P. D. and Garriga, G. (1997) 'Neuronal migrations and axon fasciculation are disrupted in ina-1 integrin mutants', *Neuron*, 19(1), pp. 51–62.

Beattie, E. C. *et al.* (2000) 'NGF signals through TrkA to increase clathrin at the plasma membrane and enhance clathrin-mediated membrane trafficking.', *The Journal of neuroscience : the official journal of the Society for Neuroscience*, 20(19), pp. 7325–33.

Becker, H. M. *et al.* (2013) 'α1β1 Integrin-Mediated Adhesion Inhibits Macrophage Exit from a Peripheral Inflammatory Lesion', *The Journal of Immunology*, 190(8), pp. 4305–4314.

Bichsel, S. J. *et al.* (2004) 'Mechanism of activation of NDR (nuclear Dbf2-related) protein kinase by the hMOB1 protein', *Journal of Biological Chemistry*, 279(34), pp. 35228–35235.

Blaess, S. *et al.* (2004) 'β1-Integrins Are Critical for Cerebellar Granule Cell Precursor Proliferation', *Journal of Neuroscience*, 24(13), pp. 3402–3412.

Bolduc, F. V *et al.* (2010) 'Fragile x mental retardation 1 and filamin a interact genetically in Drosophila long-term memory.', *Frontiers in neural circuits*, 3(January), p. 22.

Bourgin, C. *et al.* (2007) 'The EphA4 receptor regulates dendritic spine remodeling by affecting β1-integrin signaling pathways', *Journal of Cell Biology*, 178(7), pp. 1295–1307.

Bridgewater, R. E., Norman, J. C. and Caswell, P. T. (2012) 'Integrin trafficking at a glance', *Journal of Cell Science*, 125, pp. 3695–3701.

Buchsbaum, I. Y. and Cappello, S. (2019) 'Neuronal migration in the CNS during development and disease: Insights from in vivo and in vitro models', *Development (Cambridge)*, 146(1).

Burke, R. D. (1999) 'Invertebrate integrins: Structure, function, and evolution', *International Review of Cytology*, 191,

pp. 257–284.

Burns, L. H. and Wang, H.-Y. (2017) 'Altered filamin A enables amyloid beta-induced tau hyperphosphorylation and neuroinflammation in Alzheimer's disease', *Neuroimmunology and Neuroinflammation*, 4(12), p. 263.

Byfield, F. J. *et al.* (2009) 'Absence of filamin A prevents cells from responding to stiffness gradients on gels coated with collagen but not fibronectin', *Biophysical Journal*. Biophysical Society, 96(12), pp. 5095–5102.

Calderwood, D. (2004) 'Integrin activation.', *Journal of cell science*, 117, pp. 657–66.

Cameron, S. and Rao, Y. (2010) 'Molecular mechanisms of tiling and self-avoidance in neural development', *Molecular Brain*, 3(1), pp. 1–7.

Campos, L. S. *et al.* (2004) 'β1 integrins activate a MAPK signalling pathway in neural stem cells that contributes to their maintenance', *Development*, 131(14), pp. 3433–3444.

Carmeliet, G., Himpens, B. and Cassiman, J. J. (1994) 'Selective increase in the binding of the alpha 1 beta 1 integrin for collagen type IV during neurite outgrowth of human neuroblastoma TR 14 cells.', *Journal of cell science*, 107 (Pt 1, pp. 3379–3392.

Caswell, P. T., Vadrevu, S. and Norman, J. C. (2009) 'Integrins: masters and slaves of endocytic transport.', *Nature reviews. Molecular cell biology*, 10, pp. 843–853.

Chan, C.-S. *et al.* (2006) 'β1-Integrins Are Required for Hippocampal AMPA Receptor-Dependent Synaptic Transmission, Synaptic Plasticity, and Working Memory', *Journal of Neuroscience*, 26(1), pp. 223–232.

Chavez, A. *et al.* (2015) 'Highly efficient Cas9-mediated transcriptional programming', *Nature Methods*, 12(4), pp. 326–328.

Chavis, P. and Westbrook, G. (2001) 'Integrins mediate functional pre- and postsynaptic maturation at a hippocampal synapse', *Nature*, 411(6835), pp. 317–321.

Chen, H. S., Kolahi, K. S. and Mofrad, M. R. K. (2009) 'Phosphorylation facilitates the integrin binding of filamin under force', *Biophysical Journal*. Biophysical Society, 97(12), pp. 3095–3104.

Chen, J. F., Salas, A. and Springer, T. A. (2003) 'Bistable regulation of integrin adhesiveness by a bipolar metal ion cluster', *Nature Structural Biology*, 10(12), pp. 995–1001.

Chen, M. and Strachers, A. (1989) 'In Situ Phosphorylation of Platelet Actin-binding Protein by dependent Protein Kinase Stabilizes It against Proteolysis by Calpain "', *Journal of Biological Chemistry*, 264(24), pp. 14282–14289.

Chen, S. *et al.* (2015) 'Genome-wide CRISPR screen in a mouse model of tumor growth and metastasis', *Cell*. Elsevier Inc., 160(6), pp. 1246–1260.

Cho, Y., Park, D. and Cavalli, V. (2015) 'Filamin a is required in injured axons for HDAC5 activity and axon regeneration', *Journal of Biological Chemistry*, 290(37), pp. 22759–22770.

Chun, D. *et al.* (2001) 'Evidence that integrins contribute to multiple stages in the consolidation of long term potentiation in rat hippocampus', *Neuroscience*, 105(4), pp. 815–829.

Cornils, H. *et al.* (2010) 'Ablation of the Kinase NDR1 Predisposes Mice to the Development of T Cell Lymphoma', *Science Signaling*, 3(126).

Cukier, I. H., Li, Y. and Lee, J. M. (2007) 'Cyclin B1/Cdk1 binds and phosphorylates Filamin A and regulates its ability to cross-link actin', *FEBS Letters*, 581(8), pp. 1661–1672.

Culmsee, C. *et al.* (2002) 'Nerve growth factor survival signaling in cultured hippocampal neurons is mediated through TrkA and requires the common neurotrophin receptor P75', *Neuroscience*. Elsevier, 115(4), pp. 1089–1108.

Cunningham, C. C. *et al.* (1992) 'Actin-binding protein requirement for cortical stability and efficient locomotion', *Science*, 255(5042), pp. 325–327.

D'Addario, M. *et al.* (2002) 'Interaction of p38 and Sp1 in a mechanical force-induced, β1 integrin-mediated transcriptional circuit that regulates the actin-binding protein filamin-A', *Journal of Biological Chemistry*, 277(49), pp. 47541–47550.

DeFreitas, M. F. *et al.* (1995) 'Identification of integrin α3β1 as a neuronal thrombospondin receptor mediating neurite outgrowth', *Neuron*, 15(2), pp. 333–343.

Demiray, Y. E. *et al.* (2018) 'Ndr2 Kinase Controls Neurite Outgrowth and Dendritic Branching Through α1 Integrin Expression', *Frontiers in Molecular Neuroscience*, 11(March), p. 66.

Denda, S. and Reichardt, L. F. (2007) 'Studies on Integrins in the Nervous System', *Methods in Enzymology*, 426(07), pp. 203–221.

Desban, N. *et al.* (2006) 'α1β1-Integrin Engagement To Distinct Laminin-1 Domains Orchestrates Spreading, Migration and Survival of Neural Crest Cells Through Independent Signaling Pathways', *Journal of Cell Science*, 119(15), pp. 3206–3218.

Devroe, E. *et al.* (2004) 'Human Mob proteins regulate the NDR1 and NDR2 serine-threonine kinases', *Journal of Biological Chemistry*, 279(23), pp. 24444–24451.

Dijkhuizen, P. A. and Ghosh, A. (2005) 'BDNF regulates primary dendrite formation in cortical neurons via the PI3-kinase and MAP kinase signaling pathways', *Journal of Neurobiology*, 62(2), pp. 278–288.

Dominguez, R. and Holmes, K. C. (2011) 'Actin structure and function', *Annual Review of Biophysics*, 40(1), pp. 169–186.

Donada, A. *et al.* (2019) 'Disrupted filamin A/aIIbb3 interaction induces macrothrombocytopenia by increasing RhoA activity', *Blood*, 133(16), pp. 1778–1788.

Dyson, J. M. *et al.* (2003) 'SHIP-2 forms a tetrameric complex with filamin, actin, and GPIb-IX-V: Localization of SHIP-2 to the activated platelet actin cytoskeleton', *Blood*, 102(3), pp. 940–948.

Dzyubenko, E., Gottschling, C. and Faissner, A. (2016) 'Neuron-Glia Interactions in Neural Plasticity: Contributions of Neural Extracellular Matrix and Perineuronal Nets', *Neural Plasticity*, 2016.

Ehrlicher, A. J. *et al.* (2011) 'Mechanical strain in actin networks regulates FilGAP and integrin binding to filamin A', *Nature*, 478(7368), pp. 260–263.

Emoto, K. *et al.* (2006) 'The tumour suppressor Hippo acts with the NDR kinases in dendritic tiling and maintenance.', *Nature*, 443(7108), pp. 210–213.

Ewing, R. M. *et al.* (2007) 'Large-scale mapping of human protein-protein interactions by mass spectrometry', *Molecular Systems Biology*, 3(89), pp. 1–17.

Falkenberg, T. *et al.* (1992) 'Increased expression of brain-derived neurotrophic factor mRNA in rat hippocampus is associated with improved spatial memory and enriched environment', *Neuroscience letters*. Elsevier, 138(1), pp. 153–156.

Fässler, R. and Meyer, M. (1995) 'Consequences of lack of beta 1 gene expression in mice', *Genes & development*, pp. 1896–1908.

Feng, Y. *et al.* (2006) 'Filamin A (FLNA) is required for cell-cell contact in vascular development and cardiac morphogenesis.', *Proceedings of the National Academy of Sciences of the United States of America*, 103(52), pp. 19836–41.

Flanagan, L. A. *et al.* (2001) 'Filamin A, the Arp2/3 complex, and the morphology and function of cortical actin filaments in human melanoma cells', *Journal of Cell Biology*, 155(3), pp. 511–517.

van der Flier, A. and Sonnenberg, A. (2001) 'Structural and functional aspects of filamins', *Biochimica et Biophysica Acta (BBA) - Molecular Cell Research*, 1538(2–3), pp. 99–117.

Fox, J. W. *et al.* (1998) 'Mutations in filamin 1 prevent migration of cerebral cortical neurons in human Periventricular heterotopia', *Neuron*, 21(6), pp. 1315–1325.

De Franceschi, N. *et al.* (2016) 'Selective integrin endocytosis is driven by interactions between the integrin α-chain and AP2', *Nature Structural & Molecular Biology*. Nature Publishing Group, (January), pp. 1–10.

Frenz, L. M. *et al.* (2000) 'The budding yeast Dbf2 protein kinase localises to the centrosome and moves to the bud neck in late mitosis.', *J Cell Sci*, 113, pp. 3399–3408.

Fujioka, T. *et al.* (2017) 'β1 Integrin Signaling Promotes Neuronal Migration Along Vascular Scaffolds in the Post-Stroke Brain', *EBioMedicine*. 3-V Biosciences, 16, pp. 195–203.

Fusaoka-Nishioka, E. *et al.* (2011) 'Differential effects of laminin isoforms on axon and dendrite development in hippocampal neurons', *Neuroscience Research*, 71(4), pp. 421–426.

Gage, F. H. (2000) 'Mammalian neural stem cells', *Science*. American Association for the Advancement of Science, 287(5457), pp. 1433–1438.

Galileo, D. S. *et al.* (1992) 'Retrovirally introduced antisense integrin RNA inhibits neuroblast migration in vivo', *Neuron*. Cell Press, 9(6), pp. 1117–1131.

Gallegos, M. E. and Bargmann, C. I. (2004) 'Mechanosensory neurite termination and tiling depend on SAX-2 and the SAX-1 kinase', *Neuron*, 44(2), pp. 239–249.

Gao, Y. *et al.* (2019) 'Plug-and-Play Protein Modification Using Homology-Independent Universal Genome Engineering', *Neuron*. Elsevier Inc., 103(4), pp. 583-597.e8.

García, E., Stracher, A. and Jay, D. (2006) 'Calcineurin dephosphorylates the C-terminal region of filamin in an important regulatory site: A possible mechanism for filamin mobilization and cell signaling', *Archives of Biochemistry and Biophysics*, 446(2), pp. 140–150.

Gardner, H. *et al.* (1999) 'Absence of integrin α 1 β 1 in the mouse causes loss of feedback regulation of collagen synthesis in normal and wounded dermis', 272, pp. 263–272.

Gariboldi, M. *et al.* (1994) 'Comparative mapping of the actin-binding protein 280 genes in human and mouse', *Genomics*. Elsevier, 21(2), pp. 428–430.

Gehler, S. *et al.* (2009) 'Filamin A–β1 Integrin Complex Tunes Epithelial Cell Response to Matrix Tension', *Molecular Biology of the Cell*, 20, pp. 3224–3238.

Glenney, J. R., Kaulfus, P. and Weber, K. (1981) 'F-Actin Binding and Bundling Properties of Fibrin, a Major Cytoskelatal Protein of Microvilus Core Filaments', *The Journal of biological chemistry*, 256(17), pp. 9283–9288.

Glogauer, M. *et al.* (1998) 'The role of actin-binding protein 280 in integrin-dependent mechanoprotection', *Journal of Biological Chemistry*, 273(3), pp. 1689–1698.

Gógl, G. *et al.* (2015) 'The Structure of an NDR/LATS Kinase–Mob Complex Reveals a Novel Kinase–Coactivator System and Substrate Docking Mechanism', *PLoS Biology*, 13(5), pp. 1–32.

Goley, E. D. and Welch, M. D. (2006) 'The ARP2/3 complex: An actin nucleator comes of age', *Nature Reviews Molecular Cell Biology*, 7(10), pp. 713–726.

Govek, E., Newey, S. E. and Aelst, L. Van (2005) 'The role of the Rho GTPases in neuronal development', pp. 1–49.

Graus-Porta, D. *et al.* (2001) 'β1-Class integrins regulate the development of laminae and folia in the cerebral and cerebellar cortex', *Neuron*, 31(3), pp. 367–379.

Greve, J. M. and Gottlieb, D. I. (1982) 'Monoclonal Antibodies Which Alter the Morphology of Cultured Chick Myogenic Cells', *Journal of Cellular Biochemistry*, 18(2), pp. 221–229.

Gualdoni, S. *et al.* (2007) 'Normal levels of Rac1 are important for dendritic but not axonal development in hippocampal neurons', *Biology of the Cell*, 99(8), pp. 455–464.

Gushiken, F. C. *et al.* (2008) 'Protein phosphatase 2A negatively regulates integrin αIIbβ3 signaling', *Journal of Biological Chemistry*, 283(19), pp. 12862–12869.

Hall, J., Thomas, K. L. and Everitt, B. J. (2000) 'Rapid and selective induction of BDNF expression in the hippocampus during contextual learning', *Nature neuroscience*. Nature Publishing Group, 3(6), pp. 533–535.

Hall, P. E. *et al.* (2006) 'Integrins Are Markers of Human Neural Stem Cells', *Stem Cells*, 24(9), pp. 2078–2084.

Hamill, K. J. *et al.* (2009) 'Laminin deposition in the extracellular matrix: A complex picture emerges', *Journal of Cell Science*, 122(24), pp. 4409–4417.

Hanamura, K. *et al.* (2010) 'Low accumulation of drebrin at glutamatergic postsynaptic sites on GABAergic neurons', *Neuroscience*. Elsevier Inc., 169(4), pp. 1489–1500.

Hanks, S. K. and Hunter, T. (1995) ' The eukaryotic protein kinase superfamily: kinase (catalytic) domain structure and classification 1 ', *The FASEB Journal*, 9(8), pp. 576–596.

Hartwig, J. H. and Stossel, T. P. (1975) 'Isolation and properties of actin, myosin, and a new actin binding protein in rabbit alveolar macrophages', *Journal of Biological Chemistry*, 250(14), pp. 5696–5705.

Hartwig, J. H., Tyler, J. and Stössel, T. P. (1980) 'Actin-binding Protein Promotes the Bipolar and Perpendicular Branching of Actin Filaments Morphology of Actin Copolymerized with Actin-', *The Journal of cell biology*, 87(7), pp. 841–848.

Heggeness, M. H., Ash, J. F. and Singer, S. J. (1978) 'Transmembrane linkage of fibronectin to intracellular actin-containing filaments in cultured human fibroblasts.', *Annals of the New York Academy of Sciences*. United States, 312, pp. 414–417.

Hergovich, A. *et al.* (2006) 'NDR kinases regulate essential cell processes from yeast to humans.', *Nature reviews. Molecular cell biology*, 7(4), pp. 253–64.

Hergovich, A. (2016) 'The roles of NDR protein kinases in hippo signalling', *Genes*, 7(5), pp. 1–16.

Hogervorst, F. *et al.* (1990) 'Cloning and sequence analysis of beta-4 cDNA: An integrin subunit that contains a unique 118 kd cytoplasmic domain', *EMBO Journal*, 9(3), pp. 765–770.

Homma, Y. and Fukuda, M. (2016) 'Rabin8 regulates neurite outgrowth in both a GEF-activity-dependent and -independent manner.', *Molecular biology of the cell*, 27, pp. 2107–2118.

Hu, J. *et al.* (2017) 'Opposing FlnA and FlnB interactions regulate RhoA activation in guiding dynamic actin stress fiber formation and cell spreading', 26(7), pp. 1294–1304.

Huang, Z. *et al.* (2006) 'Distinct Roles of the β1-Class Integrins at the Developing and the Mature Hippocampal Excitatory Synapse', *Journal of Neuroscience*, 26(43), pp. 11208–11219.

Hutti, J. E. *et al.* (2004) 'A rapid method for determining protein kinase phosphorylation specificity', *Nature Methods*, 1(1), pp. 27–29.

Hynes, R. O. (1973) 'Alteration of cell surface proteins by viral transformation and by proteolysis', *Proceedings of the National Academy of Sciences of the United States of America*, 70(11), pp. 3170–3174.

Hynes, R. O. (2002) 'Integrins: Bidirectional, allosteric signaling machines', *Cell*, 110(6), pp. 673–687.

Hynes, R. O. and Yamada, K. M. (1982) 'Fibronectins: multifunctional modular glycoproteins.', *The Journal of cell biology*. United States, 95(2 Pt 1), pp. 369–377.

Ithychanda, S. S. *et al.* (2009) 'Migfilin, a molecular switch in regulation of integrin activation', *Journal of Biological Chemistry*, 284(7), pp. 4713–4722.

Ivankovic-Dikic, I. *et al.* (2000) 'Pyk2 and FAK regulate neurite outgrowth induced by growth factors and integrins', *Nature Cell Biology*, 2(9), pp. 574–581.

Ivins, J. K., Yurchenco, P. D. and Lander, A. D. (2000) 'Regulation of neurite outgrowth by integrin activation', *The Journal of neuroscience : the official journal of the Society for Neuroscience*, 20(17), pp. 6551–6560.

Jackson, T. R. *et al.* (1996) 'Initiation and maintenance of NGF-stimulated neurite outgrowth requires activation of a phosphoinositide 3-kinase', *Journal of Cell Science*, 109(2), pp. 289–300.

Jaworski, J. *et al.* (2005) 'Control of Dendritic Arborization by the Phosphoinositide- 3 -Kinase – Akt – Mammalian Target of Rapamycin Pathway', *The Journal of Neuroscience*, 25(49), pp. 11300–11312.

Jay, D., García, E. J. and de la Luz Ibarra, M. (2004) 'In situ determination of a PKA phosphorylation site in the C-terminal region of filamin', *Molecular and Cellular Biochemistry*, 260(1), pp. 49–53.

Ji, Y. *et al.* (2005) 'Cyclic AMP controls BDNF-induced TrkB phosphorylation and dendritic spine formation in mature hippocampal neurons', *Nature Neuroscience*, 8(2), pp. 164–172.

Ji, Z. *et al.* (2018) 'Silencing Filamin A Inhibits the Invasion and Migration of Breast Cancer Cells by Up-regulating 14-3-3σ', *Current medical science*. Springer, 38(3), pp. 461–466.

Jongbloets, B. C. *et al.* (2017) 'Stage-specific functions of Semaphorin7A during adult hippocampal neurogenesis rely on distinct receptors', *Nature Communications*. Nature Publishing Group, 8, p. 14666.

Joung, J. *et al.* (2017) 'Genome-scale CRISPR-Cas9 knockout and transcriptional activation screening', *Nature Protocols*. Nature Publishing Group, 12(4), pp. 828–863.

Kaplan, D. R. and Miller, F. D. (2000) 'Neurotrophin signal transduction in the nervous system', *Current Opinion in Neurobiology*, 10(3), pp. 381–391.

Kasza, K. E. *et al.* (2009) 'Filamin A is essential for active cell stiffening but not passive stiffening under external force', *Biophysical Journal*. Biophysical Society, 96(10), pp. 4326–4335.

Kern, A. *et al.* (1993) 'Interaction of type IV collagen with the isolated integrins α1β1 and α2β1.', *European journal of biochemistry / FEBS*, 215(1), pp. 151–9.

Kiema, T. *et al.* (2006) 'The molecular basis of filamin binding to integrins and competition with talin', *Molecular Cell*, 21(3), pp. 337–347.

Kim, H. *et al.* (2008) 'Filamin A regulates cell spreading and survival via β1 integrins', *Experimental Cell Research*, 314(4), pp. 834–846.

Kim, I. H. *et al.* (2013) 'Disruption of Arp2/3 Results in Asymmetric Structural Plasticity of Dendritic Spines and Progressive Synaptic and Behavioral Abnormalities', *Journal of Neuroscience*, 33(14), pp. 6081–6092.

Kim, S. Y. *et al.* (2016) 'Structural basis for autoinhibition and its relief of MOB1 in the Hippo pathway', *Scientific Reports*. Nature Publishing Group, 6(June), pp. 1–15.

Kim, Y. *et al.* (2004) 'A positive role of the PI3-K/Akt signaling pathway in PC12 cell differentiation', *Molecules and Cells*, 18(3), pp. 353–359.

Kim, Y. H. *et al.* (2011) 'Enhancement of neuronal cell adhesion by covalent binding of poly-d-lysine', *Journal of Neuroscience Methods*. Elsevier B.V., 202(1), pp. 38–44.

Knight, C. G. *et al.* (2000) 'The Collagen-binding A-domains of Integrins α1β1 and α2β1 Recognize the Same Specific Amino Acid Sequence, GFOGER, in Native (Triple-helical) Collagens', *The Journal of Biological Chemistry*, 275(1), pp. 35–40.

Knudsen, K. A., Horwitz, A. F. and Buck, C. A. (1985) 'A Monoclonal Antibody Identifies a Glycoprotein Complex Involved in Cell-Substratum Adhesion', *Experimental Cell Research*, 57, pp. 218–226.

Konermann, S. *et al.* (2015) 'Genome-scale transcriptional activation by an engineered CRISPR-Cas9 complex', *Nature*. Nature Publishing Group, 517(7536), pp. 583–588.

Kornberg, L. *et al.* (1992) 'Cell adhesion or integrin clustering increases phosphorylation of a focal adhesion-associated tyrosine kinase', *Journal of Biological Chemistry*, 267(33), pp. 23439–23442.

Kotani, T. *et al.* (2007) 'Constitutive activation of neuronal Src causes aberrant dendritic morphogenesis in mouse cerebellar Purkinje cells', *Neuroscience Research*, 57(2), pp. 210–219.

Kul Madencioglu, D. A. (2019) *Roles of the Hippo pathway kinase Ndr2 in neural development and behavior*. Doctoral Thesis - Otto von Guericke University.

Kulkarni, V. A. and Firestein, B. L. (2012) 'The dendritic tree and brain disorders', *Molecular and Cellular Neuroscience*. Elsevier Inc., 50(1), pp. 10–20.

Kumar, V. *et al.* (2005) 'Regulation of Dendritic Morphogenesis by Ras–PI3K–Akt-mTOR and Ras–MAPK Signaling Pathways', *The Journal of Neuroscience*, 25(49), pp. 11288–11299.

Kurabayashi, N. *et al.* (2018) 'The LPA-LPA4 axis is required for establishment of bipolar morphology and radial migration of newborn cortical neurons', *Development*, 145(17), p. dev162529.

Lange, M. *et al.* (2015) '47 patients with FLNA associated periventricular nodular heterotopia', *Orphanet Journal of Rare Diseases*. Orphanet Journal of Rare Diseases, pp. 1–11.

Lau, T. L. *et al.* (2009) 'The structure of the integrin αiIbB3 transmembrane complex explains integrin transmembrane signalling', *EMBO Journal*, 28(9), pp. 1351–1361.

Lawson, C. D. and Burridge, K. (2014) 'The on-off relationship of Rho and Rac during integrin-mediated adhesion and cell migration', *Small GTPases*, 5, p. e27958.

Lazo, O. M. *et al.* (2013) 'BDNF Regulates Rab11-Mediated Recycling Endosome Dynamics to Induce Dendritic Branching', 33(14), pp. 6112–6122.

Lei, W.-L. *et al.* (2012) 'Laminin/β1 integrin signal triggers axon formation by promoting microtubule assembly and stabilization', *Cell Research*, pp. 954–972.

Leone, D. P. *et al.* (2005) 'Regulation of neural progenitor proliferation and survival by β1 integrins', *Journal of Cell Science*, 118(12), pp. 2589–2599.

Li, L. *et al.* (2015) 'Filamin A phosphorylation by Akt promotes cell migration in response to arsenic', *Oncotarget*, 6(14), pp. 12009–12019.

Lian, G. *et al.* (2012) 'Filamin A Regulates Neural Progenitor Proliferation and Cortical Size through Wee1-Dependent Cdk1 Phosphorylation', *Journal of Neuroscience*, 32(22), pp. 7672–7684.

Lian, G. *et al.* (2019) 'Cytoskeletal associated filamin a and RhoA affect neural progenitor specification during mitosis', *Cerebral Cortex*, 29(3), pp. 1280–1290.

Lian, G. and Sheen, V. L. (2015) 'Cytoskeletal proteins in cortical development and disease: Actin associated proteins in periventricular heterotopia', *Frontiers in Cellular Neuroscience*, 9(APR), pp. 1–13.

Lim, Y. *et al.* (2008) 'PyK2 and FAK connections to p190Rho guanine nucleotide exchange factor regulate RhoA activity, focal adhesion formation, and cell motility', *Journal of Cell Biology*, 180(1), pp. 187–203.

Lin, Y.-C., Yeckel, M. F. and Koleske, A. J. (2013) 'Abl2/Arg Controls Dendritic Spine and Dendrite Arbor Stability via Distinct Cytoskeletal Control Pathways', *Journal of Neuroscience*, 33(5), pp. 1846–1857.

Liu, X. *et al.* (2016) 'PRG-1 Regulates Synaptic Plasticity via Intracellular PP2A/β1-Integrin Signaling', *Developmental Cell*, 38(3), pp. 275–290.

Loo, D. T., Kanner, S. B. and Aruffo, A. (1998) 'Filamin binds to the cytoplasmic domain of the β1-integrin: Identification of amino acids responsible for this interaction', *Journal of Biological Chemistry*, 273(36), pp. 23304–23312.

Lowry, O. H. *et al.* (1951) 'Protein measurement with the Folin phenol reagent.', *The Journal of biological chemistry*. United States, 193(1), pp. 265–275.

Loy, C. J., Sim, K. S. and Yong, E. L. (2003) 'Filamin-A fragment localizes to the nucleus to regulate androgen receptor and coactivator functions.', *Proceedings of the National Academy of Sciences of the United States of America*, 100(8), pp. 4562–7.

Luo, B.-H., Carman, C. V and Springer, T. a (2007) 'Structural basis of integrin regulation and signaling.', *Annual review of immunology*, 25, pp. 619–47.

Mah, A. S., Jang, J. and Deshaies, R. J. (2001) 'Protein kinase Cdc15 activates the Dbf2-Mob1 kinase complex', *Proceedings of the National Academy of Sciences of the United States of America*, 98(13), pp. 7325–7330.

Mali, P., Aach, J., *et al.* (2013) 'CAS9 transcriptional activators for target specificity screening and paired nickases for cooperative genome engineering', *Nature Biotechnology*. Nature Publishing Group, 31(9), pp. 833–838.

Mali, P., Yang, L., *et al.* (2013) 'RNA-guided human genome engineering via Cas9', *Science*, 339(6121), pp. 823–826.

Mammoto, A., Huang, S. and Ingber, D. E. (2007) 'Filamin links cell shape and cytoskeletal structure to Rho regulation by controlling accumulation of p190RhoGAP in lipid rafts', *Journal of Cell Science*, 120(3), pp. 456–467.

Manning, G. *et al.* (2002) 'The protein kinase complement of the human genome', *Science*. American Association for the Advancement of Science, 298(5600), pp. 1912–1934.

Marcinkiewicz, C. *et al.* (2003) 'Obtustatin: a potent selective inhibitor of alpha1beta1 integrin in vitro and angiogenesis in vivo.', *Cancer research*, 63(9), pp. 2020–2023.

Margadant, C. *et al.* (2012) 'Distinct roles of talin and kindlin in regulating integrin α5β1 function and trafficking', *Current Biology*, 22(17), pp. 1554–1563.

Marrs, G. S. *et al.* (2006) 'Dendritic arbors of developing retinal ganglion cells are stabilized by β1-integrins', *Molecular and Cellular Neuroscience*, 32(3), pp. 230–241.

Mezawa, M. *et al.* (2016) 'Filamin A regulates the organization and remodeling of the pericellular collagen matrix', *The FASEB Journal*, 30(10), pp. 3613–3627.

Millward, T. A. *et al.* (1998) 'Calcium regulation of NDR protein kinase mediated by S100 calcium-binding proteins', *EMBO Journal*, 17(20), pp. 5913–5922.

Millward, T., Cron, P. and Hemmings, B. A. (1995) 'Molecular cloning and characterization of a conserved nuclear serine(threonine) protein kinase', *Proc Natl Acad Sci U S A*, 92(May), pp. 5022–5026.

Mizuno, M. *et al.* (2000) 'Involvement of brain-derived neurotrophic factor in spatial memory formation and maintenance in a radial arm maze test in rats', *Journal of Neuroscience*. Soc Neuroscience, 20(18), pp. 7116–7121.

Monje, F. J. *et al.* (2012) 'Focal Adhesion Kinase Regulates Neuronal Growth , Synaptic Plasticity and Hippocampus-Dependent Spatial Learning and Memory', *Neurosignals*, 20, pp. 1–14.

Moreno-Murciano, M. P. *et al.* (2003) 'Amino acid sequence and homology modeling of obtustatin, a novel non-RGD-containing short disintegrin isolated from the venom of *Vipera lebetina obtusa.*', *Protein science : a publication of the Protein Society*, 12(2), pp. 366–71.

Moresco, E. M. Y. *et al.* (2005) 'Integrin-mediated dendrite branch maintenance requires Abelson (Abl) family kinases.', *The Journal of neuroscience : the official journal of the Society for Neuroscience*, 25(26), pp. 6105–6118.

Morimoto, K. *et al.* (1998) 'Time-dependent changes in neurotrophic factor mRNA expression after kindling and long-term potentiation in rats', *Brain research bulletin*. Elsevier, 45(6), pp. 599–605.

Morse, E. M., Brahme, N. N. and Calderwood, D. A. (2014) 'Integrin cytoplasmic tail interactions', *Biochemistry*, 53(5), pp. 810–820.

Moser, M. *et al.* (2008) 'Kindlin-3 is essential for integrin activation and platelet aggregation', *Nature Medicine*, 14(3), pp. 325–330.

Mould, A. P. *et al.* (2005) 'Evidence that monoclonal antibodies directed against the integrin β subunit plexin/semaphorin/integrin domain stimulate function by inducing receptor extension', *Journal of Biological Chemistry*, 280(6), pp. 4238–4246.

Muriel, O. *et al.* (2011) 'Phosphorylated filamin A regulates actin-linked caveolae dynamics.', *Journal of cell science*, 124, pp. 2763–2776.

Nakamura, F. *et al.* (2002) 'Comparison of filamin A-induced cross-linking and Arp2/3 complex-mediated branching on the mechanics of actin filaments', *Journal of Biological Chemistry*, 277(11), pp. 9148–9154.

Nakamura, F. *et al.* (2005) 'Ca2+ and calmodulin regulate the binding of filamin A to actin filaments', *Journal of Biological Chemistry*, 280(37), pp. 32426–32433.

Nakamura, F. *et al.* (2007) 'Structural basis of filamin A functions', *Journal of Cell Biology*, 179(5), pp. 1011–1025.

Nakamura, F. *et al.* (2014) 'Amino- and carboxyl-terminal domains of Filamin-A interact with CRMP1 to mediate Sema3A signalling', *Nature Communications*. Nature Publishing Group, 5, p. 5325.

Nakamura, F., Stossel, T. P. and Hartwig, J. H. (2011) 'The filamins: Organizers of cell structure and function', *Cell Adhesion and Migration*, 5(2), pp. 160–169.

Nakayama, a Y., Harms, M. B. and Luo, L. (2000) 'Small GTPases Rac and Rho in the maintenance of dendritic spines and branches in hippocampal pyramidal neurons.', *The Journal of neuroscience : the official journal of the Society for Neuroscience*, 20(14), pp. 5329–38.

Nanda, S. *et al.* (2020) 'Distinct Roles of Microtubules and Actin Filaments in Defining Dendritic Architecture', *bioRxiv*.

Naska, S. *et al.* (2006) 'An essential role for the integrin-linked kinase-glycogen synthase kinase-3β pathway during dendrite initiation and growth', *Journal of Neuroscience*, 26(51), pp. 13344–13356.

Navarro, A. I. and Rico, B. (2014) 'Focal adhesion kinase function in neuronal development', *Current Opinion in Neurobiology*. Elsevier Ltd, 27, pp. 89–95.

Neff, N. T. *et al.* (1982) 'A monoclonal antibody detaches embryonic skeletal muscle from extracellular matrices', *Journal of Cell Biology*, 95(2), pp. 654–666.

Nestor, M. W. *et al.* (2011) 'The actin binding domain of βI-spectrin regulates the morphological and functional dynamics of dendritic spines', *PLoS ONE*, 6(1).

Ni, L. *et al.* (2015) 'Structural basis for Mob1-dependent activation of the core Mst–Lats kinase cascade in Hippo signaling', *Genes and Development*, 29(13), pp. 1416–1431.

Nichols, S. A. *et al.* (2006) 'Early evolution of animal cell signaling and adhesion genes', *Proceedings of the National Academy of Sciences*, 103(33), pp. 12451–12456.

Nieuwenhuis, B. *et al.* (2018) 'Integrins promote axonal regeneration after injury of the nervous system', *Biological Reviews*, 93(3), pp. 1339–1362.

Nieves, B. *et al.* (2010) 'The NPIY motif in the integrin β1 tail dictates the requirement for talin-1 in outside-in signaling', *Journal of Cell Science*, 123(8), pp. 1216–1226.

Nilsson, S. *et al.* (2006) 'Threonine 788 in integrin subunit β1 regulates integrin activation', *Experimental Cell Research*. Elsevier Inc., 312(6), pp. 844–853.

Ning, L. *et al.* (2013) 'Interactions between ICAM-5 and β1 integrins regulate neuronal synapse formation', *Journal of Cell Science*, 126(1), pp. 77–89.

Nishida, N. *et al.* (2006) 'Activation of Leukocyte β2 Integrins by Conversion from Bent to Extended Conformations', *Immunity*, 25(4), pp. 583–594.

Noam, Y. *et al.* (2012) 'Distinct Regional and Subcellular Localization of the Actin- Binding Protein Filamin A in the Mature Rat Brain', *J Comp Neurol.*, 520(13), pp. 3013–3034.

Nunes, A. M. *et al.* (2018) 'Magnesium Activates Microsecond Dynamics to Regulate Integrin-Collagen Recognition Magnesium Activates Microsecond Dynamics to Regulate Integrin-Collagen Recognition', *Structure*, 26, pp. 1080–1090.

O'Connor, C. M., Adams, J. U. and Fairman, J. (2010) 'Essentials of cell biology', *Cambridge, MA: NPG Education*, 1, p. 54.

O'Connor, S. M. *et al.* (2001) 'Survival and neurite outgrowth of rat cortical neurons in three-dimensional agarose and collagen gel matrices', *Neuroscience Letters*, 304(3), pp. 189–193.

Ohta, Y., Hartwig, J. H. and Stossel, T. P. (2006) 'FilGAP, a Rho- and ROCK-regulated GAP for Rac binds filamin A to control actin remodelling', *Nature Cell Biology*, 8(8), pp. 803–814.

Paddison, P. J. *et al.* (2002) 'Short hairpin RNAs (shRNAs) induce sequence-specific silencing in mammalian cells', *Genes & development*, 16, pp. 948–958.

Parsons, J. T. (2003) 'Focal adhesion kinase: The first ten years', *Journal of Cell Science*, 116(8), pp. 1409–1416.

Pasterkamp, R. J. *et al.* (2003) 'Semaphorin 7A promotes axon outgrowth through integrins and MAPKs', *Nature*, 424(6947), pp. 398–405.

Pearce, L. R., Komander, D. and Alessi, D. R. (2010) 'The nuts and bolts of AGC protein kinases', *Nature Reviews Molecular Cell Biology*. Nature Publishing Group, 11(1), pp. 9–22.

Pellinen, T. *et al.* (2008) 'Integrin Trafficking Regulated by Rab21 Is Necessary for Cytokinesis', *Developmental Cell*, 15(3), pp. 371–385.

Pentikäinen, U. and Ylänne, J. (2009) 'The Regulation Mechanism for the Auto-Inhibition of Binding of Human

Filamin A to Integrin', *Journal of Molecular Biology*. Elsevier Ltd, 393(3), pp. 644–657.

Petrecca, K., Miller, D. M. and Shrier, A. (2000) 'Localization and enhanced current density of the Kv4.2 potassium channel by interaction with the actin-binding protein filamin', *J Neurosci*, 20(23), pp. 8736–8744.

Pietri, T. *et al.* (2004) 'Conditional β1-integrin gene deletion in neural crest cells causes severe developmental alterations of the peripheral nervous system', *Development*, 131(16), pp. 3871–3883.

Pinkstaff, J. K. *et al.* (1999) 'Integrin subunit gene expression is regionally differentiated in adult brain', *Journal of Neuroscience*, 19(5), pp. 1541–1556.

Pollard, T. D. and Cooper, J. A. (2009) 'Actin, a central player in cell shape and movement', *Science (New York, N.Y.)*, 326(5957), pp. 1208–1212.

Popowicz, G. M. *et al.* (2006) 'Filamins: promiscuous organizers of the cytoskeleton', *Trends in Biochemical Sciences*, 31(7), pp. 411–419.

Ran, F. A. *et al.* (2015) 'In vivo genome editing using Staphylococcus aureus Cas9', *Nature*, 520(7546), pp. 186–191.

Rantala, J. K. *et al.* (2011) 'SHARPIN is an endogenous inhibitor of β1-integrin activation', *Nature Cell Biology*. Nature Publishing Group, 13(11), pp. 1315–1324.

Rehberg, K. *et al.* (2014) 'The Serine/Threonine Kinase Ndr2 Controls Integrin Trafficking and Integrin-Dependent Neurite Growth', *Journal of Neuroscience*, 34(15), pp. 5342–5354.

Retailleau, K. *et al.* (2016) 'Arterial Myogenic Activation through Smooth Muscle Filamin A', *Cell Reports*, 14(9), pp. 2050–2058.

Richter, M. *et al.* (2007) 'Collagen Distribution and Expression of Collagen-Binding α1β1 (VLA-1) and α2β1 (VLA-2) Integrins on CD4 and CD8 T Cells during Influenza Infection', *The Journal of Immunology*, 178(7), pp. 4506–4516.

Ritter, B. *et al.* (2017) 'A lentiviral system for efficient knockdown of proteins in neuronal cultures', *MNI Open Research*, 1(May), p. 2.

Rocca, D. L. *et al.* (2008) 'Inhibition of Arp2/3-mediated actin polymerization by PICK1 regulates neuronal morphology and AMPA receptor endocytosis', *Nature Cell Biology*, 10(3), pp. 259–271.

Rodgers, E. E. and Theibert, A. B. (2002) 'Functions of PI 3-kinase in development of the nervous system', *International Journal of Developmental Neuroscience*, 20(3–5), pp. 187–197.

Rogalla, T. *et al.* (1999) 'Regulation of Hsp27 oligomerization, chaperone function, and protective activity against oxidative stress/tumor necrosis factor by phosphorylation', *Journal of Biological Chemistry*, 274(27), pp. 18947–18956.

Rognoni, L. *et al.* (2012) 'Dynamic force sensing of filamin revealed in single-molecule experiments', *Proceedings of the National Academy of Sciences*, 109(48), pp. 19679–19684.

Ruoslahti, E. and Pierschbacher, M. D. (1987) 'New perspectives in cell adhesion: RGD and integrins', *Science*. American Association for the Advancement of Science, 238(4826), pp. 491–497.

Savell, K. E. *et al.* (2019) 'A neuron-optimized CRISPR/dCas9 activation system for robust and specific gene regulation', *eNeuro*, 6(1), pp. 1–17.

Scharffetter-Kochanek, K. *et al.* (1998) 'Spontaneous skin ulceration and defective T cell function in CD18 null mice', *Journal of Experimental Medicine*, 188(1), pp. 119–131.

Schlomann, U. *et al.* (2009) 'The stimulation of dendrite growth by Sema3A requires integrin engagement and focal adhesion kinase.', *Journal of cell science*, 122(Pt 12), pp. 2034–2042.

Schmid, R. S. and Anton, E. S. (2003) 'Role of Integrins in the Development of the Cerebral Cortex', *Cerebral Cortex*, 13, pp. 219–224.

Schmits, R. *et al.* (1996) 'LFA-1-deficient mice show normal CTL responses to virus but fail to reject immunogenic tumor', *Journal of Experimental Medicine*, 183(4), pp. 1415–1426.

Sebé-Pedrós, A. *et al.* (2010) 'Ancient origin of the integrin-mediated adhesion and signaling machinery', *Proceedings of the National Academy of Sciences*, 107(22), pp. 10142 LP – 10147.

Segura, I. *et al.* (2016) 'The Oxygen Sensor PHD2 Controls Dendritic Spines and Synapses via Modification of Filamin A', *Cell Reports*, 14(11), pp. 2653–2667.

Seki, A. and Rutz, S. (2018) 'Optimized RNP transfection for highly efficient CRI SPR/Cas9-mediated gene knockout in primary T cells', *Journal of Experimental Medicine*, 215(3), pp. 985–997.

Sharma, C. P., Ezzell, R. M. and Arnaout, M. a (1995) 'Direct interaction of filamin (ABP-280) with the beta 2-integrin subunit CD18.', *Journal of immunology*, 154(8), pp. 3461–3470.

Sheen, V. L. *et al.* (2002) 'Filamin A and Filamin B are co-expressed within neurons during periods of neuronal migration and can physically interact', *Human Molecular Genetics*, 11(23), pp. 2845–2854.

Sheen, V. L. (2012) 'Periventricular Heterotopia: Shuttling of Proteins through Vesicles and Actin in Cortical Development and Disease.', *Scientifica*, 2012, p. 480129.

Shi, Y. and Ethell, I. M. (2006) 'Integrins Control Dendritic Spine Plasticity in Hippocampal Neurons through NMDA Receptor and Ca', *The Journal of Neuroscience*, 26(6), pp. 1813–1822.

Shimaoka, M. and Springer, T. A. (2003) 'Therapeutic antagonists and conformational regulation of integrin function', *Nat Rev Drug Discov*, 2, pp. 703–716.

Sholl, D. A. (1953) 'Dendritic organization in the neurons of the visual and motor cortices of the cat.', *Journal of anatomy*, 87(4), pp. 387–406.

Spence, E. F. *et al.* (2016) 'The Arp2/3 Complex Is Essential for Distinct Stages of Spine Synapse Maturation, Including Synapse Unsilencing', *Journal of Neuroscience*, 36(37), pp. 9696–9709.

Spinardi, L. *et al.* (1995) 'A recombinant tail-less integrin β4 subunit disrupts hemidesmosomes, but does not suppress α6β4-mediated cell adhesion to laminins', *Journal of Cell Biology*, 129(2), pp. 473–487.

Stankiewicz, T. R. and Linseman, D. A. (2014) 'Rho family GTPases: Key players in neuronal development, neuronal survival, and neurodegeneration', *Frontiers in Cellular Neuroscience*, 8(OCT), pp. 1–14.

Stawowy, P. *et al.* (2005) 'Protein kinase C epsilon mediates angiotensin II-induced activation of β1-integrins in cardiac fibroblasts', *Cardiovascular Research*, 67(1), pp. 50–59.

Stegert, M. R. *et al.* (2004) 'Regulation of NDR2 protein kinase by multi-site phosphorylation and the S100B calcium-binding protein', *Journal of Biological Chemistry*, 279(22), pp. 23806–23812.

Stegert, M. R. *et al.* (2005) 'Regulation of NDR Protein Kinase by Hydrophobic Motif Phosphorylation Mediated by the Mammalian Ste20-Like Kinase MST3', *Molecular and Cellular Biology*, 25(24), pp. 11019–11029.

Stephens, L. E. *et al.* (1995) 'Deletion of β1 integrins in mice results in inner cell mass failure and peri-implantation lethality', *Genes and Development*, 9(15), pp. 1883–1895.

Stork, O. *et al.* (2004) 'Neuronal functions of the novel serine/threonine kinase Ndr2', *Journal of Biological Chemistry*, 279(44), pp. 45773–45781.

Su, L. *et al.* (2007) 'Safrole oxide induces neuronal apoptosis through inhibition of integrin β4/SOD activity and

elevation of ROS/NADPH oxidase activity', *Life Sciences*, 80(11), pp. 999–1006.

Suzuki, K. and Takahashi, K. (2003) 'Reduced Cell Adhesion during Mitosis by Threonine Phosphorylation of β1 Integrin', *Journal of Cellular Physiology*, 197(2), pp. 297–305.

Szeto, S. G. Y. *et al.* (2015) 'Phosphorylation of filamin A by Cdk1 regulates filamin A localization and daughter cell separation', *Experimental Cell Research*. Elsevier, 330(2), pp. 248–266.

Takala, H. *et al.* (2008) 'β2 integrin phosphorylation on Thr758 acts as a molecular switch to regulate 14-3-3 and filamin binding.', *Blood*. United States, 112(5), pp. 1853–1862.

Tamaskovic, R. *et al.* (2003) 'Mechanism of Ca2+-mediated regulation of NDR protein kinase through autophosphorylation and phosphorylation by an upstream kinase', *Journal of Biological Chemistry*, 278(9), pp. 6710–6718.

Tamkun, J. W. *et al.* (1986) 'Structure of integrin, a glycoprotein involved in the transmembrane linkage between fibronectin and actin', *Cell*, 46(2), pp. 271–282.

Tan, C. L. *et al.* (2011) 'Integrin activation promotes axon growth on inhibitory chondroitin sulfate proteoglycans by enhancing integrin signaling', *Journal of Neuroscience*, 31(17), pp. 6289–6295.

Tan, C. L. *et al.* (2015) 'Full length talin stimulates integrin activation and axon regeneration', *Molecular and Cellular Neuroscience*. The Authors, 68, pp. 1–8.

Teckchandani, A. *et al.* (2009) 'Quantitative proteomics identifies a Dab2/integrin module regulating cell migration', *Journal of Cell Biology*, 186(1), pp. 99–111.

Thiere, M. *et al.* (2016) 'Integrin Activation Through the Hematopoietic Adapter Molecule ADAP Regulates Dendritic Development of Hippocampal Neurons', *Frontiers in Molecular Neuroscience*, 9(September), pp. 1–14.

Tigges, U. *et al.* (2003) 'The F-actin cross-linking and focal adhesion protein filamin A is a ligand and in vivo substrate for protein kinase Cα', *Journal of Biological Chemistry*, 278(26), pp. 23561–23569.

Tomaselli, K. J. *et al.* (1993) 'Expression of beta 1 integrins in sensory neurons of the dorsal root ganglion and their functions in neurite outgrowth on two laminin isoforms.', *J. Neurosci.*, 13(11), pp. 4880–4888.

Tomaselli, K. J., Damsky, C. H. and Reichardt, L. F. (1987) 'Interactions of a neuronal cell line (PC12) with laminin, collagen IV, and fibronectin: identification of integrin-related glycoproteins involved in attachment and process outgrowth', *The Journal of cell biology*. The Rockefeller University Press, 105(5), pp. 2347–2358.

Tonge, D. A. *et al.* (2012) 'Fibronectin supports neurite outgrowth and axonal regeneration of adult brain neurons in vitro', *Brain Research*. Elsevier B.V., 1453(November 2016), pp. 8–16.

Travis, M. A. *et al.* (2004) 'Interaction of filamin A with the integrin β7 cytoplasmic domain: Role of alternative splicing and phosphorylation', *FEBS Letters*, 569(1–3), pp. 185–190.

Tucker, B. A., Rahimtula, M. and Mearow, K. M. (2005) 'Integrin activation and neurotrophin signaling cooperate to enhance neurite outgrowth in sensory neurons', *Journal of Comparative Neurology*, 486(3), pp. 267–280.

Tulla, M. *et al.* (2001) 'Selective Binding of Collagen Subtypes by Integrin α1I, α2I, and α10I Domains', *Journal of Biological Chemistry*, 276(51), pp. 48206–48212.

Tulla, M. *et al.* (2008) 'Effects of conformational activation of integrin α1I and α2I domains on selective recognition of laminin and collagen subtypes', *Experimental Cell Research*, 314(8), pp. 1734–1743.

Turner, D. C., Flier, L. A. and Carbonetto, S. (1987) 'Magnesium-dependent attachment and neurite outgrowth by PC12 cells on collagen and laminin substrata', *Developmental Biology*, 121(2), pp. 510–525.

Ultanir, S. K. *et al.* (2012) 'Chemical Genetic Identification of NDR1/2 Kinase Substrates AAK1 and Rabin8 Uncovers Their Roles in Dendrite Arborization and Spine Development', *Neuron*. Elsevier Inc., 73(6), pp. 1127–1142.

Vadlamudi, R. K. *et al.* (2002) 'Filamin is essential in actin cytoskeletal assembly mediated by p21-activated kinase 1', *Nature Cell Biology*, 4(9), pp. 681–690.

Vandenberg, P. *et al.* (1991) 'Characterization of a type IV collagen major cell binding site with affinity to the α1β1 and the α2β1 integrins', *Journal of Cell Biology*, 113(6), pp. 1475–1483.

Varnum-Finney, B. *et al.* (1995) 'The integrin receptor α8β1 mediates interactions of embryonic chick motor and sensory neurons with tenascin-C', *Neuron*, 14(6), pp. 1213–1222.

Velling, T. *et al.* (2004) 'β1-Integrins induce phosphorylation of Akt on serine 473 independently of focal adhesion kinase and Src family kinases', *EMBO Reports*, 5(9), pp. 901–905.

Vichalkovski, A. *et al.* (2008) 'NDR Kinase Is Activated by RASSF1A/MST1 in Response to Fas Receptor Stimulation and Promotes Apoptosis', *Current Biology*. Elsevier Ltd, 18(23), pp. 1889–1895.

Vora, S., Cheng, J., Xiao, R., Vandusen, N. J., *et al.* (2018) 'Rational design of a compact CRISPR- - - Cas9 activator for AAV- - - mediated delivery', 9.

Vora, S., Cheng, J., Xiao, R., VanDusen, N., *et al.* (2018) 'Rational design of a compact CRISPR-Cas9 activator for AAV-mediated delivery', *bioRxiv*, 9, p. 298620.

Waldt, N. *et al.* (2018) 'Filamin A Phosphorylation at Serine 2152 by the Serine/Threonine Kinase Ndr2 Controls TCR-Induced LFA-1 Activation in T Cells', *Frontiers in Immunology*, 9(December), pp. 1–16.

Wang, H. Y. *et al.* (2012) 'Reducing amyloid-related Alzheimer's disease pathogenesis by a small molecule targeting filamin A', *Journal of Neuroscience*, 32(29), pp. 9773–9784.

Wang, H. Y. *et al.* (2017) 'PTI-125 binds and reverses an altered conformation of filamin A to reduce Alzheimer's disease pathogenesis', *Neurobiology of Aging*. Elsevier Inc, 55, pp. 99–114.

Wang, H. Y., Frankfurt, M. and Burns, L. H. (2008) 'High-affinity naloxone binding to filamin A prevents Mu opioid receptor-Gs coupling underlying opioid tolerance and dependence', *PLoS ONE*, 3(2), pp. 1–10.

Wang, K., Ash, J. F. and Singer, S. J. (1975) 'Filamin, a new high-molecular-weight protein found in smooth muscle and non-muscle cells.', *Proceedings of the National Academy of Sciences of the United States of America*, 72(11), pp. 4483–6.

Wang, K., Zhu, T. N. and Zhao, R. J. (2019) 'Filamin A regulates EGFR/ERK/Akt signaling and affects colorectal cancer cell growth and migration', *Molecular Medicine Reports*, 20(4), pp. 3671–3678.

Warren, M. S. *et al.* (2012) 'Integrin β1 Signals through Arg to Regulate Postnatal Dendritic Arborization, Synapse Density, and Behavior', *Journal of Neuroscience*, 32(8), pp. 2824–2834.

Weaver, C. D. *et al.* (1995) 'Expression and in vitro function of β1-integrin laminin receptors in the developing avian ciliary ganglion', *Journal of Neuroscience*, 15(7 II), pp. 5275–5285.

Weeks, S. D. *et al.* (2018) 'Characterization of human small heat shock protein HSPB1 α-crystallin domain localized mutants associated with hereditary motor neuron diseases', *Scientific Reports*, 8(1), p. 688.

Wheeler, D. G. and Cooper, E. (2001) 'Depolarization Strongly Induces Human Cytomegalovirus Major Immediate-Early Promoter/Enhancer Activity in Neurons', *Journal of Biological Chemistry*, 276(34), pp. 31978–31985.

Whittaker, C. A. and Hynes, R. O. (2002) 'Distribution and evolution of von Willebrand/integrin A domains: widely dispersed domains with roles in cell adhesion and elsewhere', *Molecular biology of the cell*. American Society for Cell Biology, 13(10), pp. 3369–3387.

Wiatrak, B. *et al.* (2020) 'PC12 Cell Line: Cell Types, Coating of Culture Vessels, Differentiation and Other Culture Conditions', *Cells*, 9(4), p. 958.

Willems, J. *et al.* (2020) 'ORANGE: A CRISPR/Cas9-based genome editing toolbox for epitope tagging of endogenous proteins in neurons.', *PLoS biology*, 18(4), p. e3000665.

Winograd-Katz, S. E. *et al.* (2014) 'The integrin adhesome: From genes and proteins to human disease', *Nature Reviews Molecular Cell Biology*, 15(4), pp. 273–88.

Woo, M. S. *et al.* (2004) 'Ribosomal S6 Kinase (RSK) Regulates Phosphorylation of Filamin A on an Important Regulatory Site', *Molecular and Cellular Biology*, 24(7), pp. 3025–3035.

Wu, X. and Reddy, D. S. (2012) 'Integrins as receptor targets for neurological disorders', *Pharmacology and Therapeutics*, 134(1), pp. 68–81.

Xiong, J.-P. *et al.* (2001) 'Crystal structure of the extracellular segment of integrin αVβ3', *Science*. American Association for the Advancement of Science, 294(5541), pp. 339–345.

Xiong, S. *et al.* (2018) 'Structural Basis for Auto-Inhibition of the NDR1 Kinase Domain by an Atypically Long Activation Segment', *Structure*. Elsevier Ltd., 26(8), pp. 1101-1115.e6.

Yang, J. T., Rayburn, H. and Hynes, R. O. (1995) 'Cell adhesion events mediated by α4 integrins are essential in placental and cardiac development', *Development*, 121(2), pp. 549–560.

Yang, R. *et al.* (2014) 'Rassf5 and Ndr kinases act in a novel pathway regulating neuronal polarity through Par3 phosphorylation', *Journal of Cell Science*, 127(16), pp. 3463–3476.

Yang, S. and Kim, H. M. (2012) 'The RhoA-ROCK-PTEN pathway as a molecular switch for anchorage dependent cell behavior', *Biomaterials*. Elsevier Ltd, 33(10), pp. 2902–2915.

Yeh, W. H. *et al.* (2018) 'In vivo base editing of post-mitotic sensory cells', *Nature Communications*. Springer US, 9(1), pp. 1–10.

Yousif, N. G. (2014) 'Fibronectin promotes migration and invasion of ovarian cancer cells through up-regulation of FAK-PI3K/Akt pathway', *Cell Biology International*, 38(1), pp. 85–91.

Yue, J., Huhn, S. and Shen, Z. (2013) 'Complex roles of filamin-A mediated cytoskeleton network in cancer progression.', *Cell & bioscience*, 3(1), p. 7.

Zaidel-Bar, R. *et al.* (2007) 'Functional atlas of the integrin adhesome', *Nature Cell Biology*, 9, pp. 858–867.

Zallen, J. A. *et al.* (2000) 'Neuronal Cell Shape and Neurite Initiation Are Regulated by the Ndr Kinase SAX-1 , a Member of the Orb6 / COT-1 / Warts Serine / Threonine Kinase Family', *Molecular Biology of the Cell*, 11(September), pp. 3177–3190.

Zhang, J. *et al.* (2012) 'Brefeldin A-inhibited Guanine Exchange Factor 2 Regulates Filamin A Phosphorylation and Neuronal Migration', *Journal of Neuroscience*, 32(36), pp. 12619–12629.

Zhang, J. *et al.* (2013) 'Filamin A Regulates Neuronal Migration through Brefeldin A-Inhibited Guanine Exchange Factor 2-Dependent Arf1 Activation', *Journal of Neuroscience*, 33(40), pp. 15735–15746.

Zhang, K. and Chen, J. (2012) 'The regulation of integrin function by divalent cations', *Cell adhesion & migration*. Taylor & Francis, 6(1), pp. 20–29.

Zhang, L. *et al.* (2014) 'MEK-ERK1/2-Dependent FLNA Overexpression Promotes Abnormal Dendritic Patterning in Tuberous Sclerosis Independent of mTOR', *Neuron*, 84(1), pp. 78–91.

Zhang, L. *et al.* (2020) 'Filamin A inhibition reduces seizure activity in a mouse model of focal cortical malformations',

Science Translational Medicine, 12(532), pp. 1–13.

Zhang, Z., Tarone, G. and Turner, D. C. (1993) 'Expression of integrin α1β1 is regulated by nerve growth factor and dexamethasone in PC12 cells. Functional consequences for adhesion and neurite outgrowth.', *The Journal of Biological Chemistry*, 268(8), pp. 5557–5565.

Zheng, L. *et al.* (2011) 'Drosophila Ten-m and filamin affect motor neuron growth cone guidance', *PLoS ONE*, 6(8).

Zheng, X. M., Resnick, R. J. and David, S. (2002) 'Mitotic activation of protein-tyrosine phosphatase α and regulation of its Src-mediated transforming activity by its sites of protein kinase C phosphorylation', *Journal of Biological Chemistry*, 277(24), pp. 21922–21929.

Zhu, J. *et al.* (2007) 'Tests of the Extension and Deadbolt Models of Integrin Activation *', 282(16), pp. 11914–11920.

APPENDIX

1.1 Supplementary materials

1.1.1 DNA constructs used in this study

Table 2: shRNA hairpin sequences used in this study.

Plasmid	Insert	Used in Fig#	Reference
pLL3.7 (addgene: 11795)	U6-MCS for shRNA expression and CMV-EGFP	*shRNA cloning backbone*	(Paddison *et al.*, 2002)
pLL3.7-shLuc	Firefly-luciferase targeting shRNA *ATCAGGTGGCTCCCGCTGAATTGG*	*12, 14, 16-25, 27, 40*	(Rehberg *et al.*, 2014; Demiray *et al.*, 2018)
pLL3.7-shNdr2	Mouse-Ndr2 targeting shRNA *GAAGGATTGGCAGATGAGG*	*12, 14*	(Rehberg *et al.*, 2014; Demiray *et al.*, 2018)
pLL3.7-shItgb1	Mouse-integrin-β_1 targeting shRNA *CCAGACGGAGTAACAATAA*	*21*	(Lei *et al.*, 2012; Rehberg *et al.*, 2014)
pLL3.7-shFlnA	Mouse-FlnA targeting shRNA *GCAGCTGCTCAGTAGAATACA*	*16-25, 27, 28, 30, 40*	This study
pLL3.7-shFlnA_v2	Mouse-FlnA targeting shRNA *GCATCGAGCCTACAGGCAATA*	*20*	This study
pLL3.7-shRandom	Non-targeting hairpin control TCGTCATGACGTGCATAGG	*26*	(Thiere *et al.*, 2016)
pAAV-shLuc	Firefly-luciferase targeting shRNA *ATCAGGTGGCTCCCGCTGAATTGG*	*17*	This study
pAAV-shFlnA	Mouse-FlnA targeting shRNA *GCAGCTGCTCAGTAGAATACA*	*17*	This study

Table 3: Expression vectors used in this study

Plasmid	Insert	Used in Fig#	Reference
pEGFP-C1	CMV-EGFP	*11*	Clontech
pEGFP-Ndr2	CMV-EGFP_Ndr2	*11*	(Rehberg *et al.*, 2014; Demiray *et al.*, 2018)
pcDNA-myc_WT FlnA (addgene: 8982)	CMV-myc_humanFlnA	*16, 18, 19, 21-25, 28, 30, 40*	(Woo *et al.*, 2004)
pcDNA-myc_S2152A FlnA (addgene: 8983)	CMV-myc_humanFlnA	*30*	(Woo *et al.*, 2004)
pcDNA-FlnA-myc	CMV-WT humanFlnA_myc	*29*	(Nakamura *et al.*, 2007)

pcDNA-FlnA ΔIgFlnA24-myc	CMV-ΔIgFlnA24humanFlnA_myc	*29*	(Nakamura *et al.*, 2007)
pCMV-tdTom	CMV-driven tdTomato	*11, 12,18-25, 28, 29, 30*	Clontech
pAAV-CAG-tdTom (addgene: 59462)	CAG-driven tdTomato in AAV transfer plasmid	*32*	Boyden Lab

Table 4: CRISPR vectors used in this study.

Plasmid	Insert	Used in Fig#	Reference
pLenti-SAMv2 (addgene: 75112)	ef1α-dSpCas9_vp64 and U6-sgRNA (MS2 loop)	*gRNA cloning backbone*	(Joung *et al.*, 2017)
pLenti-miniCMV$_{gRNA(MS2)}$	miniCMV$_{gRNA(MS2)}$ *GTCCCCTCCACCCCACAGTG*	*34*	This study
pLenti-FlnA-1$_{gRNA(MS2)}$	FlnA-1$_{gRNA(MS2)}$ *GGGGGCGAGGTGGGGCGGGCG*	*35, 36*	This study
pLenti-FlnA-2$_{gRNA(MS2)}$	FlnA-2$_{gRNA(MS2)}$ *GCTTCGGGGGATGGGGGCGGG*	*35, 36*	This study
pLenti-FlnA-3$_{gRNA(MS2)}$	FlnA-3$_{gRNA(MS2)}$ *GGGGGGCGGAGCCTCTGGGTG*	*35, 36*	This study
pLenti-FlnA-4$_{gRNA(MS2)}$	FlnA-4$_{gRNA(MS2)}$ *GAGCCAGAGGCAAAGTTTCCT*	*35, 36*	This study
pLenti-MPHv2 (addgene: 89308)	ef1α-MS2_p65_HSF1 activator	*34, 35, 36*	(Joung *et al.*, 2017)
pLenti-syn-dCas9VPR (addgene: 114196)	syn-dSpCas9VPR_FLAG	*37-40*	(Savell *et al.*, 2019)
pLenti-ef1α-dCas9VPR (addgene: 114195)	ef1α-dSpCas9VPR_FLAG	*37*	(Savell *et al.*, 2019)
pLenti-sgRNA(SpCas9)-mCherry (addgene: 114199)	U6-sgRNA and ef1α-mCherry	*gRNA cloning backbone*	(Savell *et al.*, 2019)
pLenti-Control$_{gRNA}$-mCherry	Non-targeting control$_{gRNA}$ GCTGAAAAAGGAAGGAGTTGA (gRNA based on Joung et al. 2017)	*31, 38, 39*	This study
pLenti-FlnA-1$_{gRNA}$-mCherry	FlnA-1$_{gRNA}$ *GGGGGCGAGGTGGGGCGGGCG*	*38, 39, 40*	This study
pLenti-FlnA-2$_{gRNA}$-mCherry	FlnA-2$_{gRNA}$ *GCTTCGGGGGATGGGGGCGGG*	*38, 39, 40*	This study
pLenti-FlnA-3$_{gRNA}$-mCherry	FlnA-3$_{gRNA}$ *GGGGGGCGGAGCCTCTGGGTG*	*38, 39, 40*	This study
pLenti-FlnA-4$_{gRNA}$-mCherry	FlnA-4$_{gRNA}$ *GAGCCAGAGGCAAAGTTTCCT*	*38, 39, 40*	This study
pLenti-FlnA-KO1$_{gRNA}$-mCherry	FlnA-KO1$_{gRNA}$ *GAAGTGGACGTTGGCAAAGATC*	*31*	This study
pLenti-FlnA-KO2$_{gRNA}$-mCherry	FlnA-KO2$_{gRNA}$ *GCATTGGTATCAAGTGTGCCCC*	*31*	This study

136

pLenti-FlnA-KO3_{gRNA}-mCherry	FlnA-KO3_{gRNA} *GTCACAGGCTTACTAGCATCCC*	*31*	This study
pLenti-FlnA-KO4_{gRNA}-mCherry	FlnA-KO4_{gRNA} *GAAGTGACAGGGACTCATAAG*	*31*	This study
pLenti-Cas9_EGFP (addgene: 63592)	EFS-SpCas9_EGFP	*31*	(Chen *et al.*, 2015)
pBR322_miniCMV-tdTom (addgene: 99652)	minimal CMV-tdTom reporter (with PAM seq. for Sa. Cas9)	*45*	Church Lab
pAAV-dCas9VPR-sgRNA (addgene: 99698)	scp1-dSaCas9VPR and U6-sgRNA (SaCas9)	*45*	(Vora, *et al.*, 2018)
pAAV-dCas9VPR-miniCMV_{gRNA}	miniCMV_{gRNA} *GTCCCCTCCACCCCACAGTG*	*45*	This study
pCR_U6-miniCMV_{gRNA} (addgene: 41817)	miniCMV_{gRNA(SpCas9)} *GTCCCCTCCACCCCACAGTG*	*37*	(Mali, Yang, *et al.*, 2013)
pCR_miniCMV-tdTom (addgene: 47320)	minimal CMV-tdTom reporter (low basal expression)	*34, 37*	(Mali, Aach, *et al.*, 2013)
pAAV-CMV-SaCas9(HA)-U6_Bsa1_{gRNA} (addgene: 61591)	Single vector AAV-Cas9 vector (pX601)	*gRNA cloning backbone*	(Ran *et al.*, 2015)
pAAV-CMV-SaCas9(HA)-U6_Control_{gRNA}	Non-targeting control_{gRNA} GCTGAAAAAGGAAGGAGTTGA	*32, 33*	This study
pAAV-CMV-SaCas9(HA)-U6_ FlnA-KO1_{gRNA}	FlnA-KO1_{gRNA} *GAAGTGGACGTTGGCAAAGATC*	*32, 33*	This study
pAAV-CMV-SaCas9(HA)-U6_ FlnA-KO2_{gRNA}	FlnA-KO2_{gRNA} *GCATTGGTATCAAGTGTGCCCC*	*32, 33*	This study
pAAV-CMV-SaCas9(HA)-U6_ FlnA-KO3_{gRNA}	FlnA-KO3_{gRNA} *GTCACAGGCTTACTAGCATCCC*	*32, 33*	This study
pAAV-CMV-SaCas9(HA)-U6_ FlnA-KO4_{gRNA}	FlnA-KO4_{gRNA} *GAAGTGACAGGGACTCATAAG*	*32, 33*	This study
pMD2.G (addgene: 12259)	VSV-G envelope expressing plasmids	*Lentivirus production*	Trono Lab
pRSV-Rev (addgene: 12253)	3rd generation lentiviral packaging plasmid (contains Rev element)	*Lentivirus production*	Trono Lab
pMDLg/pRRE (addgene: 12251)	3rd generation lentiviral packaging plasmid (contains Gag and Pol elements)	*Lentivirus production*	Trono Lab
pAAV2/1 (addgene: 112862)	AAV packaging plasmid (Rep and Cap elements)	*AAV production*	Wilson Lab
pAdDeltaF6 (addgene: 112867)	AAV helper plasmid (E4, E2a and VA elements)	*AAV production*	Wilson Lab

```
                                    MK484107.1(1619-1642)
firefly_Luc   TTAAGTACAAAGGCTATCAGGTGGCTCCCGCTGAATTGGAATCCATCTTGCTCCAACACC
shLuc         --------------ATCAGGTGGCTCCCGCTGAATTGG--------------------
                            **********************

                                 NM_172734.3 (295-313)
ms_Ndr2       AAGAAGTTAGAAGTGGCTATGGAAGAAGAAGGATTGGCAGATGAGGAGAAAAAGTTACGT
shNdr2        -------------------------GAAGGATTGGCAGATGAGG--------------
                                       ******************

                                 NM_010578.2 (1474-1492)
ms_Itgb1      TTCTGGAAAATAGCAAATTGCCAGACGGAGTAACAATAAATTACAAATCCTATTGCAAGA
shItgb1       -------------------CCAGACGGAGTAACAATAA--------------------
                                 *******************

                                 NM_010227.3 (4321-4341)
mouse_FlnA    CTTGTATGGATAATAAAGATGGCAGCTGCTCAGTAGAATACATCCCCTATGAAGCTGGAA
shFlnA        --------------------GCAGCTGCTCAGTAGAATACA-----------------
                                  ********************

                                 NM_010227.3 (967-987)
mouse_FlnA    CGAAGAAAGCCCGAGCCTATGGGCCAGGCATCGAGCCTACAGGCAATATGGTGAAGAAGA
shFlnA_2      -------------------------GCATCGAGCCTACAGGCAATA-----------
                                       ********************
```

Appendix Figure 42: Mouse transcript targeting shRNAs used in this study.
Alignment of the shRNAs used in this study against mouse RefSeq transcript database (except for control shRNA against firefly luciferase).

1.1.2 *Positional scanning peptide library*

To determine an optimal amino acid motif phosphorylated by Ndr2, purified WT Ndr2/Mob2 heterodimer was used in a positional peptide library scan (Hutti *et al.*, 2004) with radioactively labelled ATP (Figure 7A, in collaboration with Eric Devroe & Benjamin Turk). Briefly, purified kinase heterodimers combined with biotin tagged peptide mixtures for labelling with $[\gamma\text{-}^{32}P]$ATP. Peptide mixture consisted of a general sequence Y-A-X-X-X-X-X-(S/T)- X-X-X-X-A-G-K-K where X denotes for an equimolar mixture of 17 amino acids (excluding Cys, Ser and Thr) and different aliquots had a unique amino acid fixed at one of nine positions surrounding the central (S/T) phosphor acceptor residue. After 2 hours at 30 ^{0}C incubation, biotin tagged peptides were spotted on streptavidin membrane for phosphor imaging. Normalized data from two independent

runs were averaged, log transformed, and heat maps were generated in which values greater than

1 represent positive selection for the given amino acid and values less than 1 is negative selection.

1.1.3   *List of proteins containing RxP(S/T) motif in integrin adhesome*

Table 5: List of proteins in integrin adhesome network containing the recently identified Ndr2 target RxP(S/T) motif

Gene Symbol	Uniprot ID	motif start	motif start	Motif
ABI1	Q8CBW3	308	311	RtPS
ABI2	P62484	306	309	RpPS
ABI3	Q8BYZ1	120	123	RlPS
CASS4	Q08EC4	621	624	RqPT
CRKL	P47941	104	107	RyPS
FLNA	Q8BTM8	1809	1812	RmPS
FLNA	Q8BTM8	2149	2152	RaPS
GIT2	Q9JLQ2	452	455	RrPS
HSPB1	P14602	12	15	RsPS
KCNH2	O35219	148	151	RgPS
LASP1	Q61792	153	156	RrPT
LRP1	Q91ZX7	1147	1150	RpPS
LRP1	Q91ZX7	4258	4261	RcPT
LYN	P25911	34	37	RdPT
NCK2	O55033	82	85	RkPS
NISCH	Q80TM9	1370	1373	RtPS
PALLD	Q9ET54	1128	1131	RsPS
PARVB	Q9ES46	7	10	RsPT
PDE4D	Q01063	188	191	RaPS
PKD1	O08852	4060	4063	RvPT
PLD1	Q9Z280	96	99	RvPS
PTPRA	P18052	201	204	RsPS
SDC4	O35988	99	102	RvPS
SDC4	O35988	116	119	RaPS
SOS1	Q62245	568	571	RlPS
SOS1	Q62245	1051	1054	RhPT
SOS1	Q62245	1171	1174	RqPT
SRC	P05480	47	50	RgPS
SSH1	Q76I79	8	11	RsPT
SVIL	Q8K4L3	629	632	RyPS
SVIL	Q8K4L3	725	728	RlPS
TRIO	Q0KL02	1561	1564	RtPT
TRIP6	Q9Z1Y4	64	67	RgPT

| VAV2	Q60992	645	648	RpPT
VAV2	Q60992	650	653	RpPS

1.1.4 Ndr2 and FlnA S2152 phosphorylation in T-cells (Waldt et al. 2018)
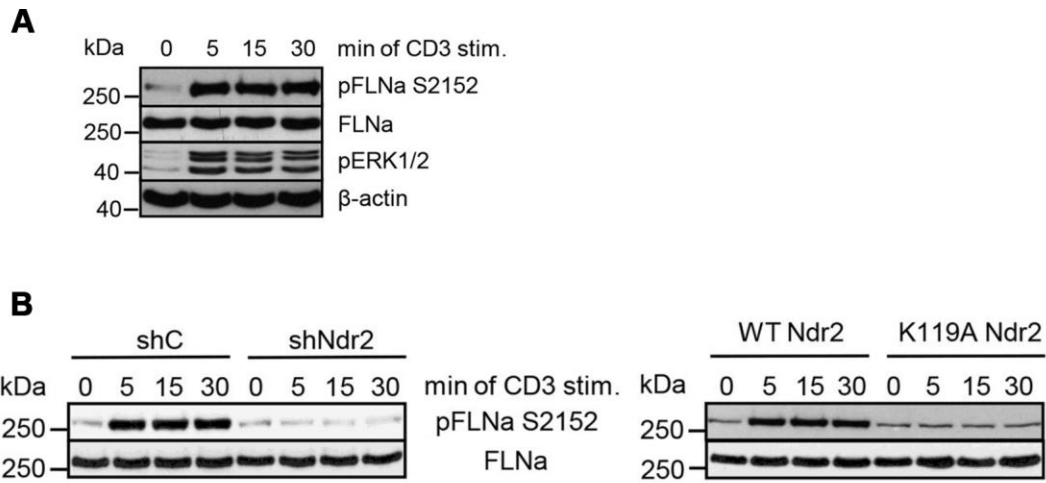
Appendix Figure 43: FlnA-S2152 phosphorylation by Ndr2 in Jurkat T cells (from Waldt *et al.*, 2018)
(A) Strong induction of FlnA-S2152 phosphorylation in Jurkat T-cells upon stimulation with CD3.
(B) Jurkat T cells were transfected with either control, shNdr2, WT Ndr2 or K119A Ndr2 mutant constructs, and 48 hours after transfection, CD3 treatment were applied at indicated time points. Western blotting against FlnA-S2152 shows disturbance in FlnA phosphorylation in shNdr2 and kinase dead Ndr2 transfected cells (in collaboration with Dr. Natalie Waldt & Dr. Stefanie Kliche).

1.1.5 Neurotrophin signaling on FlnA expression
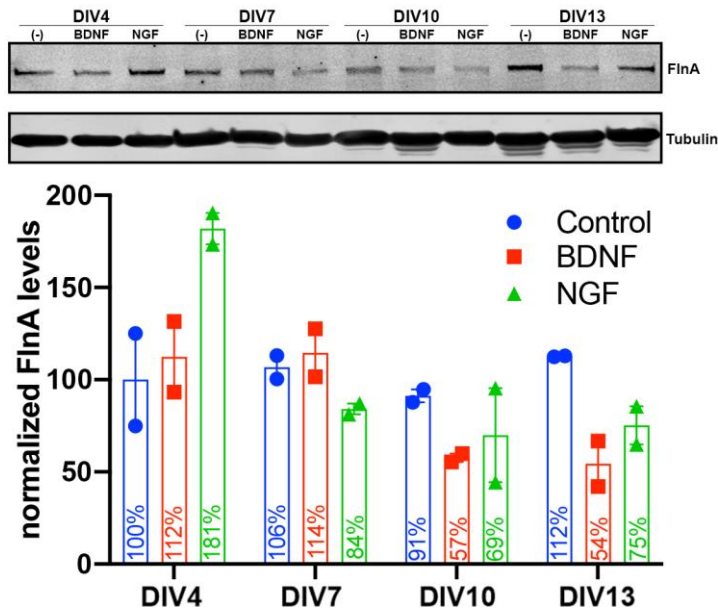
Appendix Figure 44: BDNF and NGF signaling affects FlnA expression in a time dependent manner.
Mouse cortical cultures are treated with either BDNF (25 ng/ml) or NGF (50 ng/ml) continuously from DIV1 onwards and lysed every 3rd day for western blotting. While NGF treatment results almost 2-fold increase in FlnA expression in DIV4, both NGF and BDNF treatments reduces the FlnA expression at later time points.

1.1.6 Single AAV system for transcriptional activation via dCas9-VPR
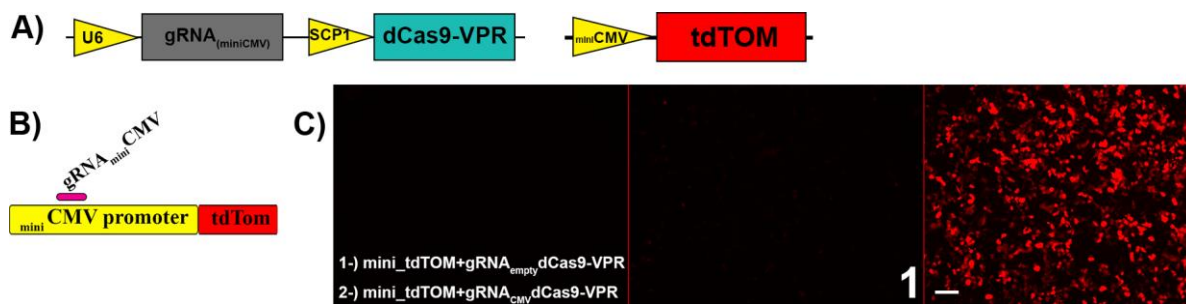
Appendix Figure 45: Single-AAV system for transcriptional activation using dCas9-VPR
(**A**) U6-gRNA$_{miniCMV}$ and SCP1-dCas9VPR cassettes were fit in an AAV transfer plasmid and used alongside miniCMV-tdTom reporter plasmid (based on Vora *et al.*, 2018). (**C**) A minimal CMV promoter (miniCMV) driven tdTom is targeted with a gRNA as a reporter for dCas9 mediated activation. (**D**) HEK293T cells are transfected with mini_tdTom reporter plasmid and co-transfected with either *(1)* empty U6-gRNA/SCP1-dCas9VPR or *(2)* U6-gRNA$_{miniCMV}$/SCP1-dCas9VPR (Scale

bar: 100μm). A strong increase of tdTom fluorescence was observed after transfection of gRNA against minimal CMV promoter.

1.2 Ehrenerklärung

Ich versichere hiermit, dass ich die vorliegende Arbeit ohne unzulässige Hilfe Dritter und ohne Benutzung anderer als der angegebenen Hilfsmittel angefertigt habe; verwendete fremde und eigene Quellen sind als solche kenntlich gemacht.

Ich habe insbesondere nicht wissentlich:

- Ergebnisse erfunden oder widersprüchlich Ergebnisse verschwiegen,

- statistische Verfahren absichtlich missbraucht, um Daten in ungerechtfertigter Weise zu interpretieren,

- fremde Ergebnisse oder Veröffentlichungen plagiiert,

- fremde Forschungsergebnisse verzerrt wiedergegeben.

Mir ist bekannt, dass Verstöße gegen das Urheberrecht Unterlassungs- und Schadensersatzansprüche des Urhebers sowie eine strafrechtliche Ahndung durch die Strafverfolgungsbe- hörden begründen kann.

Ich erkläre mich damit einverstanden, dass die Arbeit ggf. mit Mitteln der elektronischen Datenverarbeitung auf Plagiate überprüft werden kann.

Die Arbeit wurde bisher weder im Inland noch im Ausland in gleicher oder ähnlicher Form als Dissertation eingereicht und ist als Ganzes auch noch nicht veröffentlicht.

Magdeburg, 23.11.2020.

Yunus Emre Demiray